AD_____

Award Number: W81XWH-08-1-0224

TITLE: Immunotherapeutic Vaccine as an Alternative Treatment to Overcome Drug-Resistant Ovarian Cancer

PRINCIPAL INVESTIGATOR: Michael Morse, M.D.

CONTRACTING ORGANIZATION: Duke University
Durham, NC 27708

REPORT DATE: July 2012

TYPE OF REPORT: Final

PREPARED FOR: U.S. Army Medical Research and Materiel Command
Fort Detrick, Maryland 21702-5012

REPORT DOCUMENTATION PAGE

Form Approved
OMB No. 0704-0188

1. REPORT DATE	2. REPORT TYPE	3. DATES COVERED
July 2012	Final	1 July 2008 – 30 June 2012

4. TITLE AND SUBTITLE

Immunotherapeutic Vaccine as an Alternative Treatment to Overcome Drug-Resistant Ovarian Cancer

5a. CONTRACT NUMBER

5b. GRANT NUMBER
W81XWH-08-1-0224

5c. PROGRAM ELEMENT NUMBER

6. AUTHOR(S)

Michael Morse

E-Mail: michael.morse@duke.edu

5d. PROJECT NUMBER

5e. TASK NUMBER

5f. WORK UNIT NUMBER

7. PERFORMING ORGANIZATION NAME(S) AND ADDRESS(ES)

Duke University
Durham, NC 27708

8. PERFORMING ORGANIZATION REPORT NUMBER

9. SPONSORING / MONITORING AGENCY NAME(S) AND ADDRESS(ES)
U.S. Army Medical Research and Materiel Command
Fort Detrick, Maryland 21702-5012

10. SPONSOR/MONITOR'S ACRONYM(S)

11. SPONSOR/MONITOR'S REPORT NUMBER(S)

12. DISTRIBUTION / AVAILABILITY STATEMENT
Approved for Public Release; Distribution Unlimited

13. SUPPLEMENTARY NOTES

14. ABSTRACT

The overall goal is to develop a multivalent vaccine that may be administered in combination with chemotherapy or targeted therapies to address platinum-resistant ovarian cancer (Ov Ca). We identified vaccine candidate epitopes over-presented in platinum resistant Ov Ca cells and initially proposed to activate cytolytic T cells (CTL) against these epitopes in vitro and to test their cytolysis of platinum resistant cells (alone and with cisplatin and dasatinib); however, repeated attempts to expand the CTL were unsuccessful. We therefore, chose two of the genes that contained representative epitopes (EDDR1 and ADAM17/TACE) and cloned them into adenoviral vectors. We demonstrated that these vectors were immunogenic and induced immune responses against EDDR1 and TACE respectively. T cella activated against these vectors, when adoptively transferred to mice bearing a platinum resistant tumor cell line, were capable of controlling tumor growth. These data support future translation of this vaccine strategy into human clinical trials.

15. SUBJECT TERMS
Drug-resistant, ovarian cancer, adenoviral vectors, EDDR1, ADAM17

16. SECURITY CLASSIFICATION OF:			17. LIMITATION OF ABSTRACT	18. NUMBER OF PAGES	19a. NAME OF RESPONSIBLE PERSON
a. REPORT	b. ABSTRACT	c. THIS PAGE			USAMRMC
U	U	U	UU	89	19b. TELEPHONE NUMBER *(include area code)*

Table of Contents

INTRODUCTION:

The purpose of this research, performed in conjunction with the Partner PI Ramilla Philip, PhD, was to develop a novel immune therapy strategy for management of a major problem in ovarian cancer, cisplatin resistance. We hypothesized that proteins that are differentially expressed and that are processed into peptides and presented in the context of Major Histocompatibility Class I molecules by platinum-resistant ovarian cancers may serve as unique antigenic targets for the development of an immunotherapeutic vaccine that can be used in combination with other modalities to effectively prevent disease progression and metastasis of advanced-stage, platinum-resistant ovarian cancer. Specifically, we wished to identify a panel of MHC class I-associated epitopes derived from proteins that are differentially expressed by platinum-resistant ovarian tumor cells. From these antigens , we would Identify 6-12 peptide epitopes capable of activating CTL responses against tumor cells obtained from platinum-resistant ovarian cancer patients and then demonstrate that T cell responses induced against these antigens using peptide cocktails/vaccines could synergize with cisplatin or the targeted therapy dasatinib to destroy platinum resistant tumor cells. Based on challenges encountered when trying to activate CTL against the peptides, we received approval from DOD to modify the plan to develop adenoviral vector based vaccines rather than peptide vaccines to activate T cells.

BODY:

The following report details the activities of the PI (M. Morse, Duke) as described in the Statement of Work (SOW) with reference to the activities of the Partner-PI (R. Philip, Immunitope). In prior annual reports, we have described progress made on each subaim and will restate these herein and also include new progress regarding aim 3.

Specific aim 1 was to discover a panel of MHC class I-associated epitopes derived from proteins that are differentially expressed by platinum-resistant ovarian tumor cells. (Months 1-9) with the following tasks:

Task 1. Collection and processing of patient specimens): (Months 1-9 and ongoing) **(PI)**

a. Isolation of tumor cells from ascites and storage (Months 1-6 and ongoing). Initially, only ascites samples from patients with platinum resistant ovarian cancer were being collected by the PI's team (as per the SOW). However, the rate of collection of platinum resistant tumors was low and amongst the early samples, only one was found to be HLA-A2 positive. This sample was used to identify A2 associated epitopes (see below). A difficulty identified was that few patients with platinum refractory ovarian cancer actually had paracenteses performed for medical reasons. We therefore requested (and were approved by DOD) to collect samples from patients presenting with ovarian cancer and to store them in the event that they were found to be primarily platinum resistant. We would then use the tumor cells from their ascites used for further study. A total of 34 patients were enrolled but adequate samples of ascites and or tumor from 24 ovarian cancer patients were collected (See table 1).

Table 1. List of samples collected and platinum resistance status

Patient ID	Blood	Tissue	Ascites	Platinum Resistant
DODImm-001			12/1/2008	YES

DODImm-002			12/22/2008	YES
DODImm-003	3/5/2009		12/30/2008	No
DODImm-004	5/22/2009	5/29/2009	5/29/2009	No
DODImm-005	6/15/2009		6/15/2009	YES
DODImm-006	6/18/2009		6/24/2009	YES
DODImm-007	7/23/2009			No
DODImm-008	8/10/09		7/27/2009	YES
DODImm-009	7/30/2009			No
DODImm-010	8/7/2009		8/7/2009	No
DODImm-011	8/13/2009	8/14/2009	8/13/2009	No
DODImm-012	8/28/2009		8/28/09; 9/2/09; 9/1/09	YES
DOD-Imm-013	10/5/2009	10/7/2009	10/7/2009	No
DOD-Imm-021			3/5/2010	No
DOD-Imm-022		3/19/2010		No
DOD-Imm-024			4/2/2010	No
DOD-Imm-025	4/8/2010		4/2/2010	No
DOD-Imm-026	4/16/2010	4/22/2010	4/16/2010	No
DOD-Imm-027	7/7/2010	7/7/2010	7/7/2010	No
DOD-Imm-028			7/8/2010	No
DOD-Imm-029	7/9/2010		7/9/2010	No
DOD-Imm-031			7/15/2010	No
DOD-Imm-032	8/4/2010		8/4/2010	No
DOD-Imm-035	9/22/2010		9/22/2010	No

Of these samples, 6 were subsequently been identified as platinum resistant and the remainder are from patients being observed for development of platinum resistant tumor. In order to overcome the problem

of obtaining adequate samples to study peptide expression in platinum resistant patient specimens, we obtained MHC peptide data from metabolically labeled platinum resistant and sensitive ovarian cancer cell lines (see below) and therefore, the patient samples were subsequently used for characterization of CTL and selection of peptides for in vivo studies. From a budgeting standpoint, because we needed to collect more ascites, we used more supplies than originally budgeted; however, this was offset by fewer supplies used for Task 1b (see below)

b. Isolation of tumor cells from bulk tumor masses (Months 1-6) (PI): No patients with cisplatin refractory disease underwent repeat debulking to permit sampling of bulk tumor. However, these samples were not required since the ascites yielded cells that could be used for the required assays to identify tumor peptides (See task 2).

c. Isolation of normal ovarian cells from normal ovary (Months 1-6) (PI): no normal ovary tissue was available for collection on any of the patients from whom tumor was collected due to the extent of disease. However, for experiments requiring normal cells, we purchased commercially available normal organ cells (such as liver cells).

d. Initiate cultures with tumor cell lines (Months 1-9): PI: It was not possible to generate enough tumor cells in vitro to be subsequently implanted. Using other funding, we have since developed methods for growing human tumors in SCID mice on an ongoing basis and in future studies, expect to apply these techniques to human ovarian tumors.

Task 2. Identification of 10-20 candidate MHC Class I-associated peptides from proteins differentially expressed in platinum-resistant tumor cells (Partner PI).

The partner PI has performed the discovery of HLA-A2 specific epitopes associated with platinum-resistant ovarian tumor cells by immunoaffinity purification of MHC class I molecules from ovarian tumor cells isolated from ascites and ovarian cancer cell lines. Ovarian cancer cell lines OVCAR3 (platinum sensitive) and SKOV3.A2 (platinum resistant) were maintained in the presence of cisplatin and primary tumor cells from HLA-A2+ ascites were purified by differential centrifugation prior to the isolation of MHC peptides. MHC peptide complexes were isolated by immunoaffinity purification and the isolated peptides were HPLC fractionated and analyzed by LC/MS/MS experiments.

Task 3. Selection of 10 to 20 candidate peptides differentially expressed in platinum-resistant tumor cells (PI and Partner PI)

For details of the identification of the candidate peptides, see partner PI report. Following the identification of over 300 epitopes in cisplatin resistant ovarian cell lines (published by the partner PI in Shetty V et al., J Proteomics. 2012 Jun 18;75(11):3270-90), the PI and partner PI selected 11 epitopes for further validation and characterization (see partner PI report).

Specific aim 2 was to identify 6-12 peptide epitopes capable of activating CTL responses against tumor cells obtained from platinum-resistant ovarian cancer patients (6 months).

Task 1. Generation of peptide-specific CD8+ T cells using PBMC from HLA-A2+ healthy donors and ovarian cancer patients. **(PI and Partner PI)**

a. collection of peripheral blood mononuclear cells, primary tumor cells from resistant and sensitive patients; expansion in short term cultures. **(PI)**

b. Perform CTL assays using standard 51Cr assays, ELISPOT and multiparameter flow cytometry **(PI and Partner PI)**

As described above, specimens of PBMC (healthy donor and ovarian cancer) and ascites/tumor cells were collected by the PI. Both the PI and partner PI generated CTL against selected platinum-resistant ovarian cancer peptides (figure 1 is an example of an ELISPOT assay for T cells stimulated against select peptides (denoted as RLD, LLD, etc.)). In this experiment, peptide-specific CTLs were generated using peripheral blood mononuclear cells from a platinum-resistant ovarian cancer patient. The T cells were stimulated with individual peptides and IL-2/IL-7 three times prior to assay for CTL activity. *In vitro* expanded T cells were used as effectors in ELISpot assays to assess antigen-stimulated interferon-gamma (IFN-gamma) release. CTL activity was tested against peptide loaded T2 cells, platinum-resistant (SKOV3 A2+ cells +/- cisplatin treatment) and sensitive (OVCAR3) ovarian cancer cell lines and tumor cells from platinum resistant patient (A2 ascites) and HLA-A2+ normal liver cells as negative controls. CTLs specific for the selected peptides recognized both ovarian tumor cell lines and tumor cells from the platinum-resistant ovarian cancer patient suggesting endogenous presentation of these epitopes in these cells (Fig. A)**.**

Figure A: Peptide-specific CTL recognize ovarian tumor cells

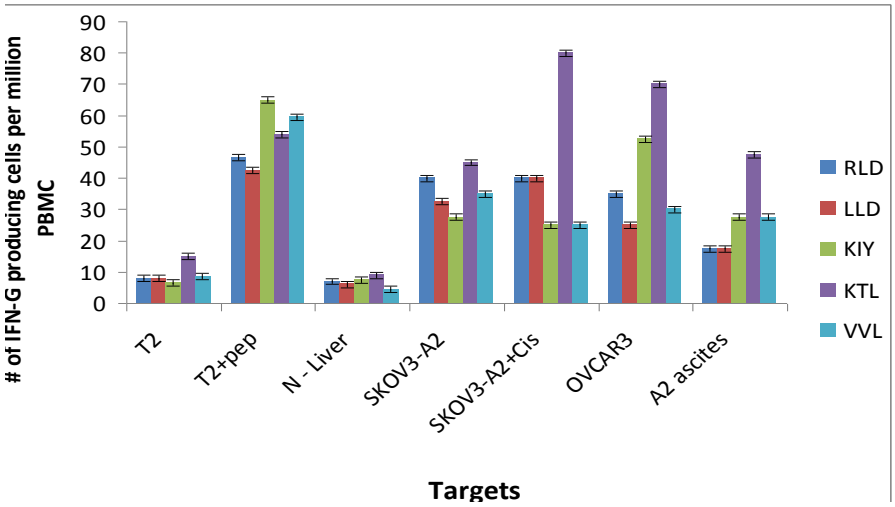

Figure A: Peptide specific CTLs were generated using PBL from an ovarian cancer patient. The CTLs were assayed for antigen-specific IFN-gamma release in an ELISpot assay. T2 with and without appropriate peptides, normal liver without peptide and platinum-resistant ovarian tumor line, SKOV3 A2 with and without cisplatin treatment (SKOV3 A2+cis) and platinum-sensitive ovarian tumor line, OVCAR3 and ascites tumor cells from platinum-resistant patient were used as targets in the ELISpot assay.

Interestingly, all the peptide specific CTLs recognized the platinum-resistant (SKOV3) and the sensitive (OVCAR3) ovarian tumor targets, suggesting that these epitopes are presented and are CTL targets on tumor cells regardless of platinum sensitivity, which makes them ideal target for all ovarian cancer patients treated with platinum drugs. Interestingly, the addition of cisplatin resulted in enhanced recognition of the SKOV3-A2 by CTL specific for the peptide denoted KTL. More importantly, the CTLs were capable of recognizing the tumor cells from the ascites sample isolated from the platinum-resistant ovarian cancer patient signifying that the peptides tested were expressed by the patient tumor and could serve as targets for T cell responses. Lack of recognition of normal liver cells suggests that these epitopes are either very low in concentration or not present on the MHC molecule of normal cells and thus tumor specific. Overall, these studies indicate that these peptides are endogenously processed and presented in the context of MHC class I molecules on ovarian tumor cells and most importantly they are presented on platinum-resistant ovarian tumor cells, which makes them potential candidates for immunotherapeutic vaccine for the treatment of drug resistant ovarian cancer.

Task 2. Identification of 6-12 epitopes for further preclinical studies **(PI and Partner PI)**
Based on the CTL activity detected in this experiment, we, in conjunction with the partner PI, chose to study the CTL response against 7 of the more potent peptides (P1-6 and P11) and were also to study two of the weaker epitopes. We attempted to generate (*in vitro*) sufficient quantities of CTL specific for the

peptides identified in the prior aims. Initially the following peptides were used to attempt to generate CTL:

Peptide#	Peptide sequence
1	RLDELGGVYL
3	LLDEKEPEV
4	VLIDYQRNV
5	LTLTMLARLA

Approximately 2x10^7 CTL per donor (4 peptide specific CTLs and 2 donors) were generated. The CTLs were tested for IFNγ release against peptide loaded T2 and cancer cell lines (SKOV3-A2 (tested with cisplatin 2mM), Ovcar3 and MDA-MB231). However, the quantities of CTL that could be reproducible amplified, even after 3 rounds of stimulation with dendritic cells loaded with peptide, were low and the antigen-specificity of these CTL was poor as evidenced by limited killing in subsequent cytotoxicity assays. Therefore, we wished to identify other methods for generating sufficient CTL to demonstrate proof of principal that CTL could synergize with cisplatin (and dasatinib) in the killing of cisplatin-resistant tumor cells. In other ongoing work in our laboratory, we have utilized adenoviral vectors encoding tumor antigens of interest to immunize mice and then have been able to show that the splenocytes from immunized mice could respond to tumor cells expressing that antigen (Morse et al., Int J Cancer. 2010 Jun 15;126(12):2893-903.). We therefore stopped work on this Task in order to generate adenoviral vectors encoding antigens expressed by platinum resistant ovarian cancers.

Although we could have chosen from amongst the antigen identified from the partner PI (reported in Shetty V et al., J Proteomics. 2012 Jun 18;75(11):3270-90), most were not derived from proteins for which we had cloned sequences available. Instead, we studied two additional proteins, EDDR1 and ADAM-17/TACE. As described in the two attached manuscripts from our group (Sinnathamby G, et al. Clin Exp Immunol. 2011 Mar;163(3):324-32 and Sinnathamby G, J. Clin Cell Immunol 2011, 2:1), we analysed the expression profile of ADAM17and EDDR1 in a variety of normal and cancer cells of human origin and found that this protein is over-expressed on the surface of several types of cancer cells including ovarian cancer compared to the normal counterparts. Furthermore, we analysed the presentation of a human leucocyte antigen (HLA)-A2-restricted epitopes from these antigens to specific T cells established from normal donors as well as ovarian cancer patients. Our analysis revealed that the HLA-A2-restricted epitopes are processed efficiently and presented by cancer cells and not by normal cells. Tumor-specific T cell activation resulted in the secretion of both interferon–γ and granzyme B that could be blocked by HLA-A2 specific antibodies. Collectively, our data presented evidence that ADAM17 and EDDR1 were ovarian cancer antigens. Because we had available complete information about these genes, we sought to develop adenoviral vectors encoding EDDR1 and ADAM-17/TACE (see aim 3).

Specific Aim 3: Demonstrate that treatment with chemotherapy or a targeted therapeutic agent will sensitize the platinum-resistant tumor to CTL responses by enhancing presentation of resistance-associated, MHC-presented epitopes on platinum-resistant tumor cells (18 months).

Task 1 Determine the *in vitro* and *in vivo* CTL responses to platinum-resistant ovarian tumors following

treatment with cisplatin**.**

Previous Task 1a: *In vitro* studies combining cisplatin with T cells against the 6-12 epitopes selected in Aim 2**.**
Revised Task 1a. *In vitro* studies combining cisplatin with T cells specific for EDDR1 and TACE, antigens expressed by platinum-resistant ovarian cancers

Previous Task 1b. In vivo studies combining cisplatin with T cells specific for the 6-12 epitopes selected in Aim 2.
Revised Task 1b. *In vivo* studies combining cisplatin with T cells specific for EDDR1 and TACE, antigens expressed by platinum-resistant ovarian cancers

Task 2 Determine the *in vitro* and i*n vivo* CTL responses to platinum-resistant ovarian tumors following treatment with targeted therapy, using dasatinib as the model targeted therapy**.**

Previous Task 1a: *In vitro* studies combining dasatinib with T cells against the 6-12 epitopes selected in Aim 2.
Revised Task 2a. *In vitro* studies combining dasatinib with T cells specific for EDDR1 and TACE, antigens expressed by platinum-resistant ovarian cancers

Previous Task 2b. In vivo studies combining dasatinib with T cells specific for the 6-12 epitopes selected in Aim 2.
Revised Task 2b. *In vivo* studies combining dasatinib with T cells specific for EDDR1 and TACE, antigens expressed by platinum-resistant ovarian cancers

As described above, we changed strategies (with DOD approval) to generate CTL specific for antigens expressed by platinum-resistant ovarian cancer. First, we chose to use adenoviruses encoding tumor antigen instead of peptides because adenovirus is associated with more potent induction of T cell responses in our experience. Second, as described above, we chose to target TACE and EDDR1 as they were available in adenovectors and because we have identified them as targets in published work (See attached Manuscripts Sinnathamby G, et al. Clin Exp Immunol. 2011 Mar;163(3):324-32 and Sinnathamby G, J. Clin Cell Immunol 2011, 2:1). Although Ad vectors encoding these antigens were thought to be available, the original batch, on further testing, was unfortunately found to have truncated genes encoded. After receiving approval for the no cost extension (NCE), we found that it was necessary to re-derive the Ad vectors encoding EDDR1 and TACE:

Constructing Ad-TACE and Ad-DDR1 (EDDR1) Virus

We constructed adenovirus (Ad5-(E1-/E3-)) encoding human TACE and DDR1 (alternatively referred to as EDDR1 or EDDR) as follows:

1. Cloning the TACE and DDR into pShuttle-CMV-vector

Full-length human TACE and DDR1 cDNA plasmids, pCMV-XL-5-TACE and pCMV-XL-DDR1 were purchased from Origene (Rockville, MD). We used Not I and Xba I restriction enzymes to cut pCMV-XL-5-TACE and pCMV-XL-DDR1 plasmids to obtain full-length TACE cDNA and DDR1 cDNA (Fig.1). TACE cDNA and DDR1 cDNA were cloned into Not I and Xba I restrict sites in the MCS of

pShuttle-CMV vectors. The cloned vectors were transformed into XL10-Gold competent cells and grown on LB/Kanamycin plates. Recombinant plasmids, pShuttle-CMV-TACE and pShuttle-CMV-DDR1, were isolated and purified from competent cell using plasmid MiniPrep kit (Qiagen, Valencia CA). The presence of TACE and DDR1 inserts were confirmed by restriction digestion (Fig 2 and Fig 3) and DNA sequencing analysis.

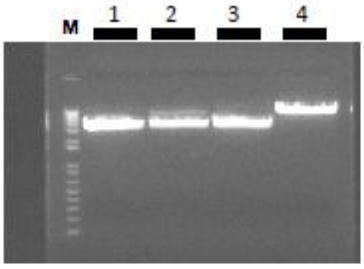

Fig 1. pCMV-XL5-DDR1 plasmid and pShuttle-CMV cut by Not I and Xha I

M: DNA marker, Lane 1, 2, and 3 were pCMC-XL5-DDR1

Lane 4 was pShuttle-CMV

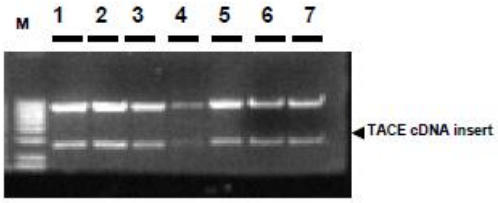

Fig 2. pShuttle-CMV-TACE cut by XhaI and Not I

M: DNA marker, Lane 1-7: pShuttle-CMV-TACE

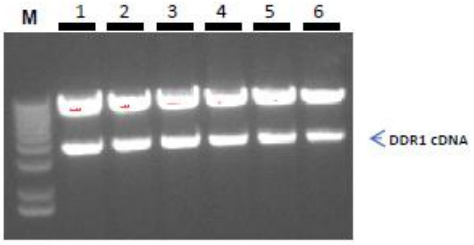

Fig 3. pShuttle-CMV-DDR1 cut by NotI and Xba I

M: DNA marker, Lane 1-6 were pShuttle-CMV-DDR1

2. Generating recombinant adenovirus plasmids using BJ5183 cells

pShuttle-CMV-TACE and pShuttle-CMV-DDR1plasmids were purified using plasmid MaxiPrep kit (Qiagen) and linearized using Pme I. Complete digestion was confirmed by agarose gel electrophoresis. Once complete digestion with Pme I was confirmed (Fig 4), the enzyme and buffer were removed by a PCR purification kit (Qiagen). Digested and purified plasmid DNA (shuttle vector plus TACE or DDR1) were further treated with alkaline phosphatase for 30 minutes at 37 ^{0}C, then separated using agarose gel electrophoresis and purified using Gel purification kit (Qiagen).

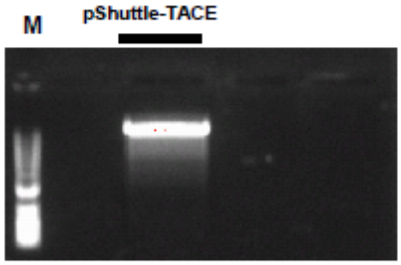

Fig 4. pShuttle-TACE cut by Pme I

M; DNA marker

1 µg of linearized and dephosphorylated shuttle vector, pShuttle-CMV-TACE or pShuttle-CMV-DDR1 and 100 ng of pAd-Easy supercoiled vector were co-pipetted into 40 µl of BJ5183 electroporation competent cell. The cells were transferred into chilled electroporation cuvettes and processed for electroporation at an electroporator (Bio-Rad, Hercules CA), then the cells were incubated at 37 ^{0}C for 1 hour, plated onto LB-Kanamycin plates, and incubated at 37 ^{0}C overnight.

10 or more of the smallest, well isolated colonies were picked from the plates into 3 ml LB-Kanamycin broth and incubated at 37 C overnight while shaking at 250 rpm. Plasmid DNA were minipreped from 2 ml of overnight culture and cut with Pac I. D digested DNA were run on a 0.8% agarose gel. Recombinant Ad plasmid DNA with Pac I treatment yielded a larger fragment of 30 kb and a smaller fragment of 3 kb or 4 kb (Fig 5 and Fig 6). Potential recombinants were transferred and amplified in XL10-Gold competent cell. PCR was used to further confirm the insert of TACE cDNA and DDR1 cDNA in recombinant Ad plasmid (Fig 7).

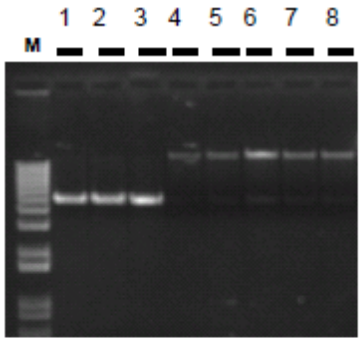

Fig 5. Ad-TACE cut by Pac I

M: DNA marker

Lane 1-8 were Ad-TACE, clones 4-8 were correct

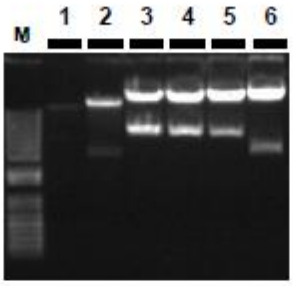

Fig 6. Ad-DDR1 digested by Pac I

M: DNA marker

Lane 1-6 were Ad-DDR1, clones 3, 4, 5 and 6 were right.

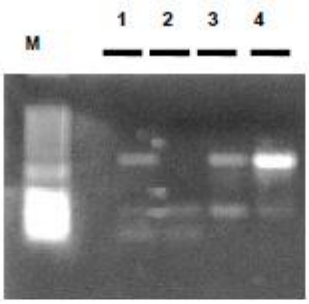

Fig 7. PCR for TACE and DDR1 insert in Ad-TACE and Ad-DDR1

M: DNA marker

Lane: 1-3 Ad-TACE; Lane 4: Ad-DDR1

Testing the immunogenicity of the Adenoviral vectors in HLA-A2 transgenic mice

In preparation for in vitro studies of the effect of anti-TACE and anti-EDDR1 in conjunction with cisplatin and to obtain splenocytes that could be used in these assays, we tested the immunogenicity of the Adenoviral vectors in HLA-A2 transgenic mice.

Method: HLA-A2 transgenic mice were vaccinated with Ad-EDDR, Ad-LacZ (2.6 x 10E10 vp/injection) or saline on days 0 and 14. Mice were euthanized on day 21, and splenocytes were harvested. These splenocytes (EDDR1 splenocytes and LacZ splenocytes) (1 M cells/well) were utilized for proliferation assay in 96 well plates. EDDR p15 peptide (final concentration; 1 µg/mL) and Ad-EDDR (moi 1000) were used as stimulating antigens, and Cap-1(6D) peptide and Ad-null were used as negative controls. Three (3) days later, 3H-thymidine (1 µci/well) was added, and 18 h later, thymidine uptake was measured. As demonstrated in figure 1A, there was greater proliferation of splenocytes (T cells) from mice immunized against EDDR1 (EDDR1-splenocytes) when exposed to Ad- EDDR1 than when exposed to the Ad-null vector suggesting that there was induction of EDDR1-specific activity beyond the expected Ad-specific activity. The EDDR1-splenocytes T cells did not proliferate against the EDDR p15 peptide, suggesting different epitope(s) than this one HLA A2 peptide were responsible for the anti-EDDR1 response.

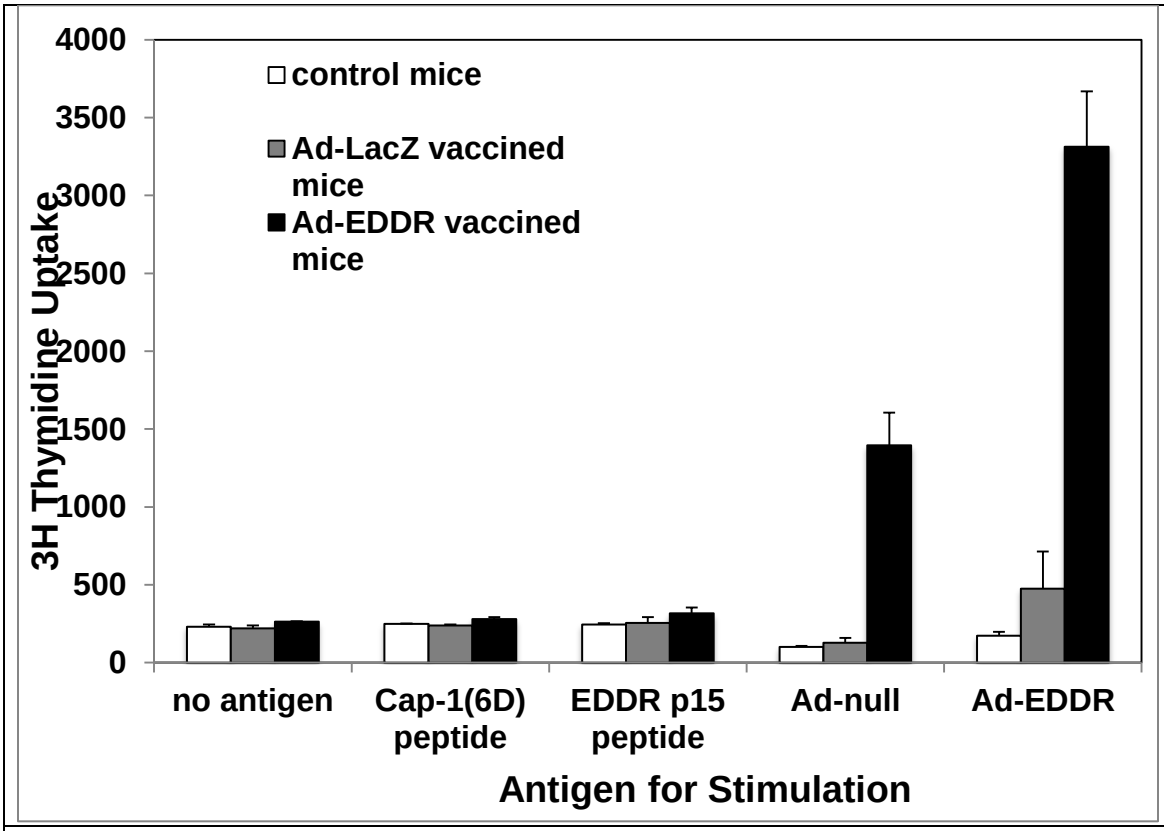

Figure 8A. Proliferation assay for splenocytes from mice immunized against Ad-EDDR versus mice immunized with Ad-LacZ. The splenocytes from mice immunized with Ad-EDDR or Ad-LacZ as control were stimulated with Ad-EDDR or Ad-null (as control) or the EDDR-derived peptide p15 (and the CEA peptide CAP1 as control). Proliferation of the splenocytes was measured by Thymidine uptake.

In order to assess the immunogenicity of the Ad-TACE vaccine, a similar experiment was performed. Specifically, HLA-A2 transgenic mice were vaccinated with Ad-TACE, Ad-LacZ (2.6 x 10E10 vp/injection) or saline on days 0 and 14. Mice were euthanized on day 21, and splenocytes were harvested. These splenocytes (TACE splenocytes and LacZ splenocytes) (1 M cells/well) were utilized for proliferation assay in 96 well plates. TACE p13 peptide (final concentration; 1 µg/mL) and Ad-TACE (moi 1000) were used as stimulating antigens, and Cap-1(6D) peptide and Ad-null were used as negative controls. Three (3) days later, 3H-thymidine (1 µci/well) was added, and 18 h later, thymidine uptake was measured. As demonstrated in figure 8B, there was greater proliferation of splenocytes (T cells) from mice immunized against EDDR1 (EDDR1-splenocytes) when exposed to Ad- EDDR1 than when exposed to the Ad-null vector suggesting that there was induction of EDDR1-specific activity beyond the expected Ad-specific activity. The EDDR1-splenocytes T cells did not proliferate against the TACE p13 peptide, suggesting different epitope(s) than this one HLA A2 peptide were responsible for the anti-TACE response.

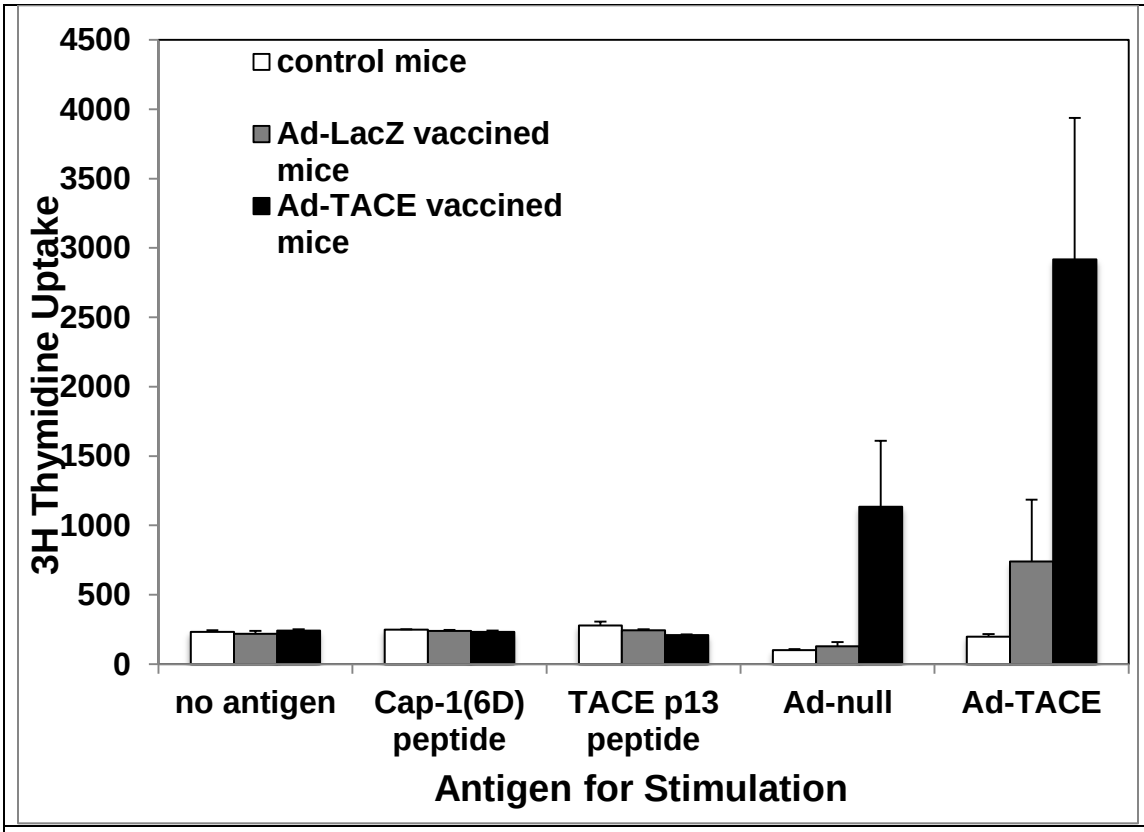

Figure 8B. Proliferation assay for splenocytes from mice immunized against Ad-TACE versus mice immunized with Ad-LacZ. The splenocytes from mice immunized with Ad-TACE or Ad-LacZ as control were stimulated with Ad-TACE or Ad-null (as control) or the TACE-derived peptide p13 (and the CEA peptide CAP1 as control). Proliferation of the splenocytes was measured by Thymidine uptake.

We also confirmed that the T cells stimulated against TACE could secrete cytokine in response to their target antigen. The splenocytes stimulated by Ad-TACE were evaluated in an ELISPOT assay for interferon-gamma production.

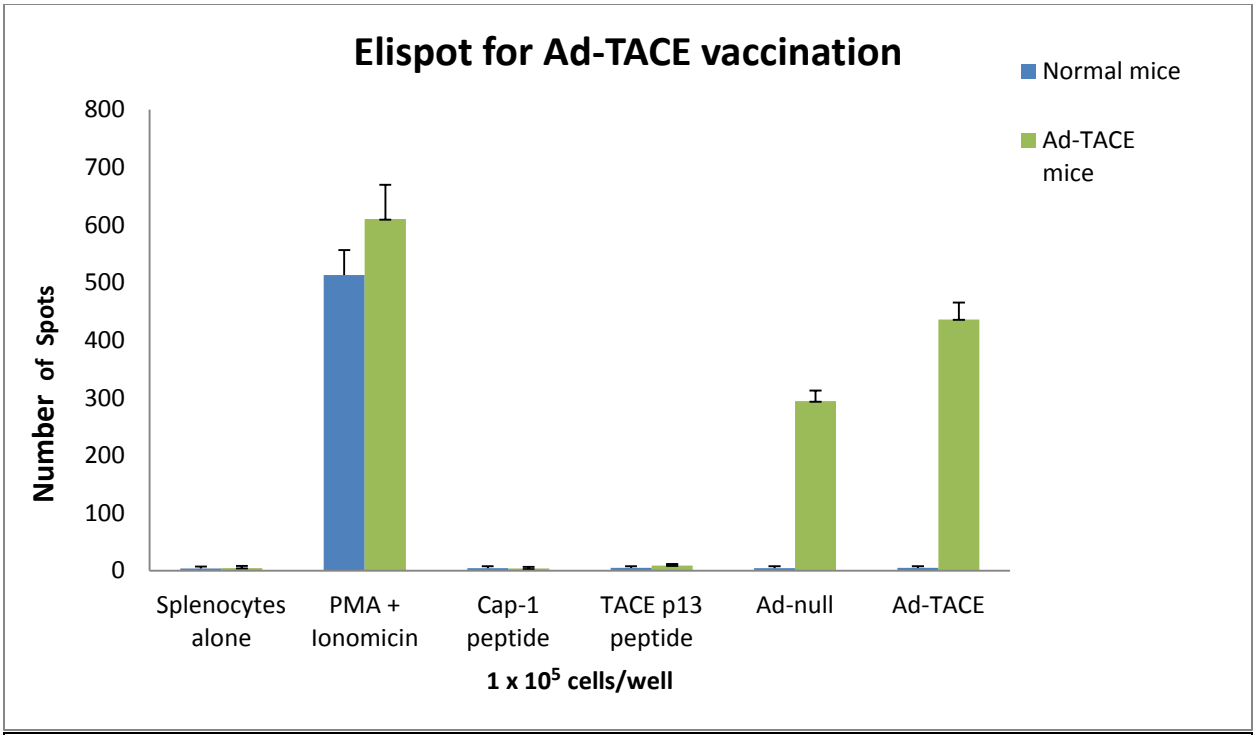

Figure 8C. ELISPOT assay for splenocytes from mice immunized against Ad-TACE versus mice immunized with Ad-LacZ. The splenocytes from mice immunized with Ad-TACE were stimulated with Ad-TACE or Ad-null (as control) or the TACE-derived peptide p13 (and the CEA peptide CAP1 as control). Interferon-secreting T cell frequency (number of spots) was determined. The splenocytes from mice immunized against Ad-TACE had a higher frequency of T cells specific for the AD-TACE than Ad-null suggesting a TACE specific immune response.

Finally, because antibody-dependent cellular cytotoxicity is a potential method of activity of the vaccines, we determined whether antibodies specific for EDDR1 or TACE were induced by the vaccinations as well. COS1 cells were infected with Ad-TACE, Ad-EDDR or irrelevant Ad vectors (moi 5000) overnight, and used as target cells. Cells were labeled with mouse serum from Ad-TACE or Ad-EDDR-vaccinated HLA-A2 transgenic mice. Control serum was obtained from unvaccinated HLA-A2 transgenic mice. Cells were labeled with mouse serum (1:50 and 1:100 dilution) and incubated for 1 hour, washed twice, and then stained with PE-conjugated goat anti-mouse IgG for 30 min. Figures 9A (1:100 dilution of serum from mice immunized against TACE) and B (1:100 dilution of serum from mice immunized against EDDR1) demonstrate that the Ad-TACE and Ad-EDDR induced antibodies capable of binding to the TACE and EDDR1-expressing targets.

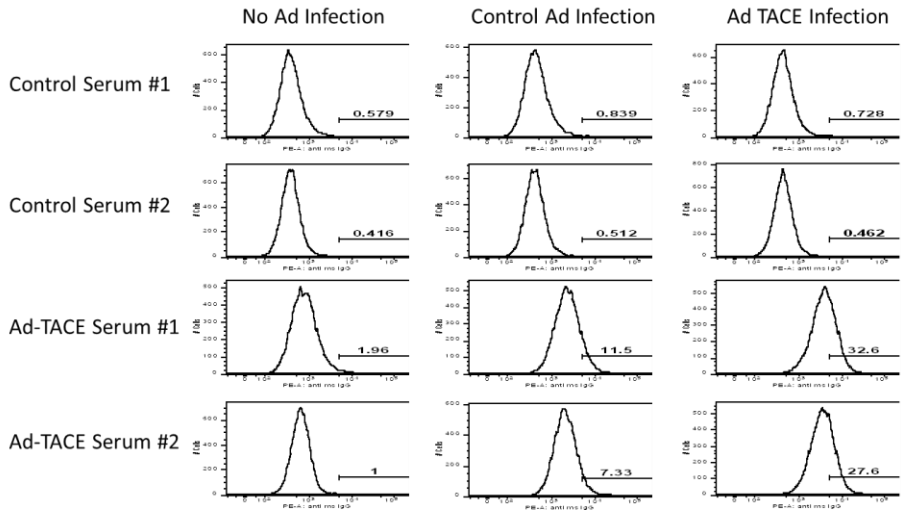

Figure 9A. Flow cytometric analysis of serum for antibody binding to TACE expressing cells.
Serum (1:100 dilution) from mice immunized with Ad-TACE was mixed with COS1 cells infected with Ad-TACE or a control Ad vector. There is a greater percentage of COS1/TACE cells binding antibody than COS1/Ad cells suggesting the presence of anti-TACE Abs.

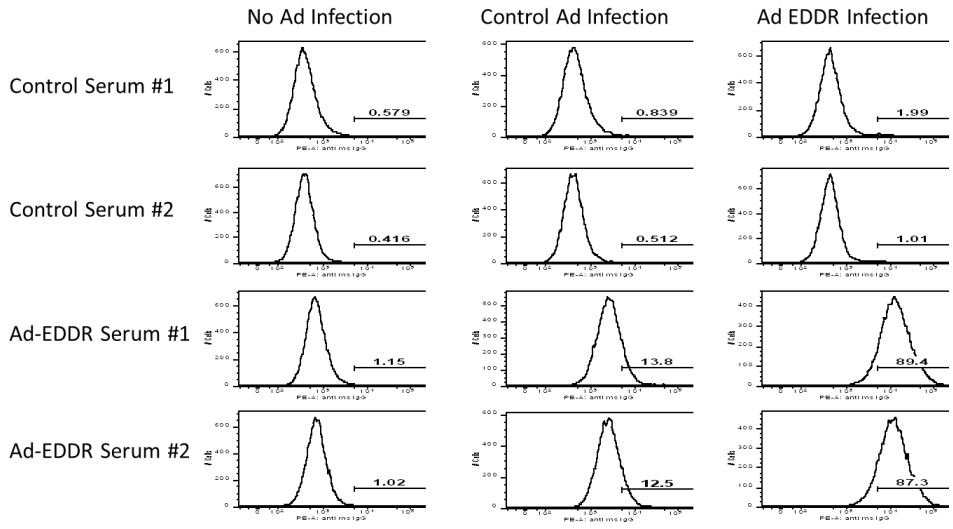

Figure 9B. Flow cytometric analysis of serum for antibody binding to EDDR1 expressing cells.
Serum (1:100 dilution) from mice immunized with Ad-TACE was mixed with COS1 cells infected with Ad-EDDR or a control Ad vector. There is a greater percentage of COS1/EDDR cells binding antibody than COS1/Ad cells suggesting the presence of anti-EDDR Abs.

Based on the above experiments, we determined that the Ad-EDDR1 and Ad-TACE vaccines induced immune responses and therefore elected to proceed to the in vivo experiments.

Ad-TACE Vaccine/Cell Transfer Experiment

We purchased and then expanded HLA-A2 transgenic mice (30) and SCID-beige mice (30). We also used the Ad-TACE: (1.07 x 10E12 vp/mL) and Ad-LacZ: (1.02 x 10E12 vp/mL) previously generated. We obtained cisplatin from the pharmacy. The procedure was as follows: HLA-A2 transgenic mice were immunized with the Ad-TACE (n=15) or Ad-LacZ (n=15) on days 0 and 14. On day 14, SKOV3-A2 cells (2 M cells/mouse) were intraperitoneally injected into female SCID-beige mice. On day 21, the HLA-A2 transgenic mice were euthanized and splenocytes were collected, pooled (i.e., Ad-TACE stimulated splenocytes were pooled and Ad-lacZ splenocytes were separately pooled), and cryopreserved. On day 22, the SCID-beige mice bearing tumor were separated into the following 6 groups (5 mice/group):

Group A) control (no splenocyte injection / no cisplatin)
Group B) Ad-LacZ splenocyte injection (20M cells, weekly), no cisplatin
Group C) Ad-TACE splenocyte injection (20M cells, weekly), no cisplatin
Group D) no splenocyte injection, cisplatin (2 mg/kg ip weekly)
Group E) Ad-LacZ splenocyte injection (20M cells, weekly), cisplatin (2 mg/kg ip weekly)
Group F) Ad-TACE splenocyte injection (20M cells, weekly), cisplatin (2 mg/kg ip weekly)

On days 29, 36, 43: Repeat injections of splenocytes and /or cisplatin were administered. Abdominal swelling of mice was monitored twice a week. When mice seemed to have abdominal pain, loss of appetite, weight loss (>15%), they were euthanized. Otherwise, on day 57, mice were sacrificed, and the tumor tissue was collected. The readouts from the experiment were pictures of the abdominal cavity, weight of tumor tissues in each mouse, and the volume of ascites if measurable.

The first observation was that the mice receiving splenocytes lost weight suggesting that there could have been an inflammatory effect. The second observation is that the adoptive transfer of T cells was associated with considerable tumor control. Figure 10 demonstrates the abdominal cavity of selected mice from each group. We observed marked tumor involvement in group A, which was slightly diminished in group D (cisplatin alone); however in the groups treated with the splenocytes, there was markedly less tumor. We could not visually determine a difference between the lacZ and TACE-splenocytes nor an additive effect with cisplatin.

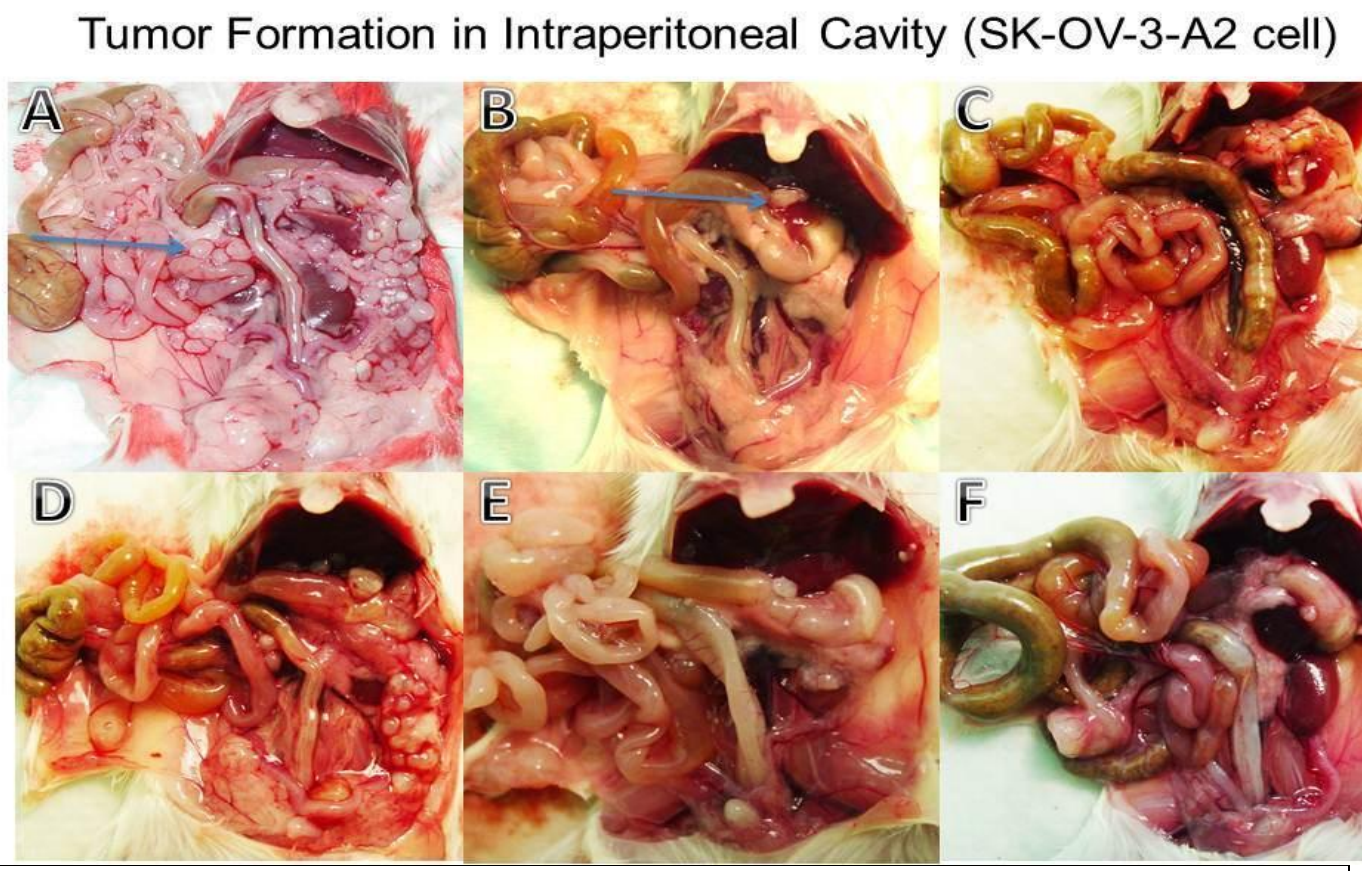

Figure 10. Abdominal cavity at time of completion of experiment from selected mice implanted (IP) with SKOV-A2 and treated as described for in each group:
Group A) control (no splenocyte injection / no cisplatin)
Group B) Ad-LacZ splenocyte injection (20M cells, weekly), no cisplatin
Group C) Ad-TACE splenocyte injection (20M cells, weekly), no cisplatin
Group D) no splenocyte injection, cisplatin (2 mg/kg ip weekly)
Group E) Ad-LacZ splenocyte injection (20M cells, weekly), cisplatin (2 mg/kg ip weekly)
Group F) Ad-TACE splenocyte injection (20M cells, weekly), cisplatin (2 mg/kg ip weekly)

We then counted the number of nodules in the abdominal cavity. As demonstrated in figure 11A, there was a marked reduction in the number of nodules for the T cell tread groups. There was also a statistically significant decrease in the number of nodules in the TACE-splenocytes compared with lac-Z splenocytes.

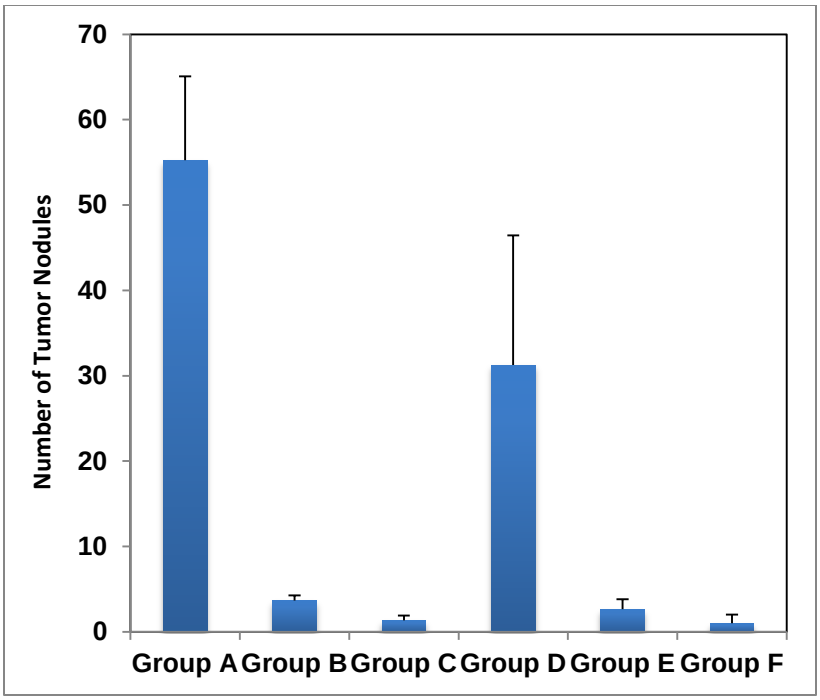

Figure 11A. Number of tumor nodules in peritoneal cavity of SCID-beige mice bearing SKOV3-A2 cells following adoptive transfer of TACE-specific splenocytes with and without cisplatin. Groups are as in Figure 10.

We also weighed the resected tumors (figure 11B)

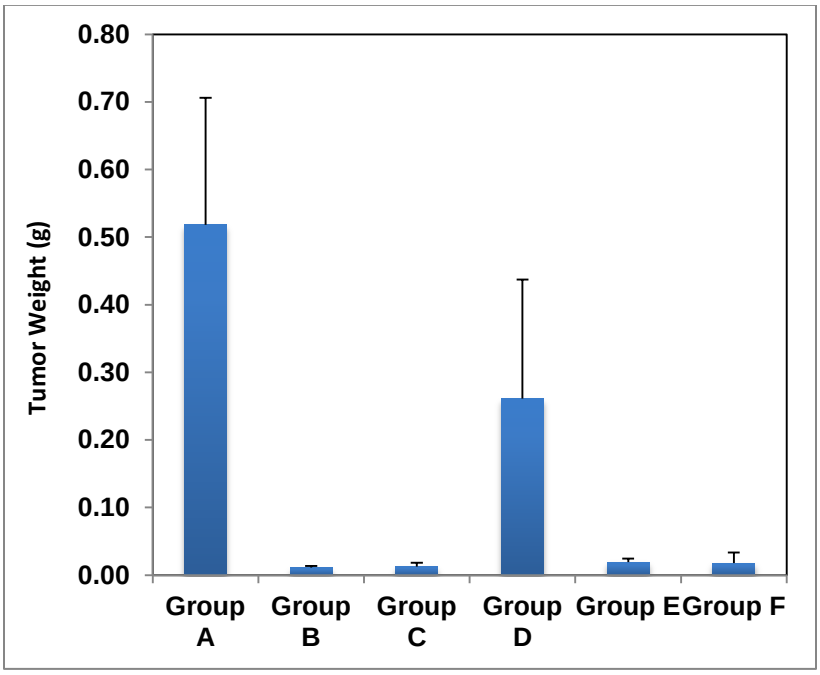

Figure 11B. Tumor weight from tumors in peritoneal cavity of SCID-beige mice bearing SKOV3-A2 cells following adoptive transfer of TACE-specific splenocytes with and without cisplatin. Groups are as described in figure 10.

These data demonstrate that the splenocytes have anti-tumor activity, but that the level of non-specific activity overwhelms our ability to accurately measure synergy with cisplatin.

Why all aims were not accomplished within the timeframe of the award:
At this point, the funding period for the second no cost extension concluded, limiting further studies. We had planned the following:

a. repeat the above experiments with lower doses of T cells for adoptive transfer in order that non-specific immune responses do not overwhelm measurement of the antigen-specific-immune response.
b. study the effect of EDDR1-specific splenocytes (combined with cisplatin).
c. study the effect of the TACE- and EDDR1-specific splenocytes when combined with dasatinib treatment. It is our intention to seek other funding to complete these experiments.

KEY RESEARCH ACCOMPLISHMENTS: Bulleted list of key research accomplishments emanating from this research.

- Identification of a panel of tumor antigens processed and presented by ovarian cancers
- Demonstration that identified tumor antigens could induce T cell responses against ovarian cancers
- Preliminary demonstration of synergy of ovarian tumor antigen-specific T cells and cisplatin in a cisplatin-resistant cell line.
- Demonstration that EDDR1 and TACE are tumor antigens in ovarian cancer.
- Demonstration that Ad-EDDR1 and Ad-TACE vaccines could induce T cell responses (identified by proliferation and ELISPOT assays)
- Demonstration that TACE-specific splenocytes (induced by vaccinating mice with Ad-TACE), adoptively transferred to SKOV-A2-bearing mice, had anti-cancer activity (reduced tumor growth).

REPORTABLE OUTCOMES: Provide a list of reportable outcomes that have resulted from this research to include:

Manuscripts

The following manuscripts were generated as a result of research on this project:

Sinnathamby G, Zerfass J, Hafner J, Block P, Nickens Z, Hobeika A, Secord AA, Lyerly HK, Morse MA, Philip R. ADAM metallopeptidase domain 17 (ADAM17) is naturally processed through major histocompatibility complex (MHC) class I molecules and is a potential immunotherapeutic target in breast, ovarian and prostate cancers. Clin Exp Immunol. 2011 Mar;163(3):324-32.

Sinnathamby G, Zerfass J, Hafner J, Block P, Nickens Z, Hobeika A, Secord AA, Lyerly HK, Morse MA, Philip R. EDDR1 is a Potential Immunotherapeutic Antigen in Ovarian, Breast, and Prostate Cancer. J. Clin Cell Immunol 2011, 2:1

Shetty V, Nickens Z, Testa J, Hafner J, Sinnathamby G, Philip R. Quantitative immunoproteomics analysis reveals novel MHC class I presented peptides in cisplatin resistant ovarian cancer cells. J Proteomics. 2012 Jun 18;75(11):3270-90.

Development of cell lines, tissue or serum repositories

We have collected and archived blood and ascites/tissue from 24 patients with ovarian cancer. Thus far 6 have been deemed platinum refractory and others will likely be identified as such in the future.

Development of new reagents

We generated the viral vectors Ad-TACE and Ad-EDDR1. These vectors have the potential, with further study, to support the translation of this project into human clinical trials. Specifically, if further study consistently demonstrates that they induce immune responses with anticancer activity, then GMP grade

vectors based on those used in our current experiments would be generated for clinical use. Indeed, we have generated clinical grade adenoviral vectors against other antigens (e.g., HER2) which are entering clinical trials currently.

CONCLUSION:

The purpose of this research was to identify antigens from platinum-resistant ovarian cancer that could serve as targets for immune therapies for women with this difficult to treat subset of ovarian cancers. We succeeded in identifying a panel of antigens expressed from platinum resistant ovarian cancer and were able to select a subset from which at least one peptide epitope could induce T cell responses that synergized with cisplatin. However, it was difficult to generate reproducibly, large numbers of T cells in vitro. This is likely due to the low precursor frequency of such T cells in humans. We found a solution to this challenge in the development of adenoviral vectors encoding two model antigens, EDDR1 and TACE/ADAM-17. These vectors have preliminarily demonstrated immunogenicity and anti-tumor activity in murine models. If further development (using future funding sources) supports the preliminary data, we envision clinical trials using these vaccines along with cisplatin or targeted therapies in the treatment of patients with ovarian cancer.

REFERENCES:

Sinnathamby G, Zerfass J, Hafner J, Block P, Nickens Z, Hobeika A, Secord AA, Lyerly HK, Morse MA, Philip R. ADAM metallopeptidase domain 17 (ADAM17) is naturally processed through major histocompatibility complex (MHC) class I molecules and is a potential immunotherapeutic target in breast, ovarian and prostate cancers. Clin Exp Immunol. 2011 Mar;163(3):324-32.

Sinnathamby G, Zerfass J, Hafner J, Block P, Nickens Z, Hobeika A, Secord AA, Lyerly HK, Morse MA, Philip R. EDDR1 is a Potential Immunotherapeutic Antigen in Ovarian, Breast, and Prostate Cancer. J. Clin Cell Immunol 2011, 2:1

Shetty V, Nickens Z, Testa J, Hafner J, Sinnathamby G, Philip R. Quantitative immunoproteomics analysis reveals novel MHC class I presented peptides in cisplatin resistant ovarian cancer cells. J Proteomics. 2012 Jun 18;75(11):3270-90.

Personnel with Salary Support from this grant

Michael A. Morse, MD, Principal Investigator,
Angeles A. Secord, Investigator
Hongtau Guo, MD, PhD Investigator
Gangjun Lei, PhD, Technician
Delila Serra, M.S., Technician
Amanda Bradshaw Summers, B.S., Research Analyst
Tim Clay, PhD, Investigator
Takuya Osada, MD, PhD, Investigator
Lisa Grace, BS, Research Technician II
Debra Davis, BS, Research Technician II

APPENDICES: Attached are the manuscripts referenced above.

Editorial Manager(tm) for OMICS PUBLISHING GROUP/Clinical
Manuscript Draft

Manuscript Number: CLINICALGROUP-10-121R2

Title: EDDR1 is a potential immunotherapeutic antigen in ovarian, breast, and prostate cancer

Short Title: Ovarian, breast and prostate cancer immunotherapy

Article Type: Research Article

Section/Category: Journal of Clinical & Cellular Immunology

Keywords: EDDR1; epitope; immunotherapy; CTL; immunohistochemistry; flow cytometry; qRT-PCR.

Corresponding Author: Ramila Philip

Corresponding Author's Institution:

First Author: Ramila Philip

Order of Authors: Ramila Philip

Manuscript Region of Origin: USA

Abstract: Selection of suitable antigens, preferably targets for cell mediated and humoral immune response is a critical step in the development of cancer vaccines. Cell surface proteins that are over-expressed in cancer cells thus constitute a very attractive class of antigens that can be targeted for effective cancer immunotherapy. Toward this goal, we characterized the relevance of Epithelial Discoidin Domain Receptor 1 (EDDR1) for such targeted therapeutics. EDDR1, a membrane expressed protein associated with adhesion, has recently emerged as a new therapeutic target in several tumor types. In the present study, we analyzed the expression profile of EDDR1 in a variety of normal and cancer cells of human origin by flow cytometry as well as immunohistochemistry. EDDR1 was found to be abundantly expressed on the surface of ovarian, prostate and breast cancer cells but not on the normal counterparts, making it a suitable candidate for antibody mediated therapy. Furthermore, a Human Leukocyte Antigen (HLA) A2-restricted epitope derived from EDDR1 was efficiently presented by various cancer cells to EDDR1 epitope-specific T cells. Collectively, our data present evidence that EDDR1 could be a potential target antigen for immunotherapy.

Suggested Reviewers: Pooja Jain
Drexel University
Pooja.Jain@drexelmed.edu
editor

Opposed Reviewers: Martin Kast
mkast@usc.edu
conflict of interest

Response to Reviewers: To
Editor
Journal of Clinical and Cellular Immunology

We are pleased to submit the revised version of our research article, "EDDR1 is a potential immunotherapeutic antigen in ovarian, breast, and prostate cancer" for publication in Journal of Clinical and Cellular Immunology. We thank the reviewers for their thoughtful and constructive comments. We have responded to the reviewers concerns as follows, which we believe strengthen the report:

Reviewer Comments to the Authors:
The authors were advised to clarify this point by including data showing no or weak expression of EDDR1 in normal tissues. In the revised manuscript Sinnathamby et al., described the IHC analysis of normal tissues. Unfortunately, the data concerning most of the normal tissues are not shown ("data not shown"). It would be more convincing to include this data in the manuscript or to provide supplementary data.

Response: As suggested by the reviewer, we have included a supplemental figure (Figure S1) to show no or weak expression of EDDR1 in various normal tissues and replaced the "data not shown" to Figure S1 in the manuscript.

Thank you again for your review of this manuscript and for the opportunity to respond to the reviewer's comments.

Sincerely,

Ramila Philip
Ph: 215 489 4955
rphilip@immunotope.com

EDDR1 is a potential immunotherapeutic antigen in ovarian, breast, and prostate cancer

Gomathinayagam Sinnathamby[1], Jennifer Zerfass[1], Julie Hafner[1], Peter Block[1], Zacharie Nickens[1], Amy Hobeika[2], Angeles Alvarez Secord[2], H. Kim Lyerly[2], Michael A. Morse[2] and Ramila Philip[1,*]

[1]Immunotope, Inc., 3805 Old Easton Road, Room 211, Doylestown, PA 18902

[2]Duke Comprehensive Cancer Center, Duke University, 25130, Morris Building, Durham NC 27710

*Address for correspondence:

Ramila Philip, PhD., Immunotope, Inc., The Pennsylvania Biotechnology Center

3805, Old Easton Road, Doylestown, PA 18902

Phone: (215)-489-4955

Fax: (215)-489-4920

Email: RPhilip@immunotope.com

Abstract

Selection of suitable antigens, preferably targets for cell mediated and humoral immune response is a critical step in the development of cancer vaccines. Cell surface proteins that are over-expressed in cancer cells thus constitute a very attractive class of antigens that can be targeted for effective cancer immunotherapy. Toward this goal, we characterized the relevance of Epithelial Discoidin Domain Receptor 1 (EDDR1) for such targeted therapeutics. EDDR1, a membrane expressed protein associated with adhesion, has recently emerged as a new therapeutic target in several tumor types. In the present study, we analyzed the expression profile of EDDR1 in a variety of normal and cancer cells of human origin by flow cytometry as well as immunohistochemistry. EDDR1 was found to be abundantly expressed on the surface of ovarian, prostate and breast cancer cells but not on the normal counterparts, making it a suitable candidate for antibody mediated therapy. Furthermore, a Human Leukocyte Antigen (HLA) A2-restricted epitope derived from EDDR1 was efficiently presented by various cancer cells to EDDR1 epitope-specific T cells. Collectively, our data present evidence that EDDR1 could be a potential target antigen for immunotherapy.

Key words

EDDR1, epitope, antigen, immunotherapy, MHC, CTL, immunohistochemistry, flow cytometry, qRT-PCR

Abbreviations

EDDR1	- Epithelial Discoidin Domain Receptor 1
MHC	-Major Histocompatibility Complex
HLA	-Human Leukocyte Antigen
CTL	-Cytotoxic T Lymphocytes
qRT-PCR	-Quantitative Reverse Transcribed Polymerase Chain Reaction
PBMC	- Peripheral blood mononuclear cells
GM-CSF	- Granulocyte Macrophage Colony Stimulating Factor
KLH	- Keyhole Limpet Hemocyanin
ELISpot	-Enzyme Linked ImmunoSpot
HRP	-Horse Radish Peroxidase
DAB	- 3,3´-diaminodbenzidine
EOC	-Epithelial Ovarian Cancer
CNS	-Central Nervous System
PCA-1	-Prostate Cancer Antigen-1

Introduction

Cancer vaccines, activating the immune system against specific antigens, have demonstrated clinical benefit and an increasing number are now in development; however, one ongoing challenge is to identify the most appropriate antigenic targets. Although tumor antigens were originally identified by cloning T cells that exhibited anti-tumor activity and then identifying the antigen to which the clones responded through genetic approaches, we have utilized a novel approach which exploits the differential expression of peptides displayed within the Major Histocompatibility Complex (MHC) [1] in tumors compared to normal cells (reviewed in [2]). We hypothesized that these MHC-presented peptides, relatively restricted to tumor cells, could be used to activate anti-tumor T cells. In addition, when we used this approach to search for ovarian cancer antigens [3], we observed that many of these peptide epitopes were derived from proteins with critical functions in tumor growth, survival and metastasis [4], suggesting that this method identifies proteins that may be indispensible to the tumor and might not be readily downregulated during attempted immune escape.

One peptide identified by our search for differentially MHC-expressed epitopes is derived from Epithelial Discoidin Domain Receptor 1 (EDDR1 or DDR1) protein [3, 5, 6]. Discoidin Domain Receptor 1 and -2, a subfamily of tyrosine kinase receptors, regulate cell adhesion, proliferation and extracellular matrix remodeling (reviewed in [7]). In this study, in order to utilize EDDR1 as part of a cancer vaccine, we characterized the T cell epitope for anti-tumor CTL activity and the range of protein

expression across several malignancies and demonstrate that it can act as a tumor associated antigen for immunotherapeutic applications.

Materials and methods

Cell lines and primary cells from human tissues

Human ovarian cancer cell lines SKOV3-A2 and OVCAR3, human breast cancer cell lines MDA-MB-231 and MCF7, and human prostate cancer cell line LNCaP were originally obtained from ATCC, Manassas, VA). SKOV3-A2, OVCAR3 and LNCaP were maintained in RPMI 1640 medium (Mediatech, Manassas, VA) supplemented with 10% fetal bovine serum (Atlanta Biologicals, Norcross, GA), L-glutamine (300mg/ml), non-essential amino acids (1× concentration), penicillin and streptomycin (1× concentration, supplements were purchased from Mediatech). MDA-MB-231 and MCF7 were maintained in DMEM medium supplemented with 10% fetal bovine serum and other supplements listed above. All cell lines were maintained at 37^0C in a humidified incubator with 5% CO_2. Kidney and liver tissues from HLA-$A2^+$ human donors were obtained from National Disease Research Interchange, Philadelphia, PA. Tissues were enzymatically digested and cell suspensions were generated as per standard methods [3, 5, 6]. Briefly, tissue samples were minced and digested with 2mg/ml collagenase, 0.1mg/ml hyaluronidase and 0.15mg/ml DNAse in DMEM supplemented with 2 × concentration of antibiotics and antimycotics (all reagents were obtained from Sigma-Aldrich, St Louis, MO) at 37^0C for 3 to 6 hours. Cell suspensions were pelleted and washed several times with PBS and DMEM supplemented with 10% FBS. Cell viability was assessed by trypan blue exclusion and cells were frozen in 90% FBS and 10% DMSO (Sigma-Aldrich) for future use.

Synthetic peptides

Synthetic peptides corresponding to the HLA-A2 presented EDDR1 epitope (p15-FLAEDALNTV) and an influenza A virus epitope derived from the matrix protein (GILGVFTL) were supplied by GenScript Corporation (Piscataway, NJ).

In vitro generation of peptide specific CTLs

Heparinized blood from healthy HLA-$A2^+$ donors was purchased from Research Blood Components, LLC (Brighton, MA). Blood samples from women with ovarian cancer undergoing surgery at Duke University Medical Center were obtained under IRB approved protocols. Peripheral blood mononuclear cells (PBMC), collected by density gradient separation over lymphocyte separation medium (Mediatech), were plated at 20×10^6 cells per well in 2 mL RPMI 1640 medium supplemented with 10% fetal bovine serum, L-glutamine (300 mg/mL), non-essential amino acids, sodium pyruvate, penicillin and streptomycin (complete medium) in 6-well tissue culture plates (BD, Franklin Lakes, NJ) overnight. Non-adherent cells were removed and saved. Plastic adherent cells were pulsed with 50 μg/mL synthetic peptide and 1.5 μg/mL human β2-microglobulin (Sigma-Aldrich) in complete medium for 2 hours. Non-adherent cells were added back in 5 mL complete medium supplemented with IL-7 at 5 ng/mL, Keyhole Limpet Hemocyanin (KLH, Sigma-Aldrich) at 5 μg/mL, Granulocyte Macrophage Colony Stimulating Factor (GM-CSF) at 25 ng/mL and IL-4 at 50 ng/mL (all cytokines and growth factors were purchased from Peprotech, Rocky Hill, NJ). Plates were incubated at 37ºC in a humidified incubator with 5% CO_2 for 12 days. Medium (2.0 mL) was removed from each well and fresh complete medium supplemented with 10 U/mL IL-2 for 2 days. T

cells were restimulated with CD4/CD8 T cell depleted autologous monocytes pulsed with synthetic peptide at 10 μg/mL and 1.5 μg/mL human β2-microglobulin in complete medium containing 5 ng/mL IL-7 and 5 μg/mL KLH for 5 days. IL-2 treatment and *in vitro* restimulation were repeated thrice at the indicated time intervals prior to use of *in vitro* expanded T cells in Enzyme Linked ImmunoSpot (ELISpot) assays.

ELISpot assays

In vitro expanded T cells were used as effectors in ELISpot assays to assess antigen stimulated interferon-γ (IFN-γ) or Granzyme B release using human IFN-γ and Granzyme B assay kits (BD-Pharmingen, San Jose, CA) (BD-Pharmingen, San Jose, CA) according to the manufacturer's instructions. Typically, a fixed number of various target cells (5×10^3 cells per well) and effector cells (2×10^5 per well), at effector to target ratios of 40:1, were used in ELISpot assays. T2 cells were pulsed with 20 μg/mL synthetic peptides and 1.5 μg/mL human β2-microglobulin in RPMI 1640 medium supplemented with 1% FBS and other additives (as above) overnight for use as targets in ELISpot assays. For antibody blocking experiments, target cells were pretreated with purified W6/32 or BB7.2 antibodies (from BD-Pharmingen) at 1:50 dilution for 1hr prior to addition to T cell cultures. ELISpot assays were performed in replicate wells. Spots were quantitated using an Immunospot reader (Cellular Technologies Limited, Shaker Heights, OH). Results are presented as the number of IFN-γ-producing cells per 1×10^6 effector cells. Error bars represent SEM of experimental replicates.

Flow cytometry

Primary cells from human liver and kidney and cancer cell lines were treated with a blocking solution (1% normal mouse serum from Sigma and 2% BSA from Sigma in PBS) on ice for 1 hr. Cells were then washed once with PBS and treated with either FITC-labeled isotype matched control antibody (Invitrogen, Carlsbad, CA) or anti-human EDDR1-specific mouse monoclonal antibody (Santa Cruz Biotechnology, Santa Cruz, CA) at 1:100 dilution in PBS containing 2% BSA for 1 hr on ice. Cells were washed three times with PBS and subjected to flow cytometry by Guava flow cytometer (Millipore). Samples were analyzed using GuavaSoft software (Millipore).

Immunohistochemistry

Paraffin coated tissue arrays comprising cancer and matched control tissue sections were purchased from Imgenex, San Diego, CA. All chemical reagents used in this protocol are purchased from Sigma unless noted otherwise. Tissue arrays were stained with anti-EDDR1 antibody and HRP-conjugated secondary reagent according to manufacturer's established procedure (www.imgenex.com). Briefly, tissue arrays were first de-paraffinized by incubating in a dry oven at 62^0C for 1h. Subsequently slides were dewaxed using xylene and hydrated using ethanol and washed in tap water. Antigen retrieval was achieved by treating slides in citrate buffer (0.01M, pH 6.0) and microwaving as suggested by the protocol. Endogenous peroxidase was quenched by treating slides with 3% hydrogen peroxide solution for 6 minutes. Slides were then blocked with blocking serum (normal mouse serum from Sigma at 1:50) for 30 minutes and treated with anti-EDDR1 antibody (1:100) for 2h at room temperature. Slides were

washed with PBS and incubated with biotinylated anti-mouse secondary antibody for 30 minutes at room temperature. Subsequently, slides were washed and incubated with Avidin-conjugated HRP (1:100) for 30 minutes at room temperature. Slides were washed with PBS and developed using DAB solution for 2 minutes. Reaction was stopped using tap water. Slides were finally counter-stained using Meyer's hematoxylin for 10 seconds and dehydrated in ethanol. Slides were then cleared using xylene and cover slides were mounted with Permount (Vectastain staining reagents were purchased from Vector Labs, Burlingame, CA). Slides were viewed under a fluorescence microscope equipped with a digital camera and micrographs were captured (Nikon Eclipse, TE 800-U).

Realtime qRT-PCR

Realtime-qRT-PCR analysis to determine the expression level of EDDR1 was carried out by SABiosciences, Frederick, MD. RNA isolated from normal liver and kidney tissues (obtained from NDRI, Philadelphia, PA) or cancer cell lines (SKOV3-A2, MDA-MB231 and LNCaP) were used for the analysis. GAPDH was used as internal control. Following first strand synthesis, Realtime RT-PCR was carried out using reagents generated by SABiosciences. Data analysis was carried out employing $\Delta\Delta C_t$ method. Results are presented as fold difference of EDDR1 mRNA expressed in cancer cell lines over the control cells obtained from a normal liver tissue.

Results

Ovarian, breast and prostate cancer cell lines endogenously express EDDR1 epitope, p15:

HLA A2-restricted peptide epitope derived from EDDR1 (called p15 (FLAEDALNTV)) was identified in a MHC class I associated epitope screen from ovarian cancer cells [3, 5, 6]. Here we studied whether T cells generated against p15 could recognize targets of various tumor histologies. We generated T cells specific for p15 from healthy HLA-A2+ donors in vitro. These p15 specific T cells were used as effectors and various cancer cell lines (ovarian, breast and prostate cancer cell lines) were used as targets in an overnight ELISpot assay to quantify IFNγ release. We first demonstrated that the CTLs were p15-specific since they could recognize T2 cells pulsed with p15 peptide. Next, we observed, as expected, that p15 specific T cells recognized ovarian cancer cells (SKOV3-A2 and OVCAR3) from which p15 peptide was originally identified [3]. In addition, two HLA-A2+ breast cancer cell lines (MDA-MB231 and MCF7) were also recognized by p15 specific T cells. Interestingly, HLA-A2+ prostate cancer cell line LNCaP were also recognized by p15 specific T cells albeit at a lower level. Other cancer cell lines we tested in culture including colon cancer cell lines did not activate p15 specific T cells (data not shown). Importantly, non-cancerous liver cells and lung and kidney cells (data not shown) were not recognized by p15-specific T cells, suggesting that p15 is not endogenously presented by normal cells. However, when pulsed with the synthetic p15 peptide, these cells readily activated T cells, thus demonstrating that these cells were capable of presenting exogenously provided peptide antigen. Thus, these results

demonstrated that EDDR1 derived p15 epitope was presented by ovarian, breast and prostate cancer cells but not cells derived from normal healthy tissue and was not necessarily universally expressed across other cancer cell lines.

HLA-A2 restricted nature of EDDR1 epitope p15 presentation to specific T cells

In order to demonstrate the HLA restricted nature of p15 presentation to specific T cells, we included antibodies specific for pan HLA-A, B, C (W6/32) or HLA-A2 (BB7.2) in the ELISpot assays. Our results indicate that the presentation of p15 from various cancer cell lines was indeed HLA-A2 restricted as evident from the effective inhibition of IFNγ release by BB7.2 antibody (Figure 2, top panel). As expected, W6/32 also blocked T cell activation. T2 cells or normal liver cells from an HLA-A2+ donor pulsed with an irrelevant peptide (influenza A matrix protein derived peptide) did not activate p15 specific T cells appreciably. When pulsed with the synthetic p15 peptide, these cells readily activated p15 specific T cells. Thus, our results demonstrated that the presentation of p15 to T cells is highly specific and HLA-A2 restricted.

EDDR1 epitope p15 specific T cells are cytolytic

In order to determine whether p15 activated T cells are cytolytic, we measured the release of Granzyme B in an ELISpot assay using various target cells. Results presented in Figure 2 (bottom panel) demonstrate that a significant portion of p15 activated T cells indeed secreted Granzyme B in response to p15 presentation by peptide loaded cells and cancer targets. This secretion could be blocked significantly by W6/32 or BB7.2

antibodies, demonstrating that the cytolytic activity was also dependent on HLA-A2 restricted peptide presentation.

EDDR1 derived epitope p15-specific T cells can be generated from ovarian cancer patients

Although T cells from healthy individuals, who may not have developed tolerance against p15, could be generated against p15, we wished to determine if T cells could be activated from PBMC of HLA-A2+ ovarian cancer patients using p15 synthetic peptide. We performed IFNγ ELISpot assay using T cells stimulated in vitro with p15 peptide and various targets. Our results shown in Figure 3 demonstrated that p15 specific T cells activated from three ovarian cancer patients recognized peptide pulsed T2 cells as well as ovarian (SKOV3-A2 and OVCAR3) and breast cancer (MDA-MB-231) cell lines (Figure 3). Thus, these results demonstrated that p15 specific T cells can be generated from ovarian cancer patients.

Expression of EDDR1 on the surface of a variety of cancer cells

In order to evaluate the expression levels of EDDR1 on the surface of normal and cancer cells, we performed flow cytometry employing an antibody that recognizes the ectodomain of EDDR1 protein. EDDR1 expression levels were high on the surface of ovarian (SKOV3-A2 and OVCAR3), breast (MDA-MB-231 and MCF7) and prostate (LNCaP) cancer cell lines (Figure 4). Notably, SKOV3-A2 and LNCaP expressed very high levels of EDDR1 although the CTL activity (described above) was greater against SKOV3-A2 than LNCaP. In contrast, primary cells prepared from healthy human liver

(Figure 4) and lung (data not shown) tissue did not express detectable levels of EDDR1 and primary cells from healthy human, kidney tissue expressed very low levels of EDDR1 on their surface. These results demonstrated that EDDR1 was highly expressed on the surface of a variety of cancer cells (ovary, breast and prostate – Figure 4; colon and lung – data not shown) but not on normal cells. Furthermore, the amount of protein expressed by flow cytometry did not necessarily correlate with CTL activity which was dependent on MHC-peptide expression.

Immunohistochemical analysis of EDDR1 expression in normal and cancer tissues

In order to confirm the EDDR1 expression levels in tissues form cancer patients, we performed immunohistochemical analysis on tissue sections from ovarian, breast and prostate cancers and tissue matched normal controls. EDDR1 was found to be expressed at very high levels in cancer tissues but its expression was low in normal tissues (Figure 5). In addition, we have tested a variety of normal tissue types (duodenum mucosa, spleen, pancreas, liver, lymph node, uterus myometrium) for EDDR1 expression (Fig S1) and found low expression profiles similar to normal ovary, breast and prostate. These results suggested that EDDR1 was not only over-expressed in cancer cell lines but also cancer tissues isolated from patients.

EDDR1 mRNA expression does not correlate with EDDR1 protein expression

In order to determine if there is a correlation between increased expression of EDDR1 protein and its transcript, we performed Realtime-qRT-PCR analysis, a powerful tool to determine the transcript levels of a given gene. We isolated RNA from normal liver and

kidney cells to use as controls. Our analysis, shown in Figure 6, demonstrated that the EDDR1 mRNA level was elevated in SKOV3-A2 and LNCaP cells compared to normal liver and kidney cells. However, the levels were slightly reduced in MDA-MB231. These data supported the notion that elevated EDDR1 expression in cancer cells was regulated at the translational/post-translational but not at transcriptional level.

Discussion

Human cancers express antigenic targets of T cells and antibodies [8-11]; however, which antigens contain the epitopes leading to the most effective T cell rejection targets is largely unknown. Starting with the MHC class I-associated peptide repertoire of ovarian cancer cells, we identified a number of differentially expressed peptides including EDDR1 [3]. In our current work, we were able to generate EDDR1-epitope specific CTL from the PBMC of healthy individuals and cancer patients suggesting the presence of EDDR1-specific precursor T cells. Furthermore, flow cytometry and immunohistochemistry analyses demonstrated that this protein is abundantly expressed on the surface of several types of cancer cells including ovarian, prostate and breast cancer cells but not on their normal counterparts (Figs 5), making it a suitable candidate for immunotherapy applications.

Our observations on EDDR protein expression mirror those of others, For example EDDR1 protein has been shown to be restricted to epithelial cells, and is significantly over-expressed in several human tumors [12] including breast, ovarian [13], hepatocellular carcinoma [14] esophageal, and high grade pediatric brain tumor [15]. The DDR1 gene is highly over expressed in all histological subtypes of epithelial ovarian cancer (EOC) compared with normal ovarian surface epithelium, identifying EDDR1 as a new biomarker of EOC [13]. DDR1 is also expressed in ovarian epithelial inclusion cysts, a site of metaplastic changes within the normal ovary, in borderline tumors and in low-grade and stage cancers suggesting the up-regulation of EDDR1, is an early event in

the development of EOC and have potential application in the early detection of disease [13]. In addition, EDDR1 has been shown to be consistently expressed in all high-grade Central Nervous System (CNS) neoplasms and by primitive cells of the embryonic ventricular zone suggests that EDDR1 is a potentially useful marker of tumor cells within the CNS [15]. Shimada et al [16] by immunohistochemical analysis of prostate carcinomas demonstrated that prostate cancer antigen 1 (PCA-1) and EDDR1 were strongly expressed in prostate cancer cells, including preneoplastic lesions with little or no expression in normal epithelium. Moreover, the expression of PCA-1 and EDDR-1 was associated with a hormone-independent state of prostate cancer suggesting PCA-1-EDDR1 signaling is a new important axis involved in malignant potential of prostate cancer associated with hormone-refractory status [16]. Furthermore, over expression of EDDR1 has been shown to increase the migration and invasion of hepatocellular carcinoma cells in association with matrix metalloproteinase [14]. Our work extends upon these other observations in that we have demonstrated not only protein expression, but also peptide epitope expression of EDDR1 in ovarian and breast cancer. Since EDDR1 is a membrane protein but is also processed and presented as peptide epitopes to T cells by MHC class I, this antigen qualifies for both cancer vaccine and antibody therapeutic applications.

One important observation is that the level of protein expression did not necessarily correlate with T cell recognition of tumors. This is not surprising since it has been observed that although protein over expression is a pre requisite for antibody or drug mediated targeting, it is not a critical factor for MHC class I processing and

presentation of the T cell epitope which primarily correlates with the level of degradation of proteins associated with misfolding, cryptic translation and other causes of high turnover [1, 2, 17]. Our approach to antigen identification differs from the more common approach which is to perform a gene expression analysis. However, gene expression may not reflect the protein level or stability and modifications of the protein [18, 19].

In summary, the characterization of EDDR1 as an immunotherapy target as well as a target for small molecule inhibitors may open up the possibility of combined approaches utilizing novel small molecules and cancer vaccines. Ongoing studies are evaluating the immunologic efficacy of EDDR1 in human cancer vaccines. Indeed the T cell epitope derived from EDDR1 has been evaluated for safety and CTL responses in patients with breast and ovarian cancers in a phase I clinical study (Morse, Secord and Philip, Clinical Cancer Research, manuscript in press).

Acknowledgements

The authors wish to acknowledge Ms. Debra Davis and Ms. Delila Serra from Duke University for ovarian cancer patient sample collection and processing.

Figure legends

Figure 1. Characterization of T cells specific for the EDDR1 derived HLA-A2 restricted p15 epitope from healthy donors: PBMC from two healthy HLA-$A2^+$ donors were *in vitro* stimulated with synthetic peptides corresponding to the EDDR1 derived HLA-A2 restricted p15 epitope (FLAEDALNTV). These cells were tested in an overnight ELISpot assay using T2 cells loaded with the p15 synthetic peptide, normal liver cell suspensions obtained from a HLA-$A2^+$ healthy donor tissue (with or without exogenously provided p15 peptide) and HLA-$A2^+$ cancer cells lines [ovarian cancer cell lines SKOV3-A2 and OVCAR3, breast cancer cell lines MDA-MB231 and MCF7 and a prostate cancer cell line LNCaP]. Interferon-γ producing cells were quantitated using Immunospot reader. Error bars represent SEM of experimental replicates.

Figure 2. HLA-A2 restricted T cell response and cytolytic potential of T cells specific for the EDDR1 derived p15 epitope: PBMC from a healthy HLA-$A2^+$ donor were *in vitro* stimulated with the synthetic peptide corresponding to the EDDR1 derived p15 epitope. (A) These cells were tested in an ELISpot assay using T2 cells or normal kidney cells (Normal) obtained from an HLA-$A2^+$ healthy donor tissue loaded with an irrelevant synthetic peptide (flu) or p15 peptide. HLA-$A2^+$ cancer cells lines [ovarian cancer cell line SKOV3-A2 and breast cancer cell line MDA-MB231] were pretreated with W6/32 or BB7.2 antibody prior to incubation with p15 specific T cells overnight. Interferon-γ producing cells were quantitated using Immunospot reader. (B) p15 specific T cells were

used in an ELISpot assay with the above mentioned targets and the release of Granzyme B was measured as described above. Error bars represent SEM of experimental replicates.

Figure 3. T cells specific for the EDDR1 derived HLA-A2 restricted p15 epitope can be generated from ovarian cancer patients: PBMC from three HLA-$A2^+$ ovarian cancer patients were *in vitro* stimulated with the p15 synthetic peptide. These cells were tested in an ELISpot assay using T2 cells loaded with the synthetic peptide, normal kidney cell suspensions obtained from a HLA-$A2^+$ healthy donor tissue (with or without exogenously provided p15 peptide) and HLA-$A2^+$ cancer cells lines [breast cancer cell line MDA-MB231 and ovarian cancer cell lines Ovcar3 and SKOV3-A2]. Interferon-γ producing cells were quantitated using Immunospot reader. Error bars represent SEM of experimental replicates.

Figure 4. Analysis of surface expression of EDDR1 in normal and cancer cells: Normal liver and kidney cell suspensions obtained from healthy HLA-A2+ donors or cancer cell lines [ovarian cancer cell lines SKOV3-A2 and Ovcar3, breast cancer cell lines MDA-MB231 and MCF7 and a prostate cancer cell line LNCaP] were treated with either FITC-labeled isotype matched control antibody or FITC-labeled EDDR1 specific antibody and subjected to flow cytometry by Guava flow cytometer. Samples were analyzed using GuavaSoft software.

Figure 5. Immunohistochemical analysis of expression of EDDR1 in normal and cancer tissues: Tissue arrays comprising of matched normal or cancer specimens (breast,

ovarian and prostate tissues) and a panel of normal tissues (Figure S1: duodenum mucosa, spleen, pancreas, liver, lymph node and uterus myometrium) were stained with a EDDR1 specific monoclonal antibody followed by treatment with an HRP-conjugated secondary antibody reagent. Slides were developed with DAB substrate and tissues were counterstained with Meyer's hematoxylin. Stained tissue sections were analyzed using a fluorescent microscope and micrographs were captured at 200× magnification.

Figure 6. Expression level of EDDR1 in normal and cancer cells by Realtime-qRT-PCR analysis: Realtime-qRT-PCR analysis was carried out using RNA isolated from normal tissues (liver and kidney) or cancer cell lines (ovarian cancer cell line SKOV3-A2, breast cancer cell line MDA-MB231 and prostate cancer cell line LNCaP) to determine the transcript levels of EDDR1. GAPDH was used as internal control. Data analysis was carried out employing $\Delta\Delta C_t$ method. Results are presented as fold difference of EDDR1 expression in cancer cell lines over the control cells obtained from a normal liver tissue.

Figures:

Figure 1

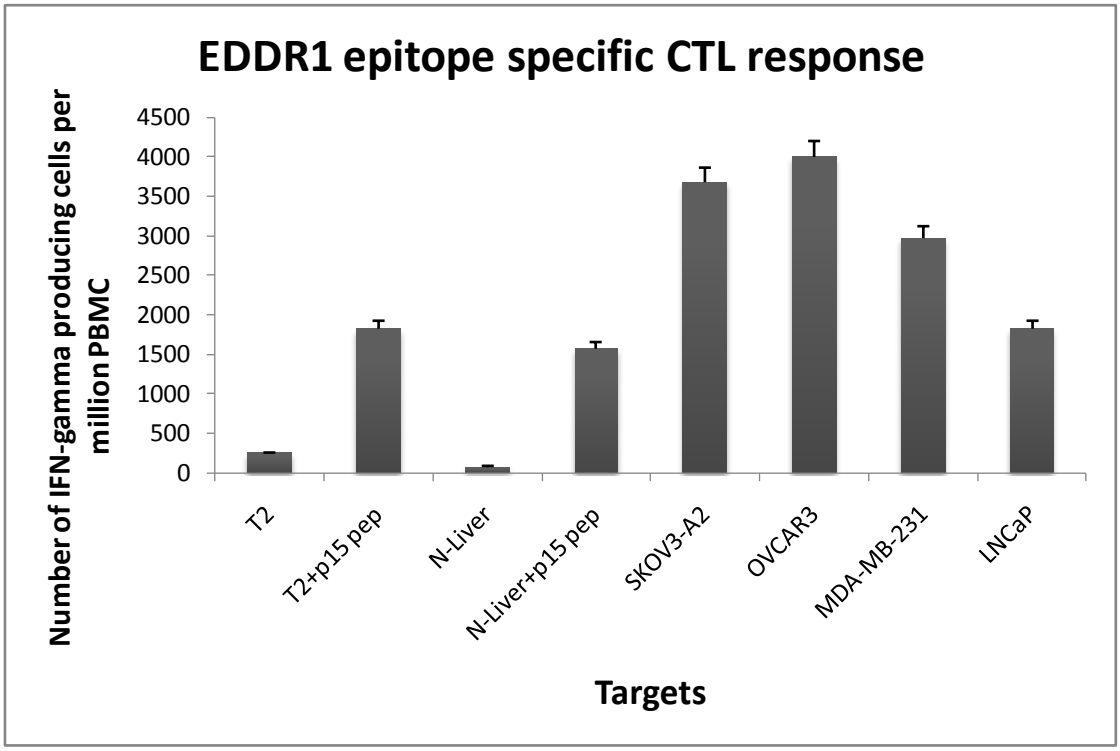

Figure 2

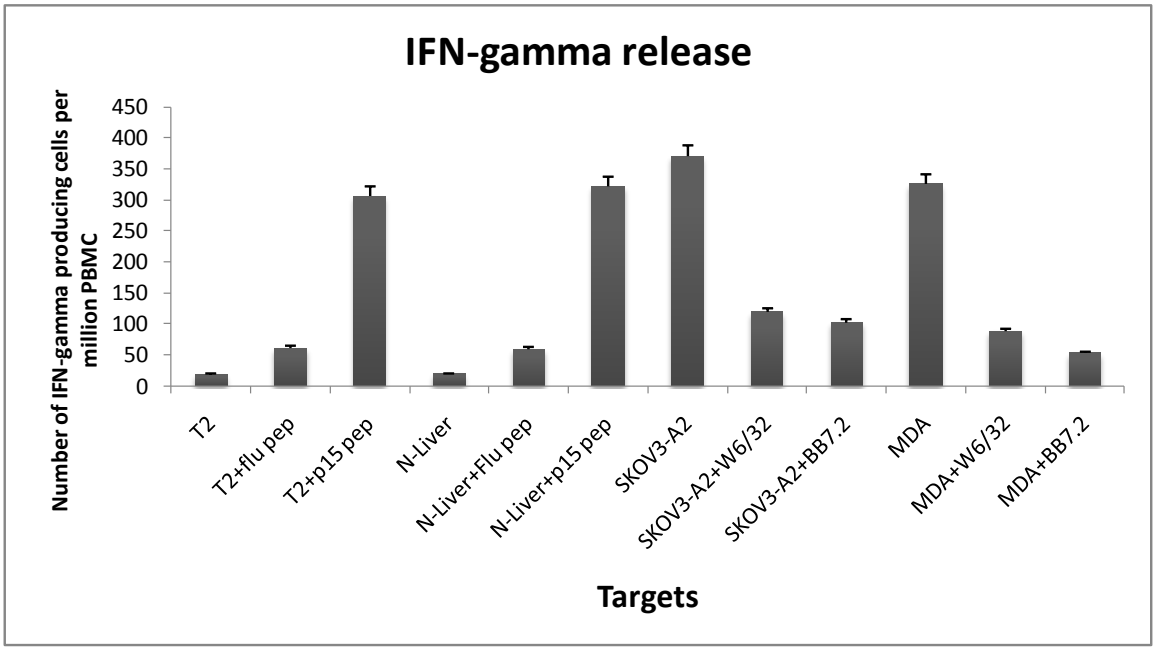
IFN-gamma release
Number of IFN-gamma producing cells per million PBMC
450
400
350
300
250
200
150
100
50
0
T2
T2+flu pep
T2+p15 pep
N-Liver
N-Liver+Flu pep
N-Liver+p15 pep
SKOV3-A2
SKOV3-A2+W6/32
SKOV3-A2+BB7.2
MDA
MDA+W6/32
MDA+BB7.2
Targets

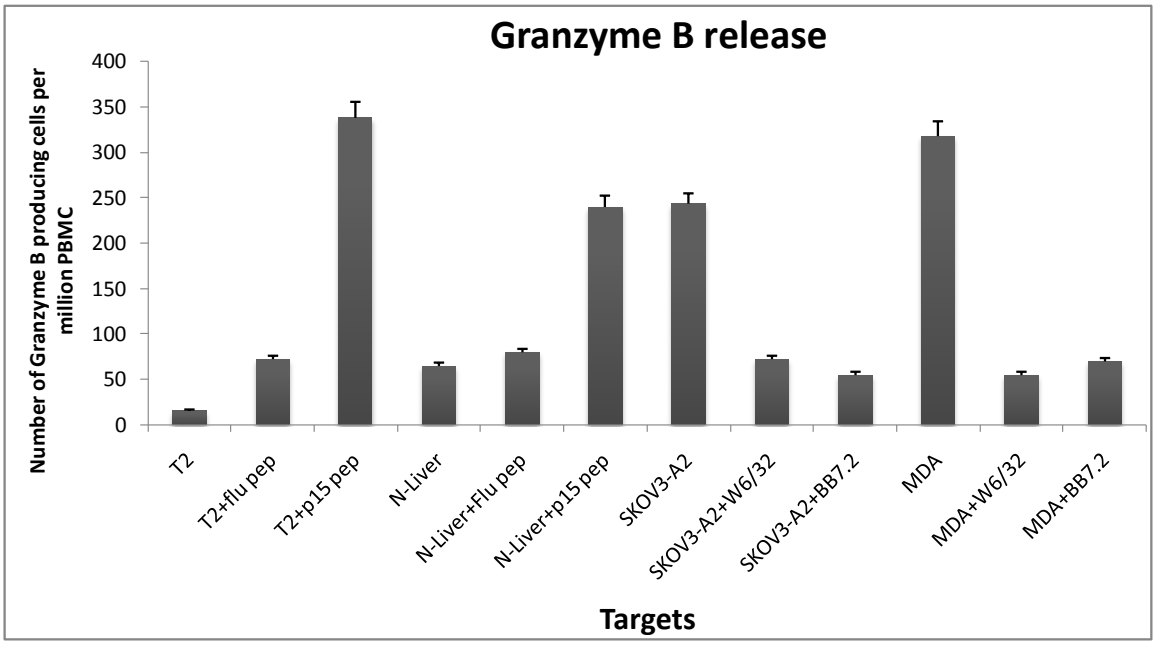
Granzyme B release
Number of Granzyme B producing cells per million PBMC
400
350
300
250
200
150
100
50
0
T2
T2+flu pep
T2+p15 pep
N-Liver
N-Liver+Flu pep
N-Liver+p15 pep
SKOV3-A2
SKOV3-A2+W6/32
SKOV3-A2+BB7.2
MDA
MDA+W6/32
MDA+BB7.2
Targets

Figure 3

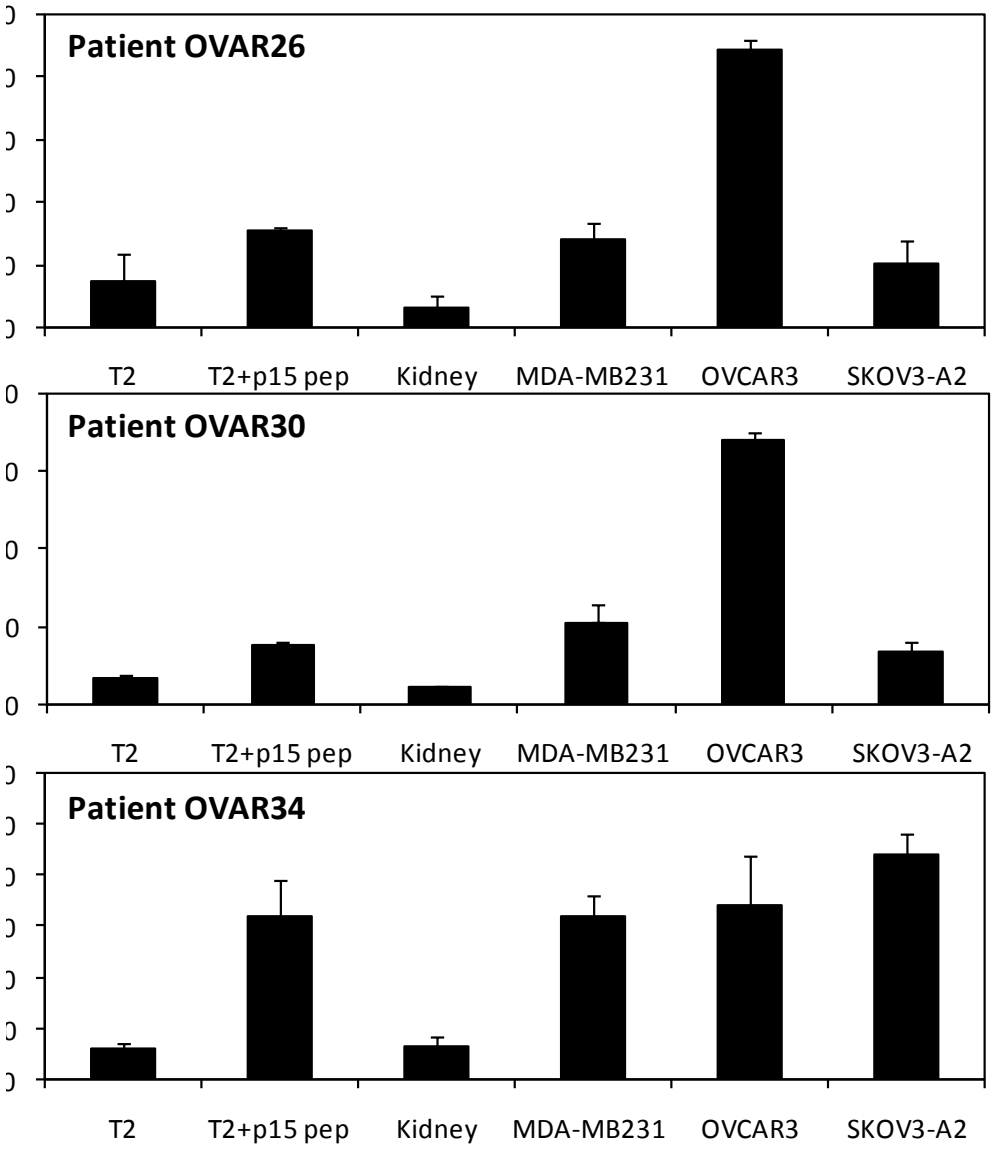
Patient OVAR26
T2
T2+p15 pep
Kidney
MDA-MB231
OVCAR3
SKOV3-A2
Patient OVAR30
T2
T2+p15 pep
Kidney
MDA-MB231
OVCAR3
SKOV3-A2
Patient OVAR34
T2
T2+p15 pep
Kidney
MDA-MB231
OVCAR3
SKOV3-A2

Figure 4

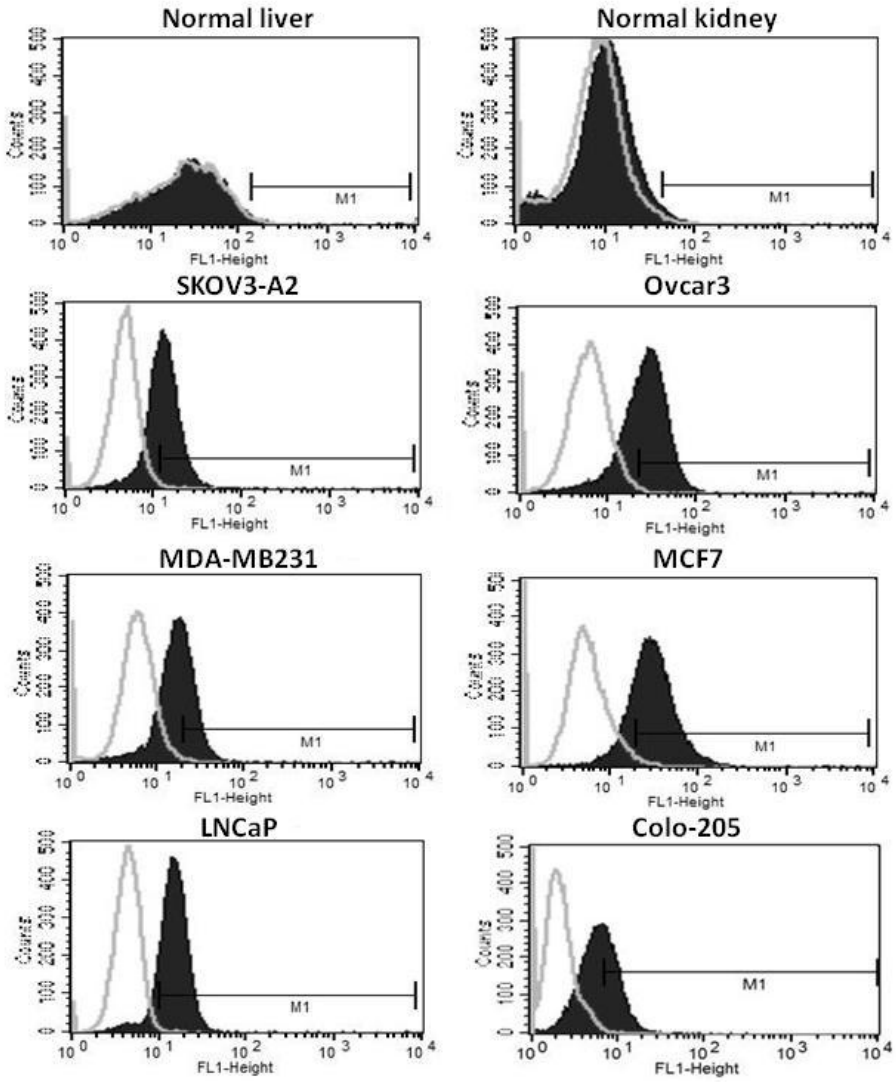
Normal liver
Normal kidney
SKOV3-A2
Ovcar3
MDA-MB231
MCF7
LNCaP
Colo-205
Counts
FL1-Height
M1

Figure 4

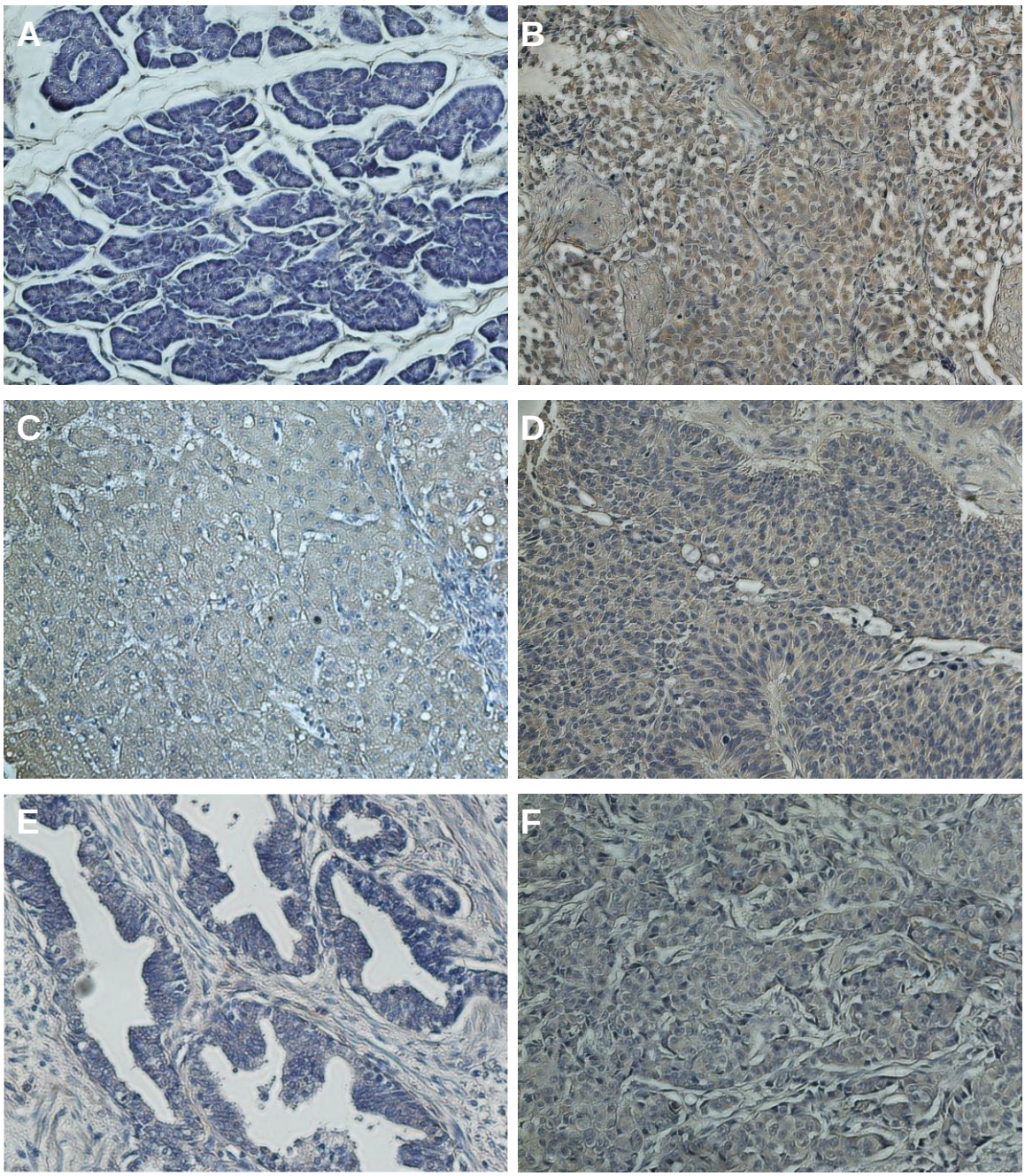

Figure 5: EDDR1 expression (200X magnification)
(**A** and **B**) Breast Normal and Cancer, (**C** and **D**) Ovarian Normal and Cancer, (**E** and **F**) Prostate Normal and Cancer.

Figure 6

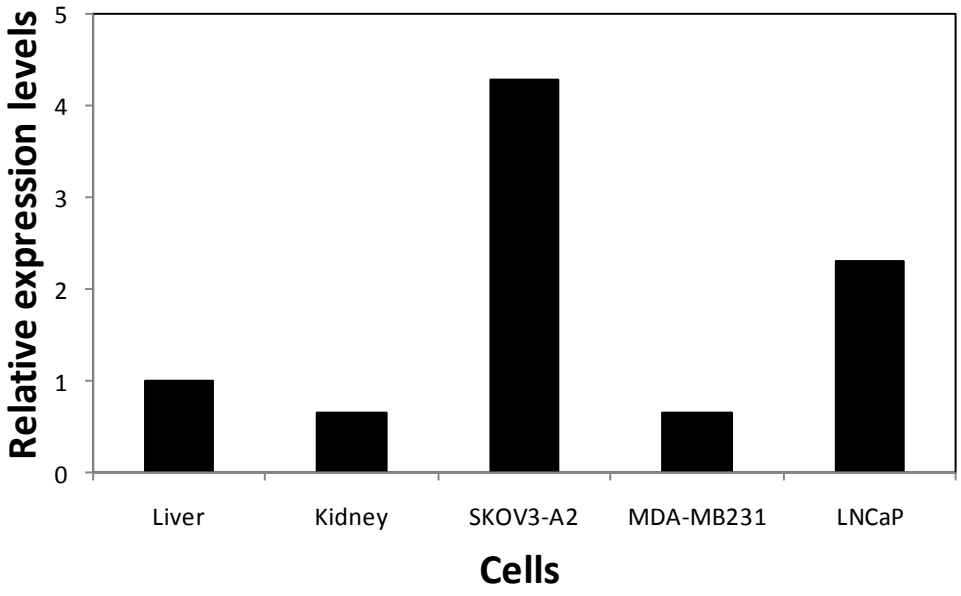
Relative expression levels
5
4
3
2
1
0
Liver
Kidney
SKOV3-A2
MDA-MB231
LNCaP
Cells

Figure S1

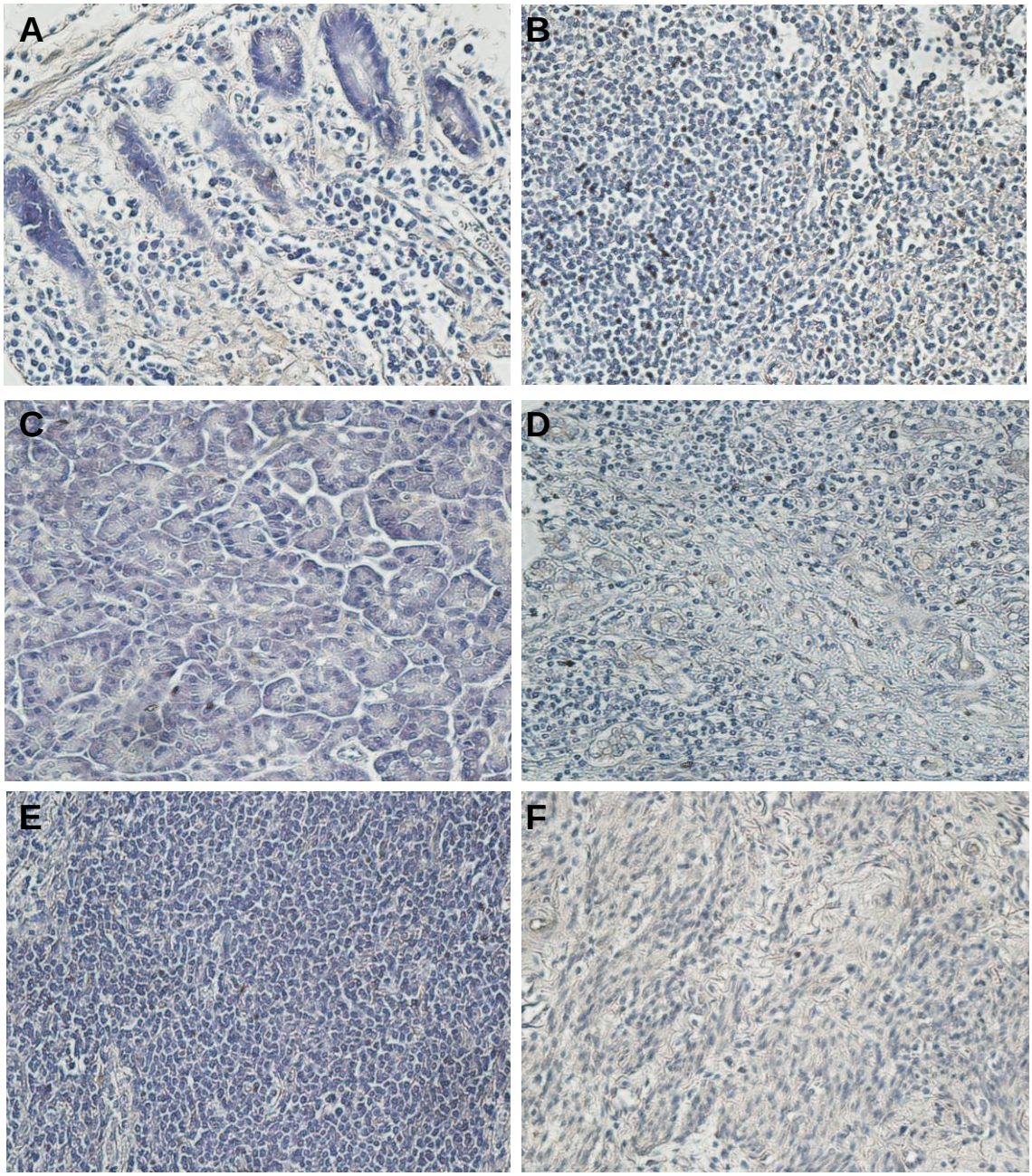

Figure S1
EDDR1(200X magnification)
Normal Samples (A) Duodenum mucosa, (B) Spleen, (C) Pancreas, (D) Liver, (E) Lymph node, and (F) Uterus myometrium

References:

1. Shastri N, Schwab S, Serwold T (2002) Producing nature's gene-chips: the generation of peptides for display by MHC class I molecules. Annu Rev Immunol 20:463-93.
2. Admon A, Barnea E, Ziv T (2003) Tumor antigens and proteomics from the point of view of the major histocompatibility complex peptides. Mol Cell Proteomics 2:388-98.
3. Ramakrishna V, Ross MM, Petersson M, Gatlin CC, Lyons CE, Miller CL, Myers HE, McDaniel M, Karns LR, Kiessling R, Parmiani G, Flyer DC (2003) Naturally occurring peptides associated with HLA-A2 in ovarian cancer cell lines identified by mass spectrometry are targets of HLA-A2-restricted cytotoxic T cells. Int Immunol 15:751-63.
4. Hanahan D, Weinberg RA (2000) The hallmarks of cancer. Cell 100:57-70.
5. Sinnathamby G, Lauer P, Zerfass J, Hanson B, Karabudak A, Krakover J, Secord AA, Clay TM, Morse MA, Dubensky TW, Jr., Brockstedt DG, Philip R, Giedlin M (2009) Priming and activation of human ovarian and breast cancer-specific CD8+ T cells by polyvalent Listeria monocytogenes-based vaccines. J Immunother 32:856-69.
6. Karkada M, Weir, G.M., Quinton,T., Sammatur, L., MacDonald, L.D., Grant, A., Liwski, R., Juskevicius, R., Sinnathamby, G., Philip, R., Mansour, M (2009) A Novel Breast/Ovarian Cancer Peptide Vaccine Platform that Promotes Specific Type-1 but not Treg/Tr1-Type Responses J Immunotherapy 33: 250-61.

7. Vogel WF, Abdulhussein R, Ford CE (2006) Sensing extracellular matrix: an update on discoidin domain receptor function. Cell Signal 18:1108-16.

8. Gilboa E (2004) The promise of cancer vaccines. Nat Rev Cancer 4:401-11.

9. van der Bruggen P, Traversari C, Chomez P, Lurquin C, De Plaen E, Van den Eynde B, Knuth A, Boon T (1991) A gene encoding an antigen recognized by cytolytic T lymphocytes on a human melanoma. Science 254:1643-7.

10. Goldman B (2002) Cancer vaccines: finding the best way to train the immune system. J Natl Cancer Inst 94:1523-6.

11. Lewis JD, Reilly BD, Bright RK (2003) Tumor-associated antigens: from discovery to immunity. Int Rev Immunol 22:81-112.

12. Shelling AN, Butler R, Jones T, Laval S, Boyle JM, Ganesan TS (1995) Localization of an epithelial-specific receptor kinase (EDDR1) to chromosome 6q16. Genomics 25:584-7.

13. Heinzelmann-Schwarz VA, Gardiner-Garden M, Henshall SM, Scurry J, Scolyer RA, Davies MJ, Heinzelmann M, Kalish LH, Bali A, Kench JG, Edwards LS, Vanden Bergh PM, Hacker NF, Sutherland RL, O'Brien PM (2004) Overexpression of the cell adhesion molecules DDR1, Claudin 3, and Ep-CAM in metaplastic ovarian epithelium and ovarian cancer. Clin Cancer Res 10:4427-36.

14. Heo SH, Lee SJ, Ryoo HM, Park JY, Cho JY (2007) Identification of putative serum glycoprotein biomarkers for human lung adenocarcinoma by multilectin affinity chromatography and LC-MS/MS. Proteomics 7:4292-302.

15. Pachuk CJ, Ciccarelli RB, Samuel M, Bayer ME, Troutman RD, Zurawski DV, Schauer JI, Higgins TJ, Weiner DB, Sosnoski DM, Zurawski VR, Satishchandran

C (2000) Characterization of a new class of DNA delivery complexes formed by the local anesthetic bupivacaine. Biochim Biophys Acta 1468:20-30.

16. Shimada K, Nakamura M, Ishida E, Higuchi T, Yamamoto H, Tsujikawa K, Konishi N (2008) Prostate cancer antigen-1 contributes to cell survival and invasion though discoidin receptor 1 in human prostate cancer. Cancer Sci 99:39-45.

17. Vierboom MP, Zwaveling S, Bos GMJ, Ooms M, Krietemeijer GM, Melief CJ, Offringa R (2000) High steady-state levels of p53 are not a prerequisite for tumor eradication by wild-type p53-specific cytotoxic T lymphocytes. Cancer Res 60:5508-13.

18. Martelange V, De Smet C, De Plaen E, Lurquin C, Boon T (2000) Identification on a human sarcoma of two new genes with tumor-specific expression. Cancer Res 60:3848-55.

19. Schultze JL, Vonderheide RH (2001) From cancer genomics to cancer immunotherapy: toward second-generation tumor antigens. Trends Immunol 22:516-23.

Clinical & Experimental Immunology
The Journal of Translational Immunology

Clinical and Experimental Immunology ORIGINAL ARTICLE doi:10.1111/j.1365-2249.2010.04298.x

ADAM metallopeptidase domain 17 (ADAM17) is naturally processed through major histocompatibility complex (MHC) class I molecules and is a potential immunotherapeutic target in breast, ovarian and prostate cancers

G. Sinnathamby,* J. Zerfass,* J. Hafner,* P. Block,* Z. Nickens,* A. Hobeika,† A. A. Secord,† H. K. Lyerly,† M. A. Morse† and R. Philip*

**Immunotope, Inc., The Pennsylvania Biotechnology Center, Doylestown, PA, and †Duke Comprehensive Cancer Center, Duke University, Durham, NC, USA*

Accepted for publication 27 October 2010
Correspondence: R. Philip, Immunotope, Inc., The Pennsylvania Biotechnology Center, 3805 Old Easton Road, Doylestown, PA 18902, USA.
E-mail: rphilip@immunotope.com

Summary

Selection of suitable antigens is critical for the development of cancer vaccines. Most desirable are over-expressed cell surface proteins that may serve as targets for both antibodies and T cells, thus maximizing a concerted immune response. Towards this goal, we characterized the relevance of tumour necrosis factor-α-converting enzyme (ADAM17) for such targeted therapeutics. ADAM17 is one of the several metalloproteinases that play a key role in epidermal growth factor receptor (EGFR) signalling and has recently emerged as a new therapeutic target in several tumour types. In the present study, we analysed the expression profile of ADAM17 in a variety of normal and cancer cells of human origin and found that this protein is over-expressed on the surface of several types of cancer cells compared to the normal counterparts. Furthermore, we analysed the presentation of a human leucocyte antigen (HLA)-A2-restricted epitope from ADAM17 protein to specific T cells established from normal donors as well as ovarian cancer patients. Our analysis revealed that the HLA-A2-restricted epitope is processed efficiently and presented by various cancer cells and not by normal cells. Tumour-specific T cell activation results in the secretion of both interferon-γ and granzyme B that can be blocked by HLA-A2 specific antibodies. Collectively, our data present evidence that ADAM17 can be a potential target antigen to devise novel immunotherapeutic strategies against ovarian, breast and prostate cancer.

Keywords: CTL, immunotherapy, MHC class I, T cell epitope, tumour antigen

Introduction

The science of tumour immunology is based on the premise that antibodies and cytotoxic T lymphocytes (CTL) can distinguish cancer cells from normal cells by recognizing specific antigens expressed differentially by the cancer. Furthermore, these antigens may be incorporated into therapeutic vaccination strategies intended to activate antibody and T cell responses capable of rejecting tumours expressing these antigens. One approach for identifying new antigens for therapeutic vaccines is to exploit differences in the peptides displayed on the cell surface by major histocompatibility complex (MHC) class I molecules [1] in tumours compared to non-malignant cells (reviewed in [2]). Importantly, the proteins from which these peptide epitopes are derived may be those with critical functions in tumour development, growth, survival and metastasis [3]. Indeed, in our search for ovarian cancer antigens, we identified and characterized a number of MHC class I-associated peptides derived from such proteins including a peptide from ADAM metallopeptidase domain 17 (ADAM17)/tumour necrosis factor (TNF)-α-converting enzyme (TACE) [4–6].

ADAM17 is a member of the metalloprotease–disintegrin family of membrane-anchored glycoproteins and is the proteinase responsible for the shedding of the proinflammatory cytokine, TNF-α [7,8] and several epidermal growth factor receptor (EGFR)-binding ligands, including transforming growth factor (TGF)-α, heparin-binding epidermal growth factor (HBEGF) and amphiregulin [9,10]. ADAM17 is up-regulated in a variety of tumours [11–13] and contributes to tumorigenesis, particularly if aberrant activity amplifies shedding of EGFR ligands with known roles in cancer, such as TGF-α, HBEGF and amphiregulin [14–16]. Thus, in recent years, there has been a growing interest in ADAM17 as a new therapeutic target in several EGFR-dependent tumour types. Identification of an MHC processed and presented ADAM17-derived peptide in ovarian and other tumour cells

would therefore make it an ideal target for immunotherapy [4–6].

In the present study, we characterized ADAM17 antigen as a potential target for cancer immunotherapy. To facilitate further development of ADAM17-based immunotherapies, we have generated critical data sets to demonstrate ADAM17 over-expression in a variety of tumours and that ADAM17 may serve as an antigen that stimulates anti-tumour immune responses against a variety of tumours.

Materials and methods

Cell lines and primary cells from human tissues

Human ovarian cancer cell lines SKOV3-A2 (kindly provided by Dr Ioannides from MD Anderson Cancer Center) and OVCAR3, human breast cancer cell lines MDA-MB231 and MCF7, human prostate cancer cell line LNCaP and colon cancer cell line Colo205 were obtained originally from the American Type Culture Collection (ATCC, Manassas, VA, USA). SKOV3-A2, OVCAR3, Colo205 and LNCaP were maintained in RPMI-1640 medium (Mediatech, Manassas, VA, USA) supplemented with 10% fetal bovine serum (FBS) (Atlanta Biologicals, Norcross, GA, USA), L-glutamine (300 mg/ml), non-essential amino acids, penicillin and streptomycin. MDA-MB231 and MCF7 were maintained in Dulbecco's modified Eagle's medium (DMEM) medium supplemented with 10% FBS and other supplements as listed above. All cell lines were maintained at 37°C in a humidified incubator with 5% CO_2. Non-malignant kidney and liver tissues from HLA-A2$^+$ human donors were obtained from the National Disease Research Interchange (NDRI, Philadelphia, PA, USA). Tissues were digested enzymatically and cell suspensions were generated as per standard methods. Briefly, tissue samples were minced and digested with 2 mg/ml collagenase, 0·1 mg/ml hyaluronidase and 0·15 mg/ml DNAse in DMEM supplemented with 2 × concentration of antibiotics and anti-mycotics (all reagents were obtained from Sigma-Aldrich, St Louis, MO, USA) at 37°C for 3–6 h. Cell suspensions were washed several times with PBS and DMEM supplemented with 10% FBS. Cell viability was assessed by trypan blue exclusion and cells were frozen in 90% FBS and 10% dimethylsulphoxide (DMSO) (Sigma-Aldrich) for future use.

In vitro generation of peptide specific cytotoxic T lymphocytes (CTLs)

Heparinized blood from healthy HLA-A2$^+$ donors was purchased from Research Blood Components, LLC (Brighton, MA, USA). Patient blood samples were obtained under International Review Board-approved protocols from women with ovarian cancer undergoing debulking surgery at Duke University Medical Center. Peripheral blood mononuclear cells were purified using lymphocyte separation medium (Mediatech) using differential centrifugation according to standard methods; 20×10^6 cells were plated per well in 2 ml RPMI-1640 medium supplemented with 10% FBS, L-glutamine (300 mg/ml), non-essential amino acids, sodium pyruvate, penicillin and streptomycin (complete medium) in six-well tissue culture plates (BD, Franklin Lakes, NJ, USA) overnight. Non-adherent cells were removed and saved. Plastic adherent cells were pulsed with 50 μg/ml synthetic peptide and 1·5 μg/ml human β2-microglobulin (Sigma-Aldrich) in complete medium for 2 h. Non-adherent cells were added back in 5 ml complete medium supplemented with interleukin (IL)-7 at 5 ng/ml, keyhole limpet haemocyanin (KLH; Sigma-Aldrich) at 5 μg/ml, granulocyte–macrophage colony-stimulating factor (GM-CSF) at 25 ng/ml and IL-4 at 50 ng/ml (all cytokines and growth factors were purchased from Peprotech, Rocky Hill, NJ, USA). Plates were incubated at 37°C in a humidified incubator with 5% CO_2 for 12 days; 2·0 ml medium was removed from each well and fresh complete medium supplemented with 10 U/ml IL-2 for 2 days. T cells were restimulated with CD4/CD8 T cell-depleted autologous monocytes pulsed with synthetic peptide at 10 μg/ml and 1·5 μg/ml human β2-microglobulin in complete medium containing 5 ng/ml IL-7 and 5 μg/ml KLH for 5 days. IL-2 treatment and *in vitro* restimulation were repeated thrice at the indicated time intervals prior to use of *in vitro* expanded T cells in enzyme-linked immunospot (ELISPOT) assays.

ELISPOT assays

In vitro-expanded T cells were used as effectors in ELISPOT assays to assess antigen-stimulated interferon (IFN)-γ release or granzyme B release using ELISPOT assay kits (BD-Pharmingen, San Jose, CA, USA), according to the manufacturer's instructions. Typically, a fixed number of various target cells (5×10^3 cells per well) and effector cells at an effector-to-target ratios of 100–40:1, were used in ELISPOT assays. T2 cells were pulsed with 20 μg/ml synthetic peptides and 1·5 μg/ml human β2-microglobulin in RPMI-1640 medium supplemented with 1% FBS overnight for use as targets in ELISPOT assays. For antibody blocking experiments, target cells were pretreated with purified W6/32 or BB7·2 antibodies (from BD-Pharmingen) at 1:50 dilution for 1 h prior to addition to T cell cultures. ELISPOT assays were performed in replicate wells. Spots were quantitated using an immunospot reader from Cellular Technologies Limited (Shaker Heights, OH, USA). Results are presented as number of IFN-γ-producing cells per 1×10^6 cells. Error bars represent standard error of the mean (s.e.m.) of experimental replicates.

Synthetic peptides

Synthetic peptides corresponding to the HLA-A2-presented ADAM17 epitope (p13-YLIELIDRV) and an influenza A

virus epitope derived from the matrix protein (GILGVFTL) were supplied by GenScript Corporation (Piscataway, NJ, USA).

Flow cytometry

Peripheral blood mononuclear cells (PBMCs) obtained from healthy donors were treated with phytohaemagglutinin (PHA) (1 μg/10^6/ml) for 48 h in culture. THP-1, a monocytic myeloma cell line, was cultured in complete RPMI-1640 media. Activated and non-activated PBMCs, THP-1 cells, normal cells from human liver and kidney and cancer cell lines were treated with a blocking solution [1% normal mouse serum from Sigma and 2% bovine serum albumin (BSA) from Sigma in phosphate-buffered saline (PBS)] on ice for 1 h. Cells were then washed once with PBS and treated with either fluorescein isothiocyanate (FITC)-labelled isotype matched control antibody or ADAM17-specific mouse monoclonal antibody at 1:100 dilution in PBS containing 2% BSA (isotype control antibody was purchased from Invitrogen, Carlsbad, CA, USA and ADAM17 ectodomain-specific monoclonal antibody from R&D Systems, Minneapolis, MN, USA) for 1 h on ice. Cells were washed thrice with PBS and subjected to flow cytometry in Guava flow cytometer (Millipore). Samples were analysed using GuavaSoft software (Millipore).

Immunohistochemistry

Paraffin-coated tissue arrays comprising cancer and matched control tissue sections were purchased from Imgenex (San Diego, CA, USA). All chemical reagents used in this protocol are purchased from Sigma unless noted otherwise. Tissue arrays were stained with anti-ADAM17 antibody and horseradish peroxidase (HRP)-conjugated secondary reagent according to the manufacturer's established procedure and can be found at Imgenex's website (http://www.imgenex.com). Briefly, tissue arrays were first deparaffinized by incubating in a dry oven at 62°C for 1 h. Subsequently slides were dewaxed using xylene and hydrated using ethanol and washed in tap water. Antigen retrieval was achieved by treating slides in citrate buffer (0·01 M, pH 6·0) and microwaving, as suggested by the protocol. Endogenous peroxidase was quenched by treating slides with 3% hydrogen peroxide solution for 6 min. Slides were then blocked with blocking serum (normal mouse serum from Sigma at 1:50) for 30 min and treated with anti-ADAM17 antibody (1:100) for 2 h at room temperature. Slides were washed with PBS and incubated with biotinylated anti-mouse secondary antibody for 30 min at room temperature. Subsequently, slides were washed and incubated with avidin-conjugated HRP (1:100) for 30 min at room temperature. Slides were washed with PBS and developed using 3,3′ diaminobenzidine (DAB) solution for 2 min. Reaction was stopped using tap water. Slides were finally counterstained using Meyer's haematoxylin for 10 s and dehydrated in ethanol. Slides were then cleared using xylene and coverslides were mounted with Permount (Vectastain staining reagents were purchased from Vector Laboratories, Burlingame, CA, USA). Slides were viewed under a fluorescence microscope equipped with a digital camera and micrographs were captured (Nikon Eclipse, TE 800-U).

Real-time quantitative reverse transcription–polymerase chain reaction (qRT–PCR)

Real-time qRT–PCR analysis to determine the expression level of ADAM17 was carried out by SABiosciences (Frederick, MD, USA). RNA isolated from normal liver and kidney tissues (obtained from NDRI) or cancer cell lines (SKOV3-A2, MDA-MB231 and LNCaP) were used for the analysis. Glyceraldehyde 3-phosphate dehydrogenase (GAPDH) was used as internal control. Following first-strand synthesis, real-time RT–PCR was carried out using reagents generated by SABiosciences. Data analysis was carried out employing the $\Delta\Delta C_t$ method. Results are presented as fold difference of ADAM17 mRNA expressed in cancer cell lines over the control cells obtained from normal liver tissue.

Results

Presentation of ADAM17-derived epitope p13 by various cancer cell lines

In order to assess the presentation of ADAM17-derived epitope p13 (YLIELIDRV) by cancer cell lines, we generated p13-specific T cells *in vitro* from healthy HLA-$A2^+$ donors. These p13-specific T cells were used as effectors and various cancer cell lines as targets in an overnight ELISPOT assay to quantify IFN-γ release. As shown in Fig. 1, *in vitro*-generated T cells recognize p13-loaded T2 cells. In addition, p13-specific T cells were tested for recognition and secretion of IFN-γ in response to primary cells obtained from healthy HLA-$A2^+$ donor or various cancer cell lines (Fig. 1). Normal liver cells are not recognized by p13-specific T cells appreciably, suggesting that p13 epitope is not generated endogenously in normal cells. However, when pulsed with the synthetic p13 peptide these cells activate T cells readily, demonstrating that these cells are capable of presenting exogenously provided peptide antigen. p13-specific T cells are activated by ovarian cancer cells (SKOV3-A2 and OVCAR3), from which p13 was isolated originally as an HLA-A2 presented peptide [4]. Breast cancer cell lines (MDA-MB-231 and MCF7) also activate p13-specific T cells significantly. Interestingly, prostate cancer cell line LNCaP also activates p13-specific T cells, albeit at a lower level. Other cancer cell lines we tested in culture, including colon cancer (Colo205, Fig. 1) and lung cancer cell lines (data not shown), do not activate p13-specific T cells. Thus, these results demonstrate that ADAM17-derived p13 epitope is presented by ovarian, breast and prostate cancer cells.

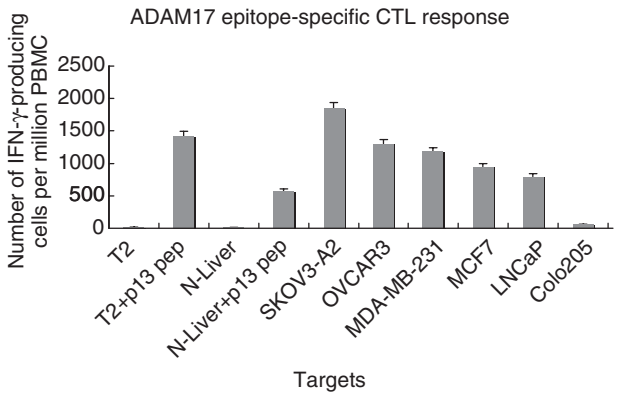

Fig. 1. Generation of T cells specific for the tumour necrosis factor-α converting enzyme (ADAM17)-derived human leucocyte antigen (HLA)-A2-restricted p13 epitope from healthy donors. Peripheral blood mononuclear cells (PBMC) from two healthy HLA-A2$^+$ donors were stimulated *in vitro* with synthetic peptides corresponding to the ADAM17-derived HLA-A2 restricted p13 epitope (YLIELIDRV). These cells were tested in an enzyme-linked immunospot assay using T2 cells loaded with the corresponding synthetic peptide, normal liver cell suspensions obtained from a HLA-A2$^+$ healthy donor tissue (with or without exogenously provided p13 peptide) and HLA-A2$^+$ cancer cell lines (ovarian cancer cell lines SKOV3-A2 and OVCAR3, breast cancer cell lines MDA-MB-231 and MCF7, a prostate cancer cell line LNCaP and a colon cancer cell line Colo205). Interferon (IFN)-γ-producing cells were quantitated using an immunospot reader. Error bars represent standard error of the mean of experimental replicates.

T cell response towards the ADAM17-derived p13 epitope is HLA-A2-restricted

In order to ascertain the HLA restriction of the presentation of p13 epitope to specific T cells, we extended our IFN-γ ELISPOT analysis to include antibodies specific for pan HLA-A, B, C (W6/32) or HLA-A2 (BB7·2) with cancer targets. Our results indicate that the presentation of p13 is HLA-A2-restricted, as evident from the effective inhibition of IFN-γ release by BB7·2 antibody (Fig. 2, top panel). As expected, W6/32 also blocked T cell activation. T2 cells or primary liver cells from an HLA-A2$^+$ donor pulsed with an irrelevant peptide (influenza A matrix protein-derived peptide) were used as negative controls, and these cells did not activate p13-specific T cells above background levels. However, as expected, when pulsed with p13 peptide, these cells activated p13-specific T cells readily. These results demonstrate that the p13 peptide-specific T cells are highly specific and the presentation of p13 peptide to these T cells is HLA-A2-restricted.

Cytolytic potential of the T cells specific for the ADAM17-derived p13 epitope

Although we observed that the p13-activated T cells could recognize p13 epitope-expressing tumour cells, we wished to determine if these p13-activated T cells were cytolytic by measuring the release of granzyme B in an ELISPOT assay in response to various targets. Results demonstrate that a significant portion of p13-activated T cells indeed secrete granzyme B in response to p13 presentation by p13 peptide-loaded T2, normal liver cells or various cancer targets, but not T2 cells or normal liver cells pulsed with a negative control peptide (Fig. 2, bottom panel). This secretion could be blocked significantly by the inclusion of W6/32 or BB7·2

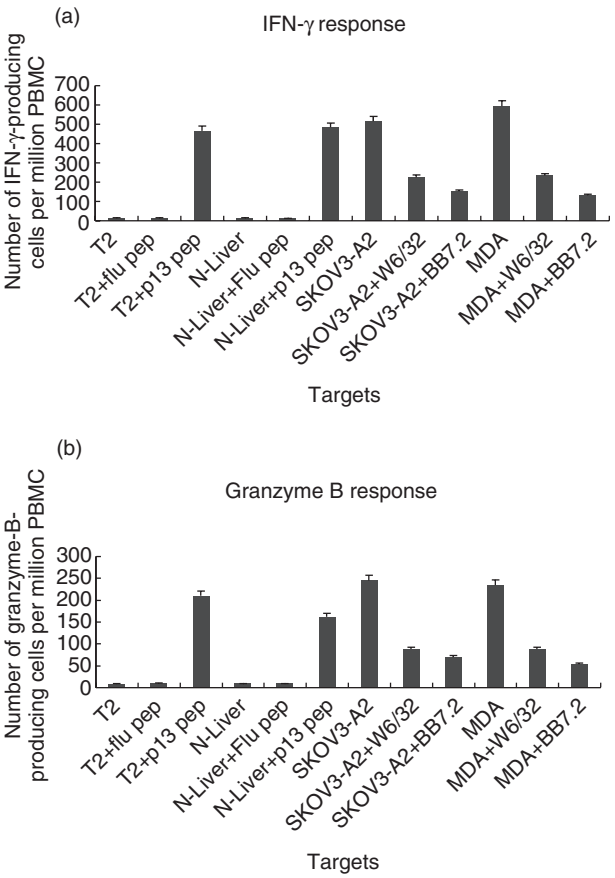

Fig. 2. T cells specific for the tumour necrosis factor (TNF)-α converting enzyme (ADAM17)-derived p13 epitope are both human leucocyte antigen (HLA)-A2-restricted and cytolytic. Peripheral blood mononuclear cells (PBMC) from a healthy HLA-A2$^+$ donor were stimulated *in vitro* with synthetic peptides corresponding to the ADAM17-derived p13 epitope (YLIELIDRV). (a) These cells were tested in an enzyme-linked immunospot (ELISPOT) assay using T2 cells or normal kidney cells obtained from an HLA-A2$^+$ healthy donor tissue loaded with an irrelevant synthetic peptide (flu) or p13 peptide. HLA-A2$^+$ cancer cell lines (ovarian cancer cell line SKOV3-A2 and breast cancer cell line MDA-MB-231) were pretreated with W6/32 or BB7·2 antibody prior to incubation with p13 specific T cells overnight. Interferon (IFN)-γ-producing cells were quantitated using an immunospot reader. (b) p13-specific T cells were used in an ELISPOT assay with the above-mentioned targets and the release of granzyme B was measured as described above. Error bars represent standard error of the mean of experimental replicates.

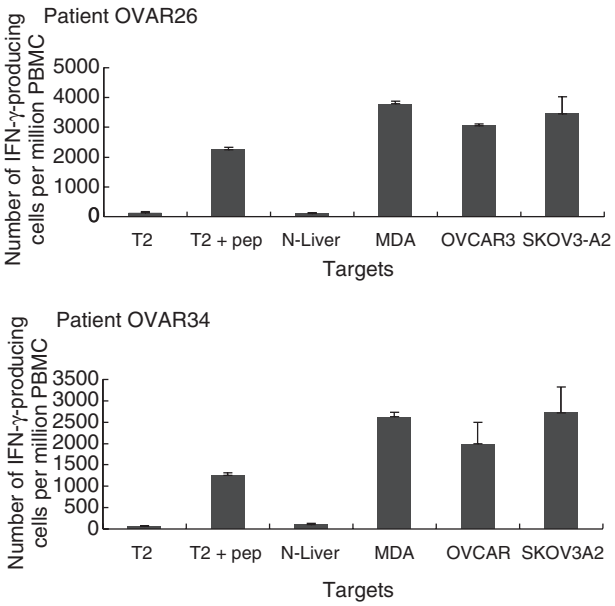

Fig. 3. Generation of T cells specific for the tumour necrosis factor-α-converting enzyme (ADAM17)-derived human leucocyte antigen (HLA)-A2-restricted p13 epitope from ovarian cancer patients. Peripheral blood mononuclear cells (PBMC) from two HLA-A2$^+$ patients with ovarian cancer were stimulated *in vitro* with the synthetic peptide corresponding to p13 peptide (YLIELIDRV). These cells were tested in an enzyme-linked immunospot assay using T2 cells loaded with the corresponding synthetic peptide, normal liver cell suspensions obtained from a HLA-A2$^+$ healthy donor tissue (with or without exogenously provided p13 peptide) and HLA-A2$^+$ cancer cells lines (breast cancer cell line MDA-MB-231 and ovarian cancer cell lines OVCAR3 and SKOV3-A2). Interferon (IFN)-γ producing cells were quantitated using an immunospot reader. Error bars represent standard error of the mean of experimental replicates.

antibodies, thus demonstrating the HLA-A2-restricted peptide presentation.

Generation of ADAM17-derived epitope p13-specific T cells from ovarian cancer patients

Our next question was to determine if T cells can be activated from PBMC obtained from HLA-A2$^+$ ovarian cancer patients using p13 synthetic peptide. IFN-γ ELISPOT assays using ovarian cancer patient T cells stimulated *in vitro* with p13 peptide and various targets demonstrate that p13 peptide-specific T cells can be activated from ovarian cancer patients, and they recognize peptide-pulsed T2 but not normal liver cells (Fig. 3). These T cells also recognize ovarian (SKOV3-A2 and OVCAR3) and breast (MDA-MB231) cancer cell lines. These results demonstrate that functional p13 peptide-specific T cells can be generated from ovarian cancer patients.

ADAM17 is over-expressed on the surface of a variety of cancer cells

In order to evaluate the expression levels of ADAM17 on the surface of normal and cancer cells, we performed flow cytometry employing a ADAM17-specific antibody that recognizes the ectodomain of ADAM17 protein. As shown in Fig. 4a, primary cells prepared from healthy human liver tissue do not express detectable levels of ADAM17. Primary cells from a healthy human kidney tissue express low levels of ADAM17 on their surface. However, ADAM17 expression is detectable at higher levels in ovarian (SKOV3-A2 and OVCAR3), breast (MDA-MB-231 and MCF7), prostate (LNCaP) and colon (Colo205) cancer cell lines. Notably, SKOV3-A2 and LNCaP express very high levels of ADAM17. These results demonstrate that ADAM17 is expressed on the surface of a variety of cancer cells, but its expression on normal cells is undetectable to extremely low. ADAM17 is involved in the release of TNF-α from activated PBMCs and monocytes. However, expression levels of TACE in these cell types have never been reported. Because we are postulating that TACE could be a potential immunotherapeutic antigen, the question of expression levels in these critical cell types needed to be addressed. Hence, we performed flow cytometry analysis of activated PBMCs and THP-1 (myelomonocytic cell line) to determine the levels of TACE in these cell types. As shown in Fig. 4b, the expression levels of ADAM17 were low in PHA-activated and non-activated PBMCs as well as THP-1 cells compared to ovarian tumour cell line SKOV3 and other tumour cell lines (Fig. 4a), demonstrating that ADAM17 can be a potential immunotherapeutic target.

ADAM17 over-expression in cancer tissues but low expression in normal tissues

We then assessed ADAM17 expression levels in cancer tissues. We chose to perform immunohistochemical analysis

Fig. 4. Analysis of surface expression of tumour necrosis factor-α converting enzyme (ADAM17) in normal and cancer cells by flow cytometry. (a) Normal cell suspensions (liver and kidney) obtained from healthy human leucocyte antigen (HLA)-A2$^+$ donors or cancer cell lines (ovarian cancer cell lines SKOV3-A2 and OVCAR3, breast cancer cell lines MDA-MB-231 and MCF7, prostate cancer cell line LNCaP and a colon cancer cell line, Colo205) were treated with either fluorescein isothiocyanate (FITC-labelled isotype-matched control antibody or FITC-labelled ADAM17-specific antibody and subjected to flow cytometry by Guava flow cytometer (Millipore). Samples were analysed using GuavaSoft software (Millipore). (b) SKOV3-A2, peripheral blood mononuclear cells (PBMC), PBMC treated with phytohaemagglutinin (PHA) and human acute monocytic leukaemia cell line (THP-1) cells were stained with either FITC-labelled isotype matched control antibody or FITC-labelled ADAM17-specific antibody and subjected to flow cytometry as described above.

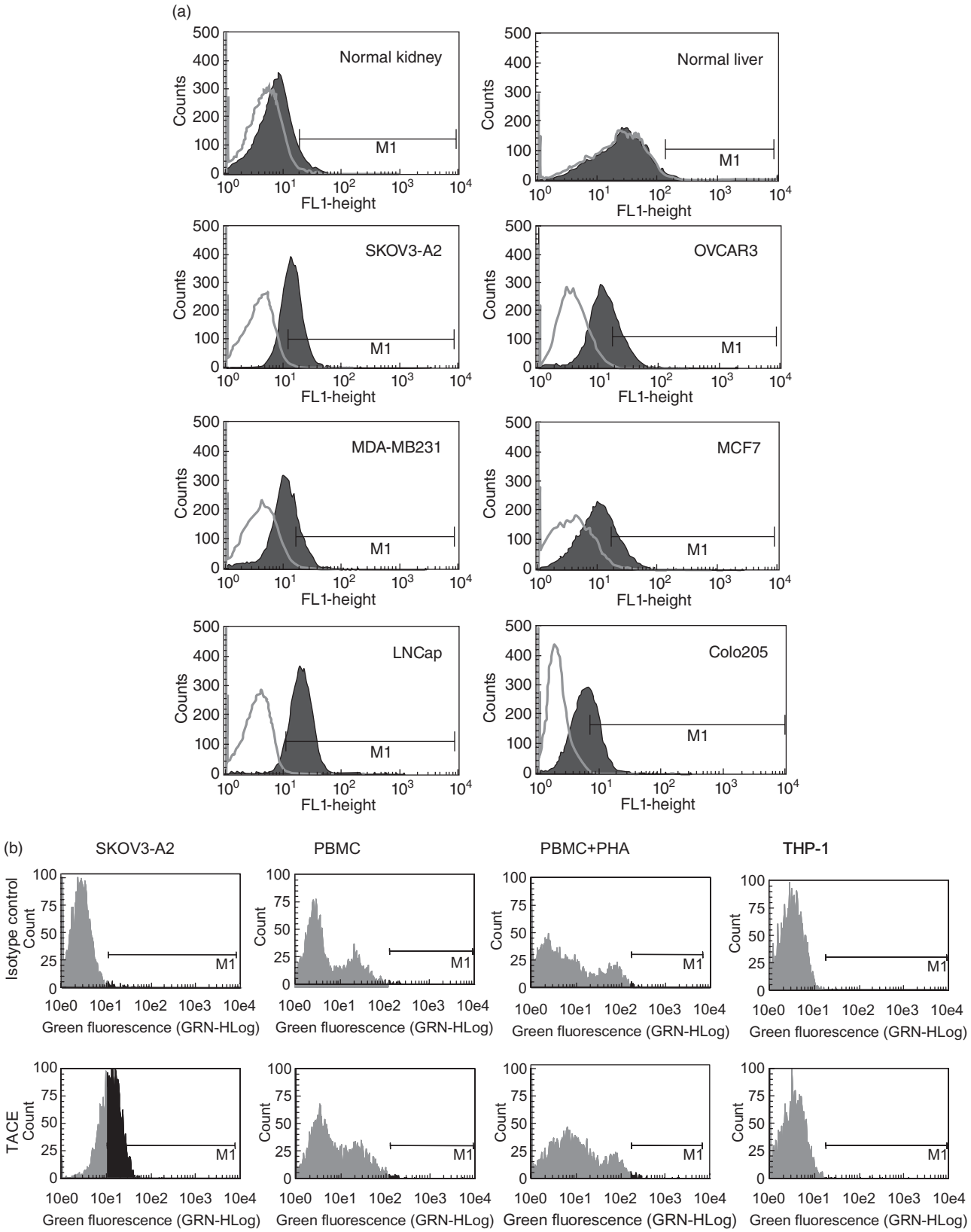
(a)
Normal kidney
Normal liver
SKOV3-A2
OVCAR3
MDA-MB231
MCF7
LNCap
Colo205
Counts
FL1-height
M1
(b)
SKOV3-A2
PBMC
PBMC+PHA
THP-1
Isotype control
TACE
Count
Green fluorescence (GRN-HLog)
M1

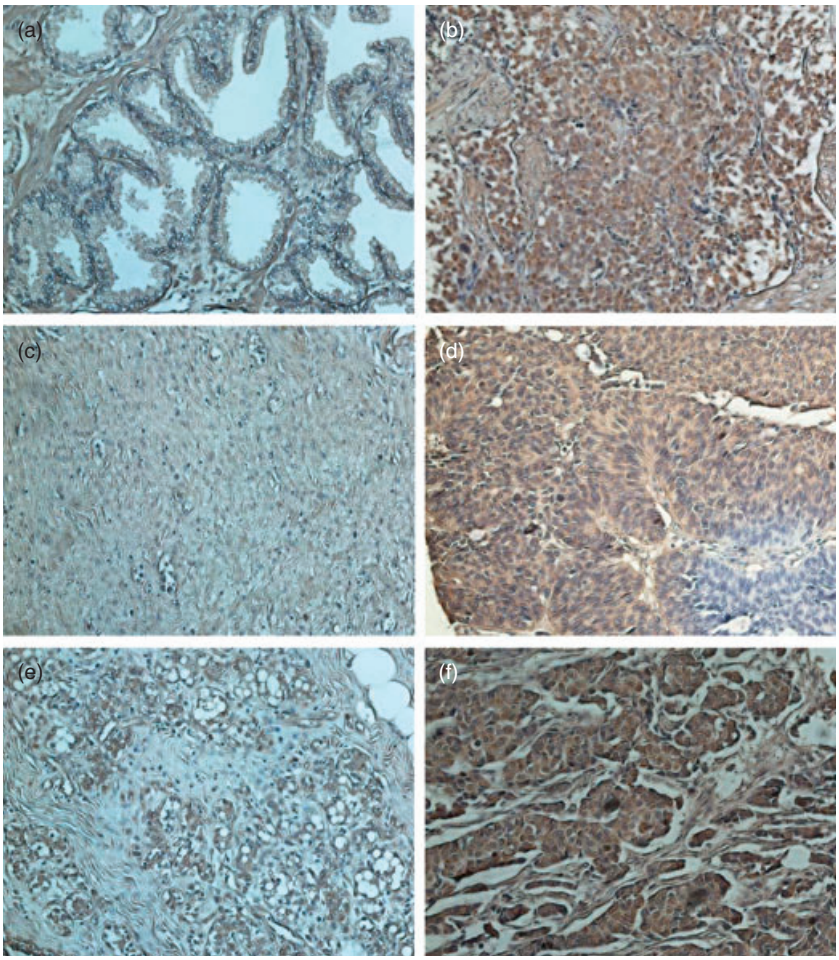

Fig. 5. Immunohistochemical analysis of expression of tumour necrosis factor (TNF)-α converting enzyme (ADAM17) in normal and cancer cells. Tissue arrays comprising of matched normal or cancer specimens (breast, ovarian and prostate tissues) were treated with an ADAM17-specific monoclonal antibody followed by treatment with a horseradish peroxidise (HRP)-conjugated secondary antibody reagent (detailed protocol is described in Materials and methods section). Slides were developed with 3,3′ diaminobenzidine (DAB) substrate and tissues were counterstained with Meyer's haematoxylin. Stained tissue sections were analysed using a fluorescent microscope and micrographs were captured at 200× magnification. (a and b) Breast normal and cancer, (c and d) ovarian normal and cancer, (e and f) prostate normal and cancer.

on tissue sections from ovarian, breast and prostate cancers and tissue-matched non-malignant controls. Results of our analysis are shown in Fig. 5. From the micrographs, it is evident that ADAM17 is expressed at very high levels in cancer tissues, but its expression is low in normal tissues. These results show that ADAM17 is not only over-expressed in cancer cell lines, but also in primary cancer tissues isolated from patients.

ADAM17 mRNA expression does not correlate with increased ADAM17 protein expression

In order to determine if increased expression of ADAM17 is regulated at the transcriptional level, we performed real-time qRT–PCR analysis, a powerful tool to determine the transcript levels of a given gene. We used RNA isolated from normal liver and kidney cells as controls. ADAM17 mRNA level is elevated slightly in SKOV3-A2 compared to normal liver and kidney cells (Fig. 6). However, the levels are reduced in MDA-MB-231 and LNCaP cells. These data support the notion that elevated ADAM17 expression in cancer cells is regulated at the translational or post-translational, but not the transcriptional level.

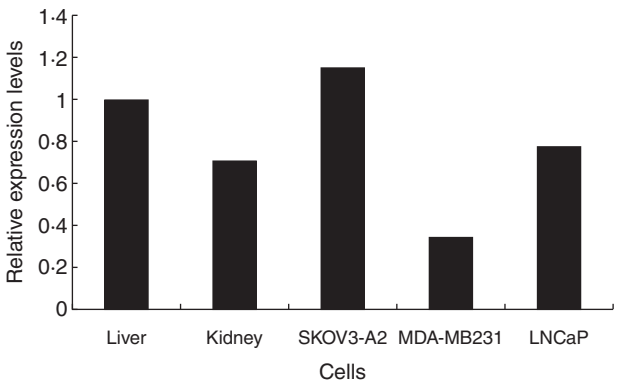

Fig. 6. Expression level of tumour necrosis factor-α-converting enzyme (ADAM17) in normal and cancer cells by real-time quantitative reverse transcription–polymerase chain reaction (qRT–PCR) analysis. Real-time qRT–PCR analysis to determine the expression levels of the genes that code ADAM17 was carried out using RNA isolated from normal tissues (liver and kidney) or cancer cell lines (ovarian cancer cell line SKOV3-A2, breast cancer cell line MDA-MB-231 and prostate cancer cell line LNCaP). Glyceraldehyde 3-phosphate dehydrogenase (GAPDH) was used as internal control. Data analysis was carried out employing the $\Delta\Delta C_t$ method. Results are presented as fold difference of ADAM17 expression in cancer cell lines over the control cells obtained from normal liver tissue.

Discussion

It is well established that human cancers express antigens that can be targeted specifically by cell-mediated and humoral immunity [17–20]. However, which antigens contain epitopes that can serve as authentic T cell rejection targets is largely unknown. We used the MHC class I-associated peptide repertoire in tumour cells as a source for identifying new tumour antigens for the development of cancer vaccines. Although a number of tumour antigens have been identified for potential use in cancer vaccines, it is essential to characterize them using various biological criteria for their translational applicability. In this study, we have characterized in depth the tumour-associated antigen ADAM17, which was discovered by analysing the MHC class I peptide repertoire in ovarian cancer cells [4]. ADAM17 protein is up-regulated and contributes to tumorigenesis in a variety of tumours [11,12,15] and has been well studied as a drug target [11,21]. However, ADAM17 as a cancer immunotherapy antigen has not been validated previously.

Herein, we report the characteristics of ADAM17 that make it suitable for both cell-mediated and humoral clinical cancer immunotherapy applications. Specifically, we have demonstrated that an HLA-A2-restricted peptide epitope of ADAM17 is capable of inducing T cell responses which can recognize ovarian, breast and prostate cancers in an HLA-A2 restricted fashion. The peptide-specific T cells not only secrete IFN-γ in response to the antigen stimulation but also secrete granzyme B, demonstrating the cytolytic potential of these *in vitro*-generated T cells. The fact that the ADAM17-epitope specific CTL could be generated from cancer patients in addition to healthy donors suggests that precursor T cells specific for ADAM17 are normally present. Flow cytometry and immunohistochemistry demonstrating that this protein is expressed abundantly on the surface of ovarian, prostate and breast cancer cell lines and patient tissues, but not on their normal counterparts, also signifies the possible use of this antigen as an antibody target. Future studies will use the serum of mice vaccinated against ADAM17 to assess for the ability of vaccine-induced antibodies to bind to surface-expressed ADAM17 and to determine the functional consequences of this binding.

One possible criticism of immunotherapeutic targeting of ADAM17, also called TNF-α-converting enzyme (TACE), is that it is involved in cleavage of TNF-α from activated T cells and monocytes [7] and thus T cells expressing the molecule might be susceptible to immune attack. It was therefore critical to assess the expression levels of ADAM17 on activated PBMC. Our flow cytometry data, using the antibody that binds to the ectodomain of ADAM17, indicates low level of expression in PHA-activated and non-activated PBMCs and a monocytic cell line, THP-1, comparable to normal tissues that we have tested (Fig. 4b). The localization of ADAM17 is speculated to be an important determinant of shedding activity. TNF-α processing has been shown to occur in the trans-Golgi network, and be connected closely to transport of soluble TNF-α to the cell surface. However, several studies suggest that the majority of mature, endogenous ADAM17 may be localized to a perinuclear compartment, with only a small amount being present on the cell surface. This perinuclear localization of ADAM17 indicates the possibility that ADAM17-mediated TNF-α shedding may also occur in the intracellular environment [22,23] suggesting less likelihood of an adverse effect on lymphoid cells caused by immunotherapeutic targeting of surface over-expression in tumours.

Our approach of antigen identification by MHC class I peptide repertoire analysis differs from the more common differential gene expression analysis of normal and cancer tissues [24,25]. However, gene expression may not reflect the protein level or stability and modifications of the protein that are relevant to immunotherapy [26–28]. As indicated by Chiriva-Internati *et al.*, it is critical to validate candidate antigens for clinical applications using a system level-based approach at the level of cells, tissues and organs beyond gene expression [29]. Indeed, our real-time qRT–PCR analysis (Fig. 6) revealed that the transcript levels of ADAM17 in cancer cells do not reflect the enhanced protein expression as detected by flow cytometry and immunohistochemistry. Furthermore, one important observation was that tumours that had high expression of ADAM 17 protein were not always the most sensitive to T cell-mediated killing, as demonstrated by the LNCaP and Colo205 data (Figs 1 and 4a). It should be noted that although protein over-expression is a prerequisite for antibody or drug-mediated targeting, it is not a critical factor for MHC class I processing and presentation of the T cell epitope, which correlates primarily with the level of degradation of proteins associated with misfolding, cryptic translation and other causes of high turnover [1,30] which occur frequently in cancer initiation, survival and progression [2].

In summary, the characterization of ADAM17 as an immunotherapy target suggests that vaccine strategies utilizing it should proceed. Indeed, the T cell epitope derived from ADAM17 has been evaluated for safety and CTL responses in patients with breast and ovarian cancers in a Phase I clinical study (Morse, Alvarez Secord and Philip, manuscript in preparation). Furthermore, because ADAM 17 is the principal sheddase for TGF-α and EGFR-ligands from a late secretory pathway compartment [31], it may be possible to combine small molecules inhibiting the EGFR pathway in conjunction with immunotherapy against ADAM17 as a combination therapy.

Acknowledgements

The authors wish to acknowledge Ms Debra Davis and Ms Delila Serra from Duke University for ovarian cancer patient sample collection and processing.

This work was supported by corporate funding to Immunotope, Inc.

Disclosure

The authors have no disclosures to declare.

References

1 Shastri N, Schwab S, Serwold T. Producing nature's gene-chips: the generation of peptides for display by MHC class I molecules. Annu Rev Immunol 2002; **20**:463–93.

2 Admon A, Barnea E, Ziv T. Tumor antigens and proteomics from the point of view of the major histocompatibility complex peptides. Mol Cell Proteomics 2003; **2**:388–98.

3 Hanahan D, Weinberg RA. The hallmarks of cancer. Cell 2000; **100**:57–70.

4 Ramakrishna V, Ross MM, Petersson M *et al.* Naturally occurring peptides associated with HLA-A2 in ovarian cancer cell lines identified by mass spectrometry are targets of HLA-A2-restricted cytotoxic T cells. Int Immunol 2003; **15**:751–63.

5 Sinnathamby G, Lauer P, Zerfass J *et al.* Priming and activation of human ovarian and breast cancer-specific CD8+ T cells by polyvalent *Listeria monocytogenes*-based vaccines. J Immunother 2009; **32**:856–69.

6 Karkada M, Weir GM, Quinton T *et al.* A novel breast/ovarian cancer peptide vaccine platform that promotes specific type-1 but not Treg/Tr1-type responses. J Immunother 2010; **33**:250–61.

7 Black RA, Rauch CT, Kozlosky CJ *et al.* A metalloproteinase disintegrin that releases tumour-necrosis factor-alpha from cells. Nature 1997; **385**:729–33.

8 Moss ML, Jin SL, Milla ME *et al.* Cloning of a disintegrin metalloproteinase that processes precursor tumour-necrosis factor-alpha. Nature 1997; **385**:733–6.

9 Lee DC, Sunnarborg SW, Hinkle CL *et al.* TACE/ADAM17 processing of EGFR ligands indicates a role as a physiological convertase. Ann NY Acad Sci 2003; **995**:22–38.

10 Le Gall SM, Bobe P, Reiss K *et al.* ADAMs 10 and 17 represent differentially regulated components of a general shedding machinery for membrane proteins such as transforming growth factor alpha, L-selectin, and tumor necrosis factor alpha. Mol Biol Cell 2009; **20**:1785–94.

11 Kenny PA, Bissell MJ. Targeting TACE-dependent EGFR ligand shedding in breast cancer. J Clin Invest 2007; **117**:337–45.

12 Merchant NB, Voskresensky I, Rogers CM *et al.* TACE/ADAM-17: a component of the epidermal growth factor receptor axis and a promising therapeutic target in colorectal cancer. Clin Cancer Res 2008; **14**:1182–91.

13 Rosso O, Piazza T, Bongarzone I *et al.* The ALCAM shedding by the metalloprotease ADAM17/TACE is involved in motility of ovarian carcinoma cells. Mol Cancer Res 2007; **5**:1246–53.

14 Ongusaha PP, Kwak JC, Zwible AJ *et al.* HB-EGF is a potent inducer of tumor growth and angiogenesis. Cancer Res 2004; **64**:5283–90.

15 Borrell-Pages M, Rojo F, Albanell J, Baselga J, Arribas J. TACE is required for the activation of the EGFR by TGF-alpha in tumors. EMBO J 2003; **22**:1114–24.

16 Berasain C, Castillo J, Perugorria MJ, Prieto J, Avila MA. Amphiregulin: a new growth factor in hepatocarcinogenesis. Cancer Lett 2007; **254**:30–41.

17 van der Bruggen P, Traversari C, Chomez P *et al.* A gene encoding an antigen recognized by cytolytic T lymphocytes on a human melanoma. Science 1991; **254**:1643–7.

18 Goldman B. Cancer vaccines: finding the best way to train the immune system. J Natl Cancer Inst 2002; **94**:1523–6.

19 Lewis JD, Reilly BD, Bright RK. Tumor-associated antigens: from discovery to immunity. Int Rev Immunol 2003; **22**:81–112.

20 Gilboa E. The promise of cancer vaccines. Nat Rev Cancer 2004; **4**:401–11.

21 Gschwind A, Hart S, Fischer OM, Ullrich A. TACE cleavage of proamphiregulin regulates GPCR-induced proliferation and motility of cancer cells. EMBO J 2003; **22**:2411–21.

22 Peiretti F, Deprez-Beauclair P, Bonardo B, Aubert H, Juhan-Vague I, Nalbone G. Identification of SAP97 as an intracellular binding partner of TACE. J Cell Sci 2003; **116**:1949–57.

23 Nelson KK, Schlondorff J, Blobel CP. Evidence for an interaction of the metalloprotease-disintegrin tumour necrosis factor alpha convertase (TACE) with mitotic arrest deficient 2 (MAD2), and of the metalloprotease-disintegrin MDC9 with a novel MAD2-related protein, MAD2beta. Biochem J 1999; **343**:673–80.

24 Martelange V, De Smet C, De Plaen E, Lurquin C, Boon T. Identification on a human sarcoma of two new genes with tumor-specific expression. Cancer Res 2000; **60**:3848–55.

25 Schultze JL, Vonderheide RH. From cancer genomics to cancer immunotherapy: toward second-generation tumor antigens. Trends Immunol 2001; **22**:516–23.

26 Mathieu MG, Linley AJ, Reeder SP *et al.* HAGE, a cancer/testis antigen expressed at the protein level in a variety of cancers. Cancer Immun 2010; **10**:2.

27 Chen G, Gharib TG, Huang CC *et al.* Discordant protein and mRNA expression in lung adenocarcinomas. Mol Cell Proteomics 2002; **1**:304–13.

28 Rogel A, Popliker M, Webb CG, Oren M. p53 cellular tumor antigen: analysis of mRNA levels in normal adult tissues, embryos, and tumors. Mol Cell Biol 1985; **5**:2851–5.

29 Chiriva-Internati M, Grizzi F, Bright RK, Martin Kast W. Cancer immunotherapy: avoiding the road to perdition. J Transl Med 2004; **2**:26.

30 Vierboom MP, Zwaveling S, Bos GMJ *et al.* High steady-state levels of p53 are not a prerequisite for tumor eradication by wild-type p53-specific cytotoxic T lymphocytes. Cancer Res 2000; **60**:5508–13.

31 Horiuchi K, Le Gall S, Schulte M *et al.* Substrate selectivity of epidermal growth factor-receptor ligand sheddases and their regulation by phorbol esters and calcium influx. Mol Biol Cell 2007; **18**:176–88.

JOURNAL OF PROTEOMICS 75 (2012) 3270–3290

Available online at www.sciencedirect.com

SciVerse ScienceDirect

www.elsevier.com/locate/jprot

Quantitative immunoproteomics analysis reveals novel MHC class I presented peptides in cisplatin-resistant ovarian cancer cells

Vivekananda Shetty, Zacharie Nickens, James Testa, Julie Hafner, Gomathinayagam Sinnathamby, Ramila Philip***

Immunotope, Inc., 3805 Old Easton Road, Doylestown, PA 18902, United States

ARTICLE INFO

Article history:
Received 2 January 2012
Accepted 25 March 2012
Available online 3 April 2012

Keywords:
Cisplatin
MHC peptides
Immunoproteomics
iTRAQ quantitation
CTL
ELISpot

ABSTRACT

Platinum-based chemotherapy is widely used to treat various cancers including ovarian cancer. However, the mortality rate for patients with ovarian cancer is extremely high, largely due to chemo-resistant progression in patients who respond initially to platinum based chemotherapy. Immunotherapy strategies, including antigen specific vaccines, are being tested to treat drug resistant ovarian cancer with variable results. The identification of drug resistant specific tumor antigens would potentially provide significant improvement in effectiveness when combined with current and emerging therapies. In this study, using an immunoproteomics method based on iTRAQ technology and an LC-MS platform, we identified 952 MHC class I presented peptides. Quantitative analysis of the iTRAQ labeled MHC peptides revealed that cisplatin-resistant ovarian cancer cells display increased levels of MHC peptides derived from proteins that are implicated in many important cancer pathways. In addition, selected differentially presented epitope specific CTL recognize cisplatin-resistant ovarian cancer cells significantly better than the sensitive cells. These over-presented, drug resistance specific MHC class I associated peptide antigens could be potential targets for the development of immunotherapeutic strategies for the treatment of ovarian cancer including the drug resistant phenotype.

1. Introduction

Ovarian cancer is the fifth most common cancer among women, and it causes more deaths than any other type of female reproductive cancer [1,2]. Standard therapy for advanced-stage ovarian cancer is surgical debulking followed by taxane plus platinum-based chemotherapy. Although patients with advanced ovarian cancer do respond to first-line platinum-based chemotherapy after cytoreductive surgery, 20–40% of patients' experience only a partial response to the treatment, and succumb to progressive disease following the initial treatment due to intrinsic drug resistance [3,4]. The poor prognosis for relapsed and refractory ovarian cancer is a highly compelling motivation to develop additional therapeutic modalities to prevent or treat disease recurrence that could be used in conjunction with or instead of other established therapies. Among these novel modalities are active immunotherapy and agents that target pathways necessary for disease

* *Corresponding author*. Tel.: +1 215 589 6327; fax: +1 215 489 4920.
** *Corresponding author*. Tel.: +1 215 489 4955; fax: +1 215 489 4920.
E-mail addresses: vivek@immunotope.com (V. Shetty), rphilip@immunotope.com (R. Philip).

1874-3919/$ – see front matter © 2012 Elsevier B.V. All rights reserved.
doi:10.1016/j.jprot.2012.03.044

progression and metastasis. Cancer vaccines in general have great promise to treat or prevent recurrence of ovarian cancer and other malignancies. It is well established that T cell infiltration into ovarian cancers is associated with improved survival [5,6] and epitopes expressed by ovarian cancers have been identified as targets for T cell responses [7,8]. Until recently, only a few T cell epitopes associated with ovarian tumors have been extensively evaluated in the clinic, including those encoded by the HER2/neu proto-oncogene [7,9,10], epithelial mucin MUC1 [11], p53 [12], CEA [13] and CA125 [14]. A limitation of these antigens is that they may not necessarily be reflective of the broad antigenic content of ovarian cancers, particularly as they become more resistant to therapy, and they may have alterations in their protein expression profiles.

A novel strategy for identifying the truly relevant tumor antigens is to analyze those actually presented by the MHC class I (MHCI) molecules on tumor cells. Tumors have a different surface expression of peptides than their normal counterparts and the MHC peptide repertoire reflects the proteome or the degradome of the cell [15,16]. The analysis of the peptide repertoire associated with the MHC class I molecules of cancer cells therefore may serve as a source of new tumor antigens for the development of cancer immunotherapy (reviewed in [15]). One of the widely used biochemical approaches for the identification of MHC associated epitopes involves recovery of the peptides from immunoaffinity-purified specific HLA molecules from the target cells, followed by analysis of the peptides by chromatography, mass spectrometry and proteomics methodologies [17–20]). iTRAQ is a novel proteomic technology that allows for the identification and quantification of the relative abundance of peptides/proteins in a complex mixture [21]. This approach involves labeling the peptides prior to LC-MS/MS with iTRAQ reagents specific to the N-terminus. This allows detection of every labeled peptide and aids in quantification of relative peptide abundance between samples.

MHC associated peptides and the parent proteins that are differentially presented by the cisplatin-resistant and -sensitive ovarian cancer cells are potential candidates for targeted treatments including immunotherapeutic strategies. Although there is enduring research in the identification of the cisplatin induced proteome [22,23], the MHC class I peptide repertoire of cisplatin-resistant ovarian cancer cells has not been previously reported. Herein, we employed iTRAQ technology in conjunction with mass spectrometry to compare the MHC peptidome of SKOV3-A2 (cisplatin-resistant), SKOV3-A2-CP (cisplatin-treated), and OVCAR3 (cisplatin-sensitive) ovarian cancer cells. We also investigated the peptide specific CTL responses for anti-tumor immunity and implications of the parent proteins in functional pathways and biological processes related to drug resistance and tumor survival.

2. Experimental procedures

2.1. Cell lines and normal tissues

Human ovarian cancer cell lines SKOV3-A2 (cisplatin-resistant expressing HLA alleles A3, A2, A68, B18, B35, Cw5), kindly provided by Dr. Ioannides (MD Anderson Cancer Center), and OVCAR3 (cisplatin-sensitive expressing HLA alleles A2, A29, B7, B58, Cw7), obtained from ATCC (Manassas, VA), were maintained in RPMI1640 complete medium (Mediatech, Manassas, VA) supplemented with 10% fetal bovine serum (Atlanta Biologicals, Norcross, GA), L-glutamine (300 mg/ml), non-essential amino acids (1× concentration), penicillin and streptomycin (1× concentration, supplements were purchased from Mediatech). A breast cancer cell line, MDA-MB-231, and a lymphoblast line, T2, were obtained from ATCC and maintained in complete RPMI1640 media. For normal liver cells, a liver from an HLA-A2+ donor was obtained from NDRI, Philadelphia, PA and was enzymatically digested to yield cell suspensions as per standard methods [8]. Briefly, tissue samples were minced and digested with 2 mg/mL collagenase, 0.1 mg/mL hyaluronidase, and 0.15 mg/mL DNAse in DMEM supplemented with 2× concentration of antibiotics and antimycotics (all reagents were obtained from Sigma-Aldrich, St. Louis, MO) at 37 °C for 3 to 6 h. Cell suspensions were pelleted and washed several times with PBS and DMEM supplemented with 10% FBS. Cell viability was assessed by trypan blue exclusion and cells were frozen in 90% FBS and 10% DMSO (Sigma-Aldrich) for future use. Additionally, ascites fluid from an HLA-A2+ patient with metastatic ovarian cancer resistant to platinum-based chemotherapy was obtained from Duke University Medical Center under their IRB approved protocols. These ascites were purified using lymphocyte separation medium for use as targets in a CTL assay.

2.2. Evaluation of cisplatin resistance

SKOV3-A2 and OVCAR3 cells (1×10^4/well) in RPMI1640 complete media were seeded in 96-well micro titer plates and exposed to increasing concentrations (0 μm, 0.4 μm, 1.2 μm, 4 μm, 12.7 μm and 40 μm) of cisplatin [Cis-diamminedichloroplatinum (II)] (Sigma) for 3 days . The cell viability was determined using the 3-(4,5-dimethylthiazol-2-yl)-2, 5-diphenyltetrazolium bromide (MTT) assay as described previously [24].

2.3. Cisplatin treatment of SKOV3-A2

SKOV3-A2 cells were plated and expanded in 225 cm^2 tissue culture flasks. When cells were ~75% confluent, they were treated with cisplatin at half maximal inhibitory concentration (IC50) overnight. Cells were then harvested using PBS-EDTA solution and washed with PBS prior to lysate preparation for the isolation of MHC peptide complexes.

2.4. Isolation of MHC peptide complexes

MHC peptides were isolated from SKOV3-A2 (cisplatin-resistant), SKOV3-A2-CP (cisplatin-treated) and OVCAR3 (cisplatin-sensitive) cells according to the following procedure. SKOV3-A2-CP cells were generated by treating the SKOV3-A2 cells with the half maximal inhibitory concentration (IC50) of cisplatin for 3 days prior to MHC peptide isolation. Cells were lysed in lysis buffer (1% NP40, 150 mM NaCl, 10 mM Na_2HPO_4, 1 mM EDTA and a cocktail of protease inhibitors) and the lysates were subjected to immunoprecipitation using the pan MHC class I antibody, W6/32 conjugated Protein A/G agarose (Pierce). Briefly, cell lysates were incubated with antibody conjugated beads overnight at 4°C with gentle rocking, cell lysates were then removed and the beads were washed thrice with PBS.

Subsequently, bound MHC class I-peptide complexes were eluted using 10% acetic acid.

2.5. Isolation and purification of MHC peptides

The MHC molecules isolated from SKOV3-A2, SKOV3-A2-CP and OVCAR3 cells were processed separately. The solutions containing the MHC peptide complexes were heated at 85 °C for 15 min to dissociate bound peptides from the MHC molecule. Then the solutions were cooled to room temperature. The peptides were then separated from the class I heavy chain and β_2-microglobulin by centrifugation on an Amicon Ultra-3 kDa device and washed with 2 mL of 10% AcOH to obtain the maximum number of MHC peptides. The peptide mixtures were purified by RPC (Reversed Phase Chromatography) and the eluted peptides were concentrated by vacuum centrifugation from approximately 200 ul down to 6 μl.

2.6. iTRAQ labeling and purification of iTRAQ labeled peptides by SCX chromatography

As outlined in Fig. 2, peptide mixtures were labeled using iTRAQ reagents (Applied Biosystems) and purified iTRAQ labeled peptides by SCX chromatography following the vendors recommended protocol.

2.7. Fractionation of SCX purified peptides by C-18 chromatography

The SCX purified iTRAQ labeled peptide mixture was fractionated by a Dionex C-18 RP column (4.6 mm diameter × 150 mm length) using an offline ultimate 3000 HPLC (Dionex, Sunnyvale, CA). Mobile phase A was 2% acetonitrile (ACN) and 0.1% formic acid (FA) in water, while mobile phase B was 0.1% FA and 90% ACN in water. Peptides were then eluted from the column with an 80 min linear gradient from 5 to 80% buffer B at a flow rate of 200 μL/min. A total of 11 fractions were collected and each fraction was concentrated to 6 μL under vacuum for LC/MS analysis.

2.8. Liquid Chromatography–Mass Spectrometry Analysis

The purified iTRAQ labeled MHC peptides were analyzed by data dependent nano LC-MS/MS experiments on an Velos LTQ-Orbtrap mass spectrometer (thermo Fisher) interfaced with a nano ultimate HPLC (Dionex). The sample was loaded onto a trap column of 100 um ID × 2 cm (L) packed with 5-μm Magic C18 AQ (200 A, 3 um, Michrom) and washed using 98% H_2O, 2% ACN, 0.05% TFA buffer at a flow rate of 10 ul/min for 5 min. The peptides were then separated by a self-packed 75 um ID × 50 cm (L) fused silica column packed with 3-μm Magic C18 AQ (200 A, 3 um, Michrom) using a linear gradient of Buffer B from 4% to 55% in 50 min at a flow rate of 300 nl/min. The buffer compositions were as follows: Buffer A was 0.1% formic acid in water, buffer B was 0.1% formic acid, 80% acetonitrile. The analytical column was coupled to the mass spectrometer via a nano ion source (Proxeon) with a metal emitter. The peptides were analyzed in the Orbitrap operated at 60,000 resolution in full scan (300–2000 m/z) followed by 10 Data-Dependent HCD MS/MS scans (100–2000 m/z) with 7500 resolution and normalized collision energy of 45%. Survey scans were acquired in profile mode and MS/MS scans were acquired in centroid mode. Maximum injection times for MS and MS/MS were set to 500 and 1000 ms, respectively. The precursor isolation width was set at ±1.2 Da and monoisotopic precursor selection was enabled to exclude singly charged ions from MS/MS. The minimum intensity threshold for MS/MS fragmentation in the orbitrap analyzer was 5000 counts and the dynamic exclusion was set to 60 s with repeat count as one.

2.9. Peptide identification and quantification

MHC peptides and their corresponding proteins were identified by searching the LC-MS/MS raw data using proteome discoverer software (v 1.3) with Sequest search algorithm (Thermo). The data generation and database search parameters were: m.wt range: 375 Da–1500 Da, threshold: 200 counts, charge state—auto, MS^n level—MS^2, activation type—HCD, precursor ion tolerance: 20 ppm, fragment ion tolerance—0.02 Da, minimum ion count: 10, in database—Swissprot human, oxidation of M: 16 Da, N-terminus/K modification by iTRAQ reagents: 144 Da, enzyme—no enzyme. The search results were also verified manually to confidently identify the correct peptide sequence. Quantitation was done by selecting a 4-plex iTRAQ default method which contains the isobaric correction parameters for all the iTRAQ labels, however, only 3 labels (114,115,116) were selected for quantitation of MHC peptides. Peptides quantified with ≥1.5 fold increase and with ≤1.5 fold decrease in concentration were considered as up regulated and down regulated, respectively, in the current analysis.

2.10. Gene Ontology and pathway analysis

To classify the proteins from which the MHC peptides were derived from into functional categories, Gene Ontology (GO) analysis was performed using protein center software feature available in proteome discoverer software (v 1.3) software. Pathway analysis was carried out using National Cancer Institute (NCI) pathway interaction database (http://pid.nci.nih.gov/search/batch_query.shtml).

2.11. Validation of iTRAQ labeled MHC peptides by synthetic analogs

Synthetic peptides for validating the selected peptides identified in this study were obtained from Genscript Corporation (Piscataway, NJ). Peptide solutions were prepared in 2% ACN and 0.1% FA in water buffer, mixed them according to ~1 pm/ul concentration. All the peptide solutions were combined, and divided into 3 parts. Then these peptide solution parts 1, 2 and 3 were labeled by 114, 115 and 116 iTRAQ reagents, respectively, combined again and purified by SCX chromatography as described above for the MHC peptides. All the iTRAQ labeled synthetic peptides were analyzed by a Dionex 3000 nano ultimate HPLC (Sunnyvale CA), coupled with a LTQ ITMS (Thermo Electron, San Jose, CA) that equipped with an advanced nanospray source. As a part of the on-line sample clean-up step, the peptides were first concentrated using a

300 μm ID×5 mm C18 RP trap column (Dionex, Sunnyvale CA) and then separated using a 75 μm ID×15 cm C18 RP analytical column (Dionex, Sunnyvale CA), equilibrated in 4% ACN/0.1% FA at 250 nL/min flow rate. Mobile phase A was 2% ACN and 0.1% FA in water, while mobile phase B was 0.1% FA and 90% ACN in water. Peptide mixture was separated with a gradient of 4% to 50% B in 60 min and 50% to 80% in 90 min and eluted directly into an ITMS. The mass range in MS mode was 350 Da to 1500 Da and in MS/MS mode it was set as 100 Da to 1500 Da. PQD technique was used to fragment the iTRAQ labeled synthetic peptides. The instrument method was set to acquire fragment ion (MS/MS) spectra on the 4 most abundant precursor ions from each MS scan with a repeat count set of 1 and a repeat duration of 30 s. Dynamic exclusion was enabled for 180 s. The MS/MS spectra of the synthetic peptides were compared with the experimentally observed MS/MS spectra of MHC peptides to identify true positive peptides.

2.12. *In vitro generation of peptide-specific cytotoxic T lymphocytes*

Unpurified buffy coats from healthy HLA-A2+ donors were purchased from Research Blood Components, LLC (Brighton, MA). Peripheral blood mononuclear cells (PBMC) were purified using lymphocyte separation medium (Mediatech) using differential centrifugation according to standard methods. PBMC (2×10^7 per well) were plated in 2 mL of complete RPMI 1640 medium in 6-well tissue culture plates (BD, Franklin Lakes, NJ) overnight. Non-adherent cells were removed and saved. Plastic adherent cells were pulsed with 50 μg/mL synthetic peptide and 1.5 μg/mL human β2-microglobulin (Sigma-Aldrich) in complete medium for 2 h. Non-adherent cells were added back in 5 mL complete medium supplemented with IL-7 at 5 ng/mL, Keyhole Limpet Hemocyanin (KLH, Sigma-Aldrich) at 5 μg/mL, Granulocyte Monocyte Colony Stimulating Factor (GM-CSF) at 25 ng/mL and IL-4 at 50 ng/mL (all cytokines and growth factors were purchased from eBioscience, San Diego, CA). Plates were incubated at 37 °C in a humidified incubator with 5% CO2 for 12 days. T cells were restimulated with CD4+ and autologous CD8+ T cell-depleted monocytes pulsed with synthetic peptide at 10 μg/mL and 1.5 μg/mL human β2-microglobulin in complete medium containing 5 ng/mL IL-15, 12.5 ng/mL GM-CSF, and 10 U/mL IL-2 for 5 days. Medium (2.0 mL) was substituted from each well with 2.0 mL fresh complete medium supplemented with the same cytokines. In vitro restimulation was repeated three times at the indicated time intervals prior to use in ELISpot assays.

2.13. *ELISpot assays*

In vitro expanded T cell function was analyzed using antigen stimulated interferon-γ (IFN-γ) release as a measure of cytokine secretion performed using an ELISpot assay kit (BD-Pharmingen, San Jose, CA) according to the manufacturer's instructions. Typically, a fixed number of various target cells (5×10^3 cells per well) and effector cells (5×10^5 cells per well; effector to target ratio of 100:1) were cultured in triplicate wells overnight. Spots were quantitated using an ELISpot Reader System (AID). Results are presented as the number of IFN-γ producing cells per 1×10^6 PBMCs. Each assay was performed with PBMCs from at least 3 different healthy HLA-A2+ donors.

3. Results

We first determined the cisplatin resistance level of the SKOV3-A2 cell line using the MTT assay. We found that the IC50 of 2.4 μg/mL for the resistant cell line (SKOV3-A2) and 0.3 μg/mL for the sensitive cell line (OVCAR3). Thus, the intrinsically-resistant cell line SKOV3-A2 presented an almost an eight fold higher IC50 compared to its sensitive counterpart (Fig. 1).

3.1. *Identification of MHC class I presented peptides*

The general strategy involved in the discovery of the differential ovarian cancer MHC class I-presented peptide repertoire is shown in Fig. 2. MHC class I associated peptides isolated from ovarian cancer cells were subjected to LC/MS/MS analysis to identify the peptides and their corresponding proteins. Employing this strategy, 1500 MHC peptides were identified in the database search following the criteria described in the materials and methods section. Out of 1500 peptides, 952 peptides, derived from 834 proteins, were identified with high confidence based on the high XCorr values of identified peptides as well as the manual inspection of the characteristic fragment ions observed in their tandem mass spectra. The final list of peptides identified, their XCorr values, precursor proteins, and accession IDs, and gene IDs are given in Supplemental Table S1. The majority of these peptides varied in length from 8 to 11 amino acids and a few of them were >11 amino acids. About 10% of the proteins were identified with more than one MHC associated peptide and the peptide number ranged from 2 to 7. Since we used a pan-MHC class I antibody for the isolation of MHC peptide complexes, we identified hundreds of peptides associated with all the HLA molecules, including HLA-A2, A3, B7, B35, and B18, expressed on the ovarian cancer cells used in the

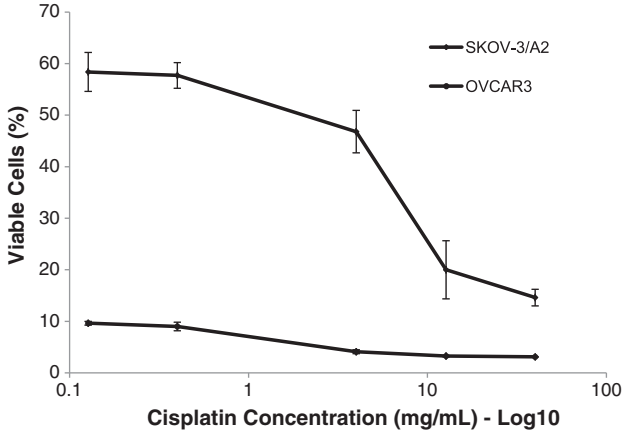

Fig. 1 – Evaluation of cell line resistance to cisplatin. Comparative cytotoxicity of cisplatin in SKOV3-A2 and OVCAR3 cells, as determined by the reduction of MTT, 6 days after a 2 h exposure to different concentrations of CDDP. The results are expressed as a percentage of viable cells compared to control cells.

study. In total, we identified 611 peptides corresponding to various HLA types (Table 1a) with the sequences that fit consensus binding motifs suggesting that they are potentially authentic MHC ligands (Table S1). We have calculated the binding scores and half life for dissociation of all the identified peptides by SYFPEITHI and Bimass software programs [25,26] and majority of them were found to have significant binding affinities to the corresponding HLA molecules. A small percentage of these peptides were reported previously by other research groups and the corresponding references and/or links are provided in Table S1. In this analysis, we identified 462 novel MHC peptides (100-A2, 323-A3, 15-B18, 15-B35, and 9-B7) and to the best of our knowledge there are no reports on the identification of these peptides using the immunoproteomics approaches.

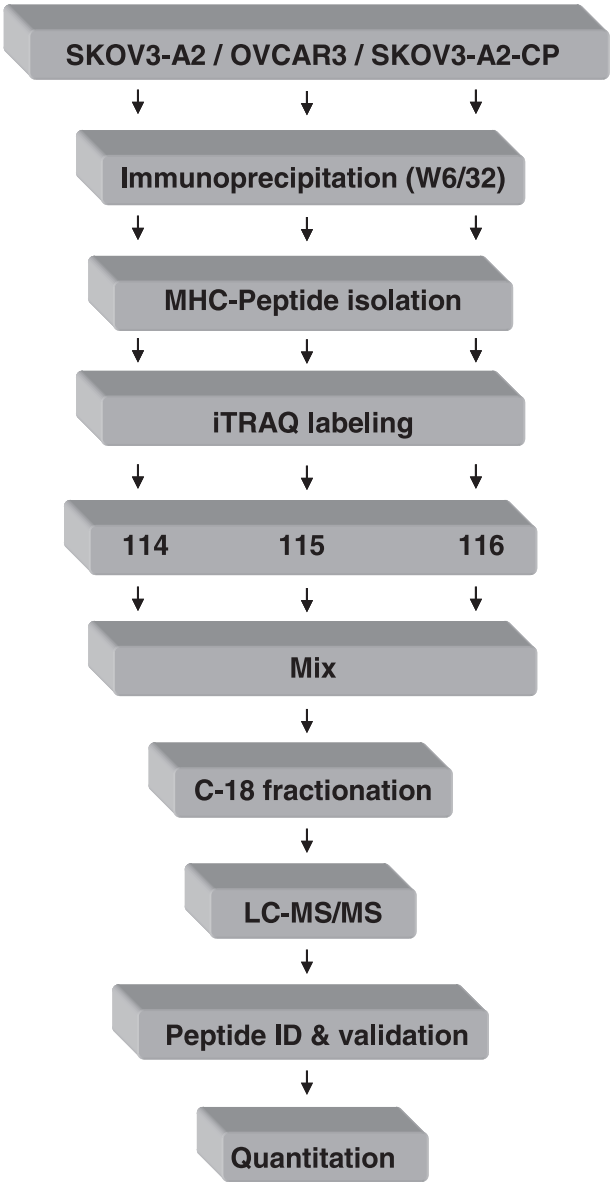

Fig. 2 – Immunoproteomics. Strategy used for the identification, validation and quantitation of cisplatin induced peptide epitopes presented by MHC class I molecules in ovarian cancer.

3.2. *Validation of MHC peptides*

To validate the results of MHC peptide identification, nine experimentally observed peptides, sTRkDYPAAk (Myc proto-oncogene protein) [27,28] ILDKkVEkV (Heat shock protein HSP 90-beta) [29], rLAADDFRV (Keratin, type I cytoskeletal 18) [30], rVAPRSGLAAk (Deoxyuridine 5′-triphosphate nucleotidohydrolase, mitochondrial) [31], rVIGTLEEV (Ran GTPase-activating protein 1) [32], yLAPHVRTL (COP9 signalosome complex subunit 1) [33,34], aLSDGVHkI (Fas apoptotic inhibitory molecule 1) [35], rTLAEIAkV (Non-POU domain-containing octamer-binding protein) [22], and vLIDYQRNV (Exportin-1) [36] were selected for synthesis (Table 2) based on the vital role of their precursor proteins in drug-resistant ovarian cancer [22,27–37]. The tandem mass spectrometry data of the experimentally observed peptides and their corresponding synthetic analogs are given in Fig. 3. The HCD MS/MS data of the experimentally observed peptides are given in Fig. 3A: 1a–9a. All the spectra in Fig. 3: 1a–9a shows several characteristic b and y fragment ions suggesting the correct peptide sequence. Furthermore, the high mass accuracy of the fragment ion masses of the experimentally observed peptides, as verified by the theoretical masses (insets Fig. 3: 1a–9a), corroborates the true positive identification of these peptides. Furthermore, these sequences were confirmed by the PQD MS/MS data of iTRAQ labeled synthetic peptides (Fig. 3: 1b–9b). The HCD MS/MS spectra and PQD MS/MS spectra of all the experimentally observed peptides and synthetic peptides, respectively, exhibit similar fragment ions with minor differences in their relative abundance. In addition, the presence of similar b and y signature ions in both the spectra, although the data were acquired by two different techniques (HCD and PQD), confirms not only that the peptides were labeled at the N-terminus/epsilon amino group of lysines by iTRAQ reagents, but also the accuracy of the sequences of the endogenously presented and experimentally observed MHC peptides.

3.3. *Quantitative analysis*

We have performed quantitative analysis in order to investigate the effect of cisplatin treatment of ovarian cancer cells on the processing and presentation of MHC peptides on the cell surface and to gain information on the MHC peptide repertoire of different ovarian cancer cell types with varying degree of sensitivity to cisplatin. The results of the differentially presented MHC peptides in SKOV3-A2-CP (cisplatin-resistant cells treated with cisplatin) cells compared to SKOV3-A2 (untreated cisplatin-resistant cells) are given in Table 3. The data comparing the peptides from SKOV3-A2-CP cells and SKOV3-A2 cells with OVCAR3 (cisplatin-sensitive) cells are summarized in Table 4. Quantitative analysis was carried out by setting the ratio threshold to 1.5 fold change. The summary of the differentially presented peptides of various HLA types from cisplatin treated (SKOV3-A2-CP) and untreated (SKOV3-A2) ovarian cancer cells is given in Table 1b. We observed that 75 peptides were up-regulated and 13 peptides were down-regulated in SKOV3-A2-CP cells (Table 3). The number of differentially presented peptides in both SKOV3-A2 cells and SKOV3-A2-CP cells compared to OVCAR3 cells are summarized in Tables 1c and 1d. One of the significant findings in this study is that we observed major differences between

Table 1 – Summary of the total number of MHC peptides identified in each HLA type. a) MHC peptide identification: Summary of the total number of MHC peptides identified in each HLA type b) Quantitative analysis of MHC peptides. Summary of the number of differentially presented peptides of various HLA types between cisplatin treated (SKOV3-A2-CP) and untreated (SKOV3-A2) ovarian cancer cells c) Quantitative analysis of MHC peptides. Summary of the number of differentially presented peptides in SKOV3-A2 cells compared to OVCAR3 cells d) Quantitative analysis of MHC peptides. Summary of the number of differentially presented peptides in SKOV3-A2-CP cells compared to OVCAR3 cells.

A

motif	A2	A3	B35	B18	B7	Un-classified	Total
# peptides identified	146	416	19	16	14	341	952

B

motif	A2	A3	B35	B18	Total
# up regulated peptides SKOV3-A2-CP (116)/SKOV3-A2 (114)	27	43	2	3	75
# down regulated peptides SKOV3-A2-CP (116)/SKOV3-A2 (114)	6	7	–	–	13

C

motif	A2	B7	Total
# up regulated peptides SKOV3-A2(114)/OVCAR3 (115)	126	2	128
# down regulated peptides SKOV3-A2(114)/OVCAR3 (115)	6	7	13

D

motif	A2	B7	Total
# up regulated peptides SKOV3-A2-CP (116)/OVCAR3 (115)	126	2	128
# down regulated peptides SKOV3-A2-CP (116)/OVCAR3 (115)	5	7	12

SKOV3-A2 and OVCAR3 peptide repertoire for the shared HLA type (HLA-A2). Large numbers of A2 motif containing peptides were found to be up-regulated and very few peptides were down-regulated in both SKOV3-A2 and SKOV3-A2-CP cells compared to OVCAR3 cells (Table 4). The concentration of a significant number of MHC peptides were highly elevated and some as much as 100 fold in both SKOV3-A2 and SKOV3-A2-CP cells. Indeed, a majority of the peptides that were up-regulated in SKOV3-A2 cells were also further up-regulated in SKOV3-A2-CP cells compared to OVCAR3 cells.

3.4. *Functional pathway analysis*

The proteins corresponding to the up-regulated peptides in SKOV3-A2-CP cells were analyzed by an NCI cancer pathway tool to investigate the altered functional pathways associated with cisplatin resistance. Interestingly, many important pathways were found to be altered in cisplatin-resistant cells (SKOV3-A2-CP and SKOV3-A2) compared to the sensitive cells (OVCAR3) (Supplemental Table S2). One such example is the regulation of the telomerase pathway by HDAC1 (Histone deacetylase 1), and MYC (proto-oncogene protein) genes. The peptide, rmLPHAPGV corresponding to Histone deacetylase proteins was found to be up-regulated by 1.50 fold, and 4.57 fold in SKOV3-A2-CP cells compared to SKOV3-A2 and OVCAR3 cells, respectively. Whereas, the peptide sTRkDY-PAAk corresponding to proto-oncogene protein was found to be up-regulated by 3.47 fold, and 30.58 fold in SKOV3-A2-CP cells compared to SKOV3-A2 and OVCAR3 cells, respectively, as showed by the tandem mass spectrometry data and the iTRAQ ratio in Fig. 3: 1a. Similar up-regulation profiles were found for many significant proteins that are implicated in cancer pathways and pathways involved in chemotherapy response.

3.5. *Gene Ontology of proteins corresponding to the differentially presented MHC peptides*

Using the protein center feature in the proteome discover 1.3 software, we obtained the GO terms for the proteins corresponding to all 952 MHC peptides identified in this study. We compared the functional as well as biological process GO terms between the total proteins and proteins corresponding to the differentially presented peptides in SKOV3-A2-CP cells (Supplemental Fig. S1). The functional analysis revealed that both structural, molecular activity and translation activity were increased by 3% each upon cisplatin resistance and treatment, whereas, transcription regulation activity was decreased by 10%. With regard to biological processes, cell differentiation and defense response were increased by 1% each in the cisplatin resistance phenotype.

3.6. *Antigen-specific CD8+ T cells generated against differentially presented ovarian cancer epitopes recognize platinum-resistant ovarian cancer cells*

To analyze the function of the differentially presented T cell epitopes, we performed CTL analysis. T cell activation, a direct assessment of MHCI epitope presentation, was ascertained by antigen specific IFN-γ release and measured by ELISpot assay.

Table 2 – List of MHC peptides selected for validation experiments. The list of selected true positive peptides, their sequences, motif's, protein names, ID's, gene ID's, Xcorr scores, number of amino acids (#AA) SYFPEITHI scores and Bimas scores, implication of parent protein in cancer and references.

Acc ID	Gene ID	Protein	Peptide sequence	XCorr	Motif	#AA	SYFPEITHI score [a]	Bimas score [a]	SKOV3-A2(114)/ OVCAR3 (115) ratio	SKOV3-A2-CP (116)/ OVCAR3 (115) ratio	Significance of parent protein in drug resistance	Implication of parent proteins in cancer
P01106	MYC	Myc proto-oncogene protein	sTRkDYPAAk [b]	2.8	A2	10	9	0	8.82	30.58	Involved in acquisition of cisplatin resistance	Ovarian cancer [27]
P08238	HSP90AB1	Heat shock protein HSP 90-beta	ILDKkVEkV	2.7	A2	9	29	53.302	3.18	2.99	Increases P-glycoprotein-mediated multi-drug resistance	Colon adenocarcinoma [29]
P05783	KRT18	Keratin, type I cyto-skeletal 18	rLAADDFRV	3.8	A2	9	22	403.402	0.45	0.57	Differentially associated with cisplatin sensitivity	Ovarian adenocarcinoma [30]
P33316	DUT	Deoxyuridine 5′-triphosphate nucleotidohydrolase, mitochondrial	rVAPRSGLAAk	3.4	A2	11	12	0.435	3.58	1.25	Implicated in chemo-resistance, and repression of tumor suppressor in many cancers	Neuroblastoma colon, hepatocellular carcinoma [31,51–53]
P46060	RANGAP1	Ran GTPase-activating protein 1	rVIGTLEEV	2.6	A2	9	24	6.859	1.2	1.30	Over expressed in cisplatin-resistant cells	Ovarian cancer [32]
Q13098	GPS1	COP9 signalosome complex subunit 1	yLAPHVRTL	3.6	A2	9	32	45.203	9.21	12.45	Involved in ovarian cancer taxol-chemotherapy response	Ovarian carcinoma [33]
Q9NVQ4	FAIM1	Fas apoptotic inhibitory molecule 1	aLSDGVHkI [b]	3.2	A2	9	30	98.381	1.93	4.90	Involved in resistance to apoptotic cell death	Nasopharyngeal carcinoma [35]
Q15233	NONO	Non-POU domain-containing octamer-binding protein	rTLAEIAkV	3.0	A2	9	24	8.221	1.37	1.86	Over expressed in cisplatin-induced apoptotic cells	Leukaemia [22]
O14980	XPO1	Exportin-1	vLIDYQRNV	2.1	A2	9	25	96.955	11.34	11.90	Over expressed in aggressive ovarian carcinomas and related to poor prognosis	Colorectal cancer [36,54]

[a] Calculated score based on halftime for dissociation of the peptide (in min) from HLA molecule.
[b] These peptides are further elevated in ovarian cancer resistant cells (SKOV3-A2-CP) upon cisplatin treatment.

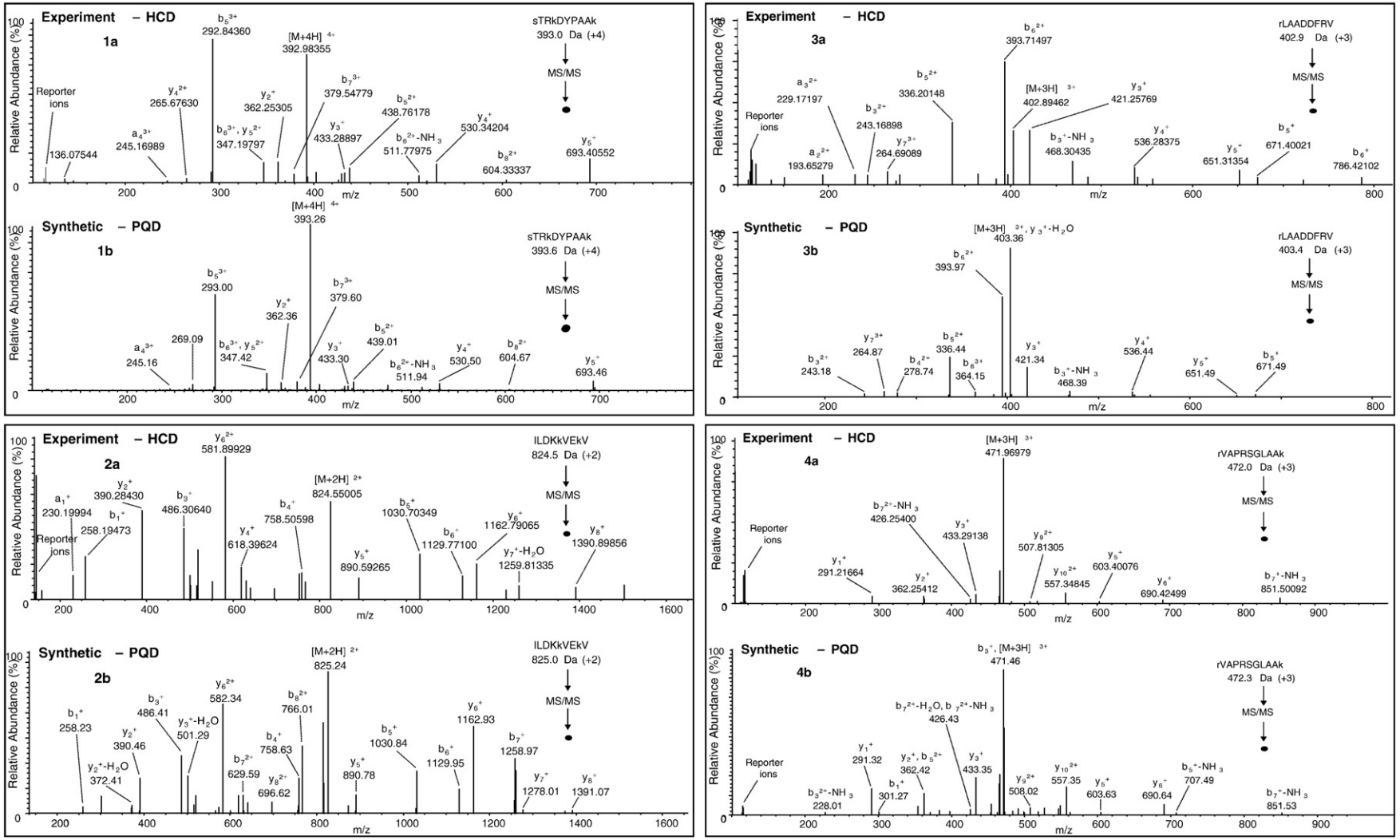

Fig. 3 – Identification and validation of MHC peptides by tandem mass spectrometry. MS/MS spectra of experimentally observed peptides (1a–9a) and synthetic peptides (1b–9b) acquired by HCD (Orbitrap) and PQD (LTQ ion trap) techniques, respectively.

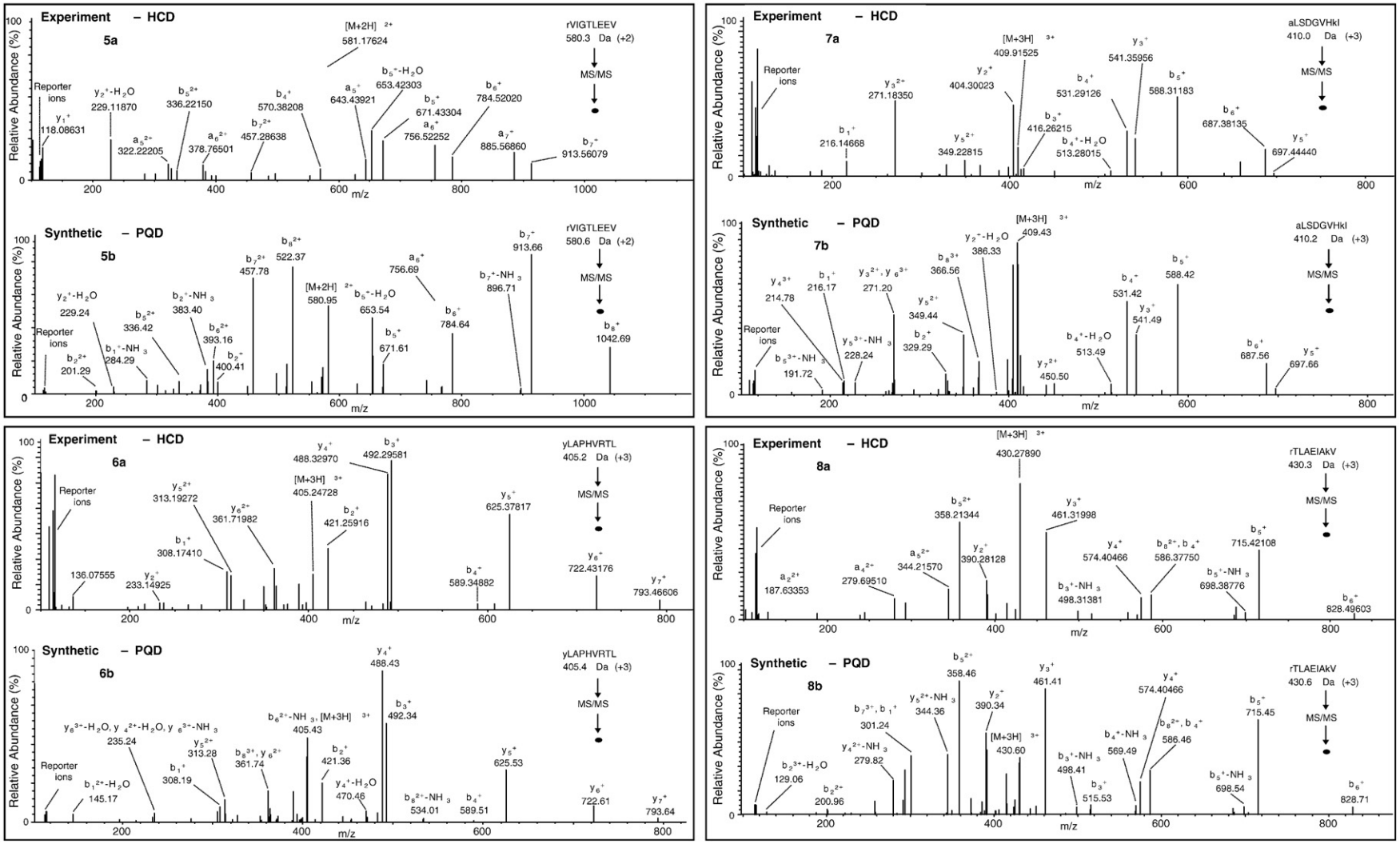

Fig. 3 (*continued*).

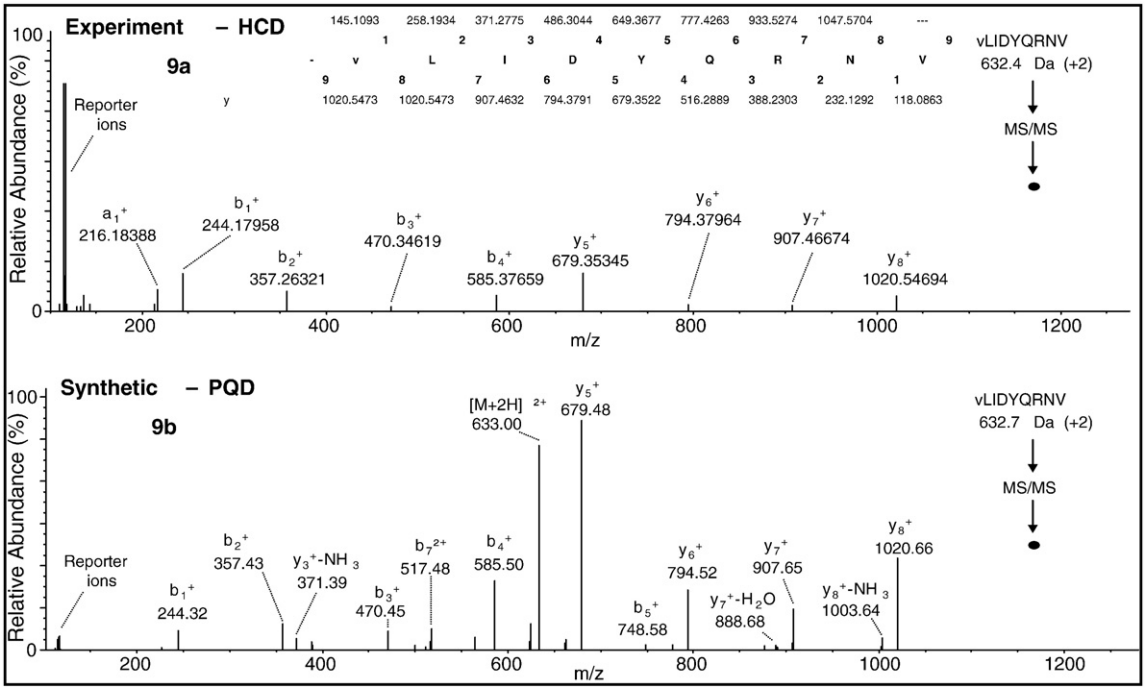

Fig. 3 (*continued*).

As illustrated in Fig. 4, all of the 9 confirmed differentially presented peptides generated a CTL response against peptide-loaded targets. More importantly, we also observe CTL recognition of ovarian tumor targets. Specifically, the CTL responses were significantly higher against intrinsically cisplatin-resistant ovarian cancer cells (SKOV3-A2) as compared to the sensitive cells (OVCAR3), suggesting that these peptides were over-presented by the resistant cells. Furthermore, there was a slight increase in CTL recognition of the cisplatin-treated SKOV3-A2 cells indicating the upregulation of these epitopes by the selection pressure caused by cisplatin treatment. Interestingly, most of the peptide specific CTLs also efficiently recognized cisplatin-resistant tumor cells from ovarian cancer patient ascites and a triple negative, multidrug resistant breast cancer cell line (MDA-MB-231). Furthermore, the peptide specific CTLs failed to recognize normal liver cells without any exogenous peptide loading indicating these peptide presentations is specific for cancer cells.

4. Discussion

MHC class I associated peptides, derived from tumor-associated antigens and uniquely presented on cancer cells have attracted attention in recent years, as candidates for the development of cancer vaccines [15,38]. A number of such tumor-specific peptides have already been identified and some have been successfully tested as cancer vaccines in humans, most notably for immunotherapy of melanoma [39] and other cancers including ovarian cancer [40]. In the present study, employing a quantitative immunoproteomics method, we identified 952 MHC peptides in cisplatin-sensitive and resistant ovarian cancer cells (SKOV3-A2, SKOV3-A2-CP and OVCAR3) with a large number of them up-regulated in the cisplatin-resistant ovarian cancer cells. In addition to the identification of 461 novel, unreported MHC peptides, we also identified a set of peptides that are reported by others and directly implicated in ovarian and other cancers (Tables 2 and 3), which is highly significant to the development of a therapeutic vaccine, specifically for the platinum resistant phenotype of ovarian cancer. For example, antigenic peptides from Histone H1.2 and Melanoma-associated antigen B2 proteins have been reported earlier from the analysis of UO1 107 ovarian carcinoma cells [38]. Similarly, peptides from Dynein light chain roadblock-type 1 protein, which has been implicated in renal cell carcinoma [41].

4.1. *Chemotherapeutic agents alter MHC peptide repertoire*

About 33% of the total MHC peptides (corresponding to HLA types given in Table 1) identified in our study are up-regulated and about 4% are down-regulated in cisplatin-resistant cells (SKOV3-A2-CP/SKOV3-A2-CP) compared to the sensitive cells (OVCAR3). We hypothesized that the relatively high number of up-regulated peptides compared to down-regulated peptides in the resistant cells and further elevation of these peptides upon cisplatin treatment of the resistant cells could be attributed to the high levels of protein expression and/or protein degradation resulting in higher MHC class I antigen processing correlated to drug resistance. Indeed, an increase in MHC class I (HLA-A,B,C) expression upon treatment with cisplatin has been reported earlier [42], correlating the relative expression of MHC class I cell surface antigens with the chemotherapeutic response and overall survival among a cohort of patients with aneuploid ovarian cancers. Further evidence comes from the increased expression of MHC class I molecules in colorectal cancer cell lines exposed to chemotherapy drugs [43]. It is postulated that chemotherapeutic agents activate the immune system and cancer-specific immunotherapy may be more effective when

used in combination with systemic chemotherapy. Furthermore, by identifying immunologically relevant drug induced MHC peptide presentation, it may be possible to target the over-presented antigens for efficient immunotherapeutic tumor response to overcome drug resistant disease progression.

4.2. *Identification of altered functional pathways in cisplatin-resistant cells*

Pathway analysis of the source proteins of differentially presented peptides revealed cancer specific pathways including the regulation of the telomerase pathway by HDAC1 (Histone deacetylase 1), and MYC (proto-oncogene protein) genes (Table S2 and Fig. 4). It is known that more than 90% of malignant tumors, including ovarian tumors, express telomerase [44], a ribonucleoprotein that adds DNA telomeric repeat sequences to the ends of linear chromosomes [45]. The hyper-activity of the telomerase pathway occur only in ovarian tumor cells derived from ascites, peritoneal fluid, and metastatic lesions [45,46] implicating telomerase activation specifically in drug resistant form of ovarian cancer. HDAC1, MYC genes also affect the two other important signaling pathways including the regulation of nuclear beta catenin signaling mediated, target gene transcription and nuclear SMAD2/3 signaling. Furthermore, several up-regulated peptides were derived from proteins involved in multiple malignant pathways including notch, hedgehog and IL-6 signaling events (Table S2), reflecting the pathological changes occurring in drug resistant ovarian cancer cells. Similar up regulation of MHC peptides derived from tumor transcriptome has been reported by others [16], indicating the significance of MHC peptide repertoire in search for tumor antigens [15].

4.3. *Poor correlation of changes in MHC peptide repertoire with protein expression levels*

Even though we did not investigate the differential expression of the proteins from which the MHC peptides were derived from in the cisplatin-resistant cells, we have surveyed the literature for corroborative data on the differentially expressed proteins in various types of ovarian cancer cells that were treated with cisplatin (Supplemental Table S3). We found that there is a considerable overlap between the list of proteins identified in our study and differentially expressed (both up and down regulated) proteins reported in the literature. Interestingly, 34 proteins corresponding to the differentially presented MHC peptides in cisplatin-resistant cells, are known to be directly or indirectly implicated in various types of cancers (Tables 2 and 3). Additionally, the majority of the proteins corresponding to the up regulated peptides in the resistant cells are implicated specifically in ovarian cancer. For example, we identified peptides derived from elongation factor 2 and MMP7 proteins, which were found to be differentially expressed in serous and mucinous ovarian carcinomas [47]. This implies that the peptides derived from these proteins (Tables 2, 3, S3) could be potential targets for further screening with CTL analysis and immunotherapy development. Although many of the proteins are implicated in several cancer related hallmark pathways [48], the majority of the parent proteins of the up-regulated MHC peptides in resistant cells, do not overlap with the over-expressed proteins reported in ovarian cancer literature. This suggests that not all over-expressed proteins in cancer go through the proteosomal degradation pathway that yields peptides which would be presented on the cell surface by the MHC molecules [15] which is essential for CTL recognition and has significant implication on the therapeutic vaccine response.

4.4. *MHC peptide repertoire reflect neoplastic transformation*

In a recent comparative study with normal and cancer cells, Fortier et al. [16] reported that the MHC class I peptide repertoire of cancer cells reflected the pathological status of the cell and reported that the majority of those peptides were derived from molecules directly implicated in neoplastic transformation. Furthermore, in a study reported by Weinzierl et al. [49], that integrated mass spectrometry and microarray data on renal cell carcinomas and autologous normal kidney tissues showed poor correlation between changes in peptide expression and mRNA copy numbers in normal versus cancer cells. Neoplastic transformation is associated with many genomic and proteomic changes. How these changes may alter the MHC peptide repertoire is a critical question for cancer immunotherapy that can be addressed directly only by immunoproteomics-based analysis of the MHC peptide signature of the cancer cell. Our data supports the conclusions of Weinzierl et al [49] and Fortier et al. [16] that alterations in the MHC peptidome of the transformed or chemotherapy treated neoplastic cells is caused by post transcriptional mechanisms and only proteomics based profiling approaches would be able to determine these alterations that would otherwise be missed by estimation of only the transcript levels.

4.5. *MHC peptides as candidate ovarian cancer specific antigens*

Analysis of the peptide repertoire associated with the MHC class I molecules of cancer cells provide a source for new tumor antigens for the development of cancer immunotherapy [15]. In order to begin to evaluate the potential immunotherapy application of the peptide identified in this study for ovarian cancer vaccine development, we selected and analytically confirmed a few candidates based on the significance of their parent proteins involvement in multiple cancer pathways and specifically implicated in the development of chemo-resistant (cisplatin and other drugs) and aggressive ovarian cancer [48] (Table 2). We selected peptides which showed expression in both cisplatin-sensitive (OVCAR3) and intrinsically-resistant (SKOV3-A2) cells for T cell functional analysis, because of the need for a therapeutic vaccine applicable to ovarian cancer in general, including the drug resistant phenotype. However, levels of some of the peptides, sTRkDYPAAk (Myc proto-oncogene protein) and aLSDGVHkI (Fas apoptotic inhibitory molecule 1), were further elevated in the cisplatin-resistant cells (Table 2) indicating that the up-regulation may be specifically associated to the effect of cisplatin treatment. Increased peptide specific CD8+ T cell responses against the resistant cell types (Fig. 4) further confirm that these differentially presented peptides are immunologically relevant and have the potential to serve as immunotherapeutic antigens. Though further work is needed

Table 3 – Quantitative analysis of differentially presented MHC peptides. List of up-regulated and down-regulated MHC peptides in SKOV3-A2-CP compared to SKOV3—A2 cells, their sequences, motif's, protein names, ID's, gene ID's, Xcorr scores, number of amino acids (#AA) SYFPEITHI scores and Bimas scores, implication of parent protein in cancer and references.

Accession ID	Gene ID	Protein	Peptide sequence	XCorr	Motif	SKOV3-A2-CP (116)/SKOV3-A2 (114) ratio	AA #	SYFPEITHI score	Bimas score	Implication of parent proteins in cancer
Up-regulated										
P01106	MYC	Myc proto-oncogene protein	sTRkDYPAAk	2.8	A2	3.47	10	9	0.0	Ovarian and breast
Q6P1A2	LPCAT3	Lysophospholipid acyltransferase 5	rLIQESPTL	2.4	A2	1.63	9	25	21.4	
O00244	ATOX1	Copper transport protein ATOX1	rVLNkLGGVk	2.4	A2	1.56	10	6	0.0	
O60318	MCM3AP	80 kDa MCM3-associated protein	rILANWLKVK	2.5	A2	1.61	10	13	0.0	Breast and colorectal
O14787	TNPO2	Transportin-2	aLLGDLTkA	2.4	A2	1.73	9	26	42.3	
P08579	SNRPB2	U2 small nuclear ribonucleoprotein B″	nQFPGFkEV	2.2	A2	6.69	9	16	49.6	Breast and colorectal
Q9BYV8	TSGA14	Centrosomal protein of 41 kDa	rLDTGNSmTk	2.5	A2	1.66	10	12	0.0	
Q9NVQ4	FAIM	Fas apoptotic inhibitory molecule 1	aLSDGVHkI	3.2	A2	2.53	9	30	98.4	
Q9Y5Y0	FLVCR1	Feline leukemia virus subgroup C receptor-related protein 1	aVAPGHPLAk	3.1	A2	1.64	10	12	0.0	
O15372	EIF3H	Eukaryotic translation initiation factor 3 subunit H	rLTPkLmEV	2.9	A2	2.21	9	28	160.0	
Q96QD9	FYTTD1	UAP56-interacting factor	rTAVPSFLTk	4.0	A2	1.94	10	9	0.0	
Q14258	TRIM25	E3 ubiquitin/ISG15 ligase TRIM25	aVYQARPQLHk	4.0	A2	**1.72**	11	18	0.0	Anaplastic large cell lymphomas
P11217	PYGM	Glycogen phosphorylase, muscle form	nLAENISRV	2.7	A2	1.59	9	28	655.9	
Q9Y678	COPG	Coatomer subunit gamma	aIVDkVPSV	2.2	A2	3.64	9	29	90.2	
Q99436	PSMB7	Proteasome subunit beta type-7	rVVTANRmLk	3.0	A2	1.91	10	4	0.0	Colorectal
Q9Y5W9	SNX11	Sorting nexin-11	hTNSkAFTAk	5.1	A2	1.79	10	6	0.0	
Q14697	GANAB	Neutral alpha-glucosidase AB	hLIHEVTkV	4.5	A2	1.78	9	28	5.4	
Q02543	RPL18A	60S ribosomal protein L18a	rIFAPNHVVAk	3.8	A2	1.55	11	21	1.0	Cervix carcinoma
P46781	RPS9	40S ribosomal protein S9	gLAkSIHHA	3.7	A2	2.30	9	22	11.4	Colorectal
P84098	RPL19	60S ribosomal protein L19	iLmEHIHkL	3.7	A2	1.55	9	32	1267.1	Breast
P42766	RPL35	60S ribosomal protein L35	rVAkVTGGAASk	3.5	A2	1.66	12	13	0.1	
P63220	RPS21	40S ribosomal protein S21	nVAEVDkVTGR	3.3	A2	1.73	11	11	0.0	
			sASNRIIGAk	2.5	A2	1.51	10	11	0.0	
Q13547	HDAC1	Histone deacetylase 1	rmLPHAPGV	3.2	A2	1.50	9	24	185.9	
P13639	EEF2	Elongation factor 2	tTFEHAHNmRV	4.5	A2	3.13	11	12	0.0	
P62269	RPS18	40S ribosomal protein S18	fAITAIkGVGR	2.7	A2	2.50	11	21	0.0	
O15479	MAGEB2	Melanoma-associated antigen B2	gVYDGEEHSV	2.8	A2[a]	1.54	9			
P60709	ACTB	Actin, cytoplasmic 1	aVFPSIVGRPR	3.2	A3	3.57	11	24	0.02	Lung
P58876	HIST1H2BD	Histone H2B type 1-D	sVYVYkVLk[b]	3.4	A3	2.42	9	29	30.0	
O60814	HIST1H2BK	Histone H2B type 1-K	sVYVYkVLk[b]	3.4	A3	2.42	9	29	30.0	
P16403	HIST1H1C	Histone H1.2	gTGASGSFk	2.2	A3	1.73	9	18	3.0	Breast
			aVFPSIVGRPR	3.2	A3	3.57	11	24	0.0	
Q14204	DYNC1H1	Cytoplasmic dynein 1 heavy chain 1	sVYQIkVHR	3.4	A3	1.81	9	23	3.0	
Q0VD67	YP032	Putative uncharacterized protein LOC440356	hLNPVPIkk	2.7	A3	1.72	9	25	90.0	
P62917	RPL8	60S ribosomal protein L8	rVkLPSGSk	4.7	A3	1.66	9	29	0.9	Anaplastic large cell lymphomas
P62280	RPS11	40S ribosomal protein S11	rILSGVVTk	3.8	A3	1.65	9	34	9.0	
P47914	RPL29	60S ribosomal protein L29	rLAYIAHPkLG	3.5	A3	1.56	11	28	0.6	Breast
P62269	RPS18	40S ribosomal protein S18	tAIkGVGRR	2.9	A3	1.78	9	10	0.1	

(continued on next page)

Table 3 *(continued)*

Accession ID	Gene ID	Protein	Peptide sequence	XCorr	Motif	SKOV3-A2-CP (116)/SKOV3-A2 (114) ratio	AA #	SYFPEITHI score	Bimas score	Implication of parent proteins in cancer
P62081	RPS7	40S ribosomal protein S7	eTFSGVYkk	3.4	A3	1.65	9	12	13.5	
P26373	RPL13	60S ribosomal protein L13	aTWFNQPARk	4.3	A3	1.65	10	17	5.0	
Q6NVV1	R13AX	Putative 60S ribosomal protein L13a-like MGC87657	rmVVPAALk	4.1	A3	1.63	9	20	45.0	
O14977	AZIN1	Antizyme inhibitor 1	nTIPEVHkk	3.5	A3	1.60	9	16	6.8	
O43660	PLRG1	Pleiotropic regulator 1	aVALPLQTk	3.2	A3	1.54	9	29	4.5	
Q9BUN8	DERL1	Derlin-1	tVAVPLVGk	2.8	A3	1.67	9	25	4.5	
Q9BY32	ITPA	Inosine triphosphate pyrophosphatase	iVFVTGNAk	3.5	A3	2.18	9	26	10.0	
A0JLT2	MED19	Mediator of RNA polymerase II transcription subunit 19	rLmHIQPPk	3.2	A3	1.59	9	24	45.0	
P11926	ODC1	Ornithine decarboxylase	iLYDHAHVk	5.6	A3	1.56	9	34	100.0	Breast
P41091	EIF2S3	Eukaryotic translation initiation factor 2 subunit 3	gTIGHVAHGk	4.5	A3	1.64	10	18	10.1	
O15525	MAFG	Transcription factor MafG	aTSVITIVk	2.8	A3	2.16	9	17	3.0	
Q9UFW8	CGGBP1	CGG triplet repeat-binding protein 1	vTAPPARNR	2.5	A3	1.64	9	11	0.0	
Q9NRN9	METTL5	Methyltransferase-like protein 5	rTAVYSLHk	4.0	A3	1.57	9	18	6.0	
O00487	PSMD14	26S proteasome non-ATPase regulatory subunit 14	sLALLkmLK	2.9	A3	1.54	9	24	40.0	Anaplastic large cell lymphomas
Q9NVA1	UQCC	Ubiquinol-cytochrome c reductase complex chaperone CBP3 homolog	gVNPYILkk	4.0	A3	1.69	9	26	81.0	Breast and colorectal
Q9H3K2	GHITM	Growth hormone-inducible transmembrane protein	rVFHPAFTk	4.2	A3	1.91	9	31	45.0	
O60675	MAFK	Transcription factor MafK	tTSVITIVk	2.5	A3	1.97	9	14	3.0	
Q96SK2	TMEM209	Transmembrane protein 209	hVYNLPkGR	3.3	A3	2.20	9	20	1.0	
Q12986	NFX1	Transcriptional repressor NF-X1	rLDSNRIGR	3.3	A3	1.55	9	19	8.0	Cervical cancer
P10809	HSPD1	60 kDa heat shock protein, mitochondrial	akDVkFGAD	2.4		1.61				Anaplastic large cell lymphomas
Q14146	URB2	Unhealthy ribosome biogenesis protein 2 homolog	aVYSGISLk	2.4	A3	2.32	9	32	15.0	
Q9Y3D0	FAM96B	Protein FAM96B	aVNkQLADk	2.4	A3	1.62	9	26	3.0	
Q8N442	GUF1	GTP-binding protein GUF1 homolog	aLFDGVVSk	2.3	A3	1.63	9	32	300.0	
Q9P281	BAHCC1	BAH and coiled-coil domain-containing protein 1	aVALARQk	2.2	A3	2.23	8	N/A	N/A	
Q92817	EVPL	Envoplakin	aVAkLQAR	2.1	A3	2.44	8	N/A	N/A	Esophageal cancer
Q9H9Y6	POLR1B	DNA-directed RNA polymerase I subunit RPA2	vISPPTVPk	2.2	A3	1.85	9	25	4.5	
Q2NL82	TSR1	Pre-rRNA-processing protein TSR1 homolog	aAHRPGPLk	3.4	A3	1.76	9	19	0.3	

P46695	IER3	Radiation-inducible immediate-early gene IEX-1	vLYPRVVRR	2.9	A3	3.57	9	27	90.0	Pancreatic carcinoma
P29317	EPHA2	Ephrin type-A receptor 2	gVRLPGHQk	2.7	A3	1.63	9	30	9.0	Lung cancer
Q5JV73	FRMPD3	FERM and PDZ domain-containing protein 3	vLHTHQSPk	2.6	A3	2.18	9	23	20.0	
Q9UBR1	UPB1	Beta-ureidopropionase	vLYGKELRKLDL	2.4	A3	1.62	12	30	0.7	
P62306	SNRPF	Small nuclear ribonucleoprotein F	lTGkPVmVk	2.4	A3	1.67	9	15	9.0	
O15446	CD3EAP	DNA-directed RNA polymerase I subunit RPA34	vLFPSTTkk	2.3	A3	1.64	9	24	150.0	
Q8N983	MRPL43	39S ribosomal protein L43, mitochondrial	rRNPGVVIY	2.7	B35	1.66	9	N/A, N/A	0.4, 22.4	
Q96SB8	SMC6	Structural maintenance of chromosomes protein 6	aYRQGHFTY	3.6	B35	1.53	9	N/A, N/A	0.6, 12	Colorectal cancer
P35579	MYH9	Myosin-9	lEAHIDSANkNRD	2.6	B18	5.67	13	12		Lung, prostate , breast and colorectal
Q9NP99	TREM1	Triggering receptor expressed on myeloid cells 1	lEKFASSQkA	2.6	B18	1.53	9	10	N/A	Breast and colorectal
O95835	LATS1	Serine/threonine–protein kinase LATS1	yESISkPS	2.4	B18	1.81	8	12	N/A	Multiple cancers
Down-regulated										
P62805	HIST1H4A	Histone H4	nIQGITkPAIRR	3.0	A2	0.65	12	15	1.435	Lung cancer
Q5JTW2	CEP78	Centrosomal protein of 78 kDa	sVkEPSKTAk	3.5	A2	0.51	10	8	0	
P13693	TPT1	Translationally-controlled tumor protein	kLEEQRPERVk	2.8	A2	0.65	11	22	31.3	Prostate cancer
Q96NU1	SAMD11	Sterile alpha motif domain-containing protein 11	gLRPAGDLLGk	2.6	A2	0.59	11	23	0.006	
Q01082	SPTBN1	Spectrin beta chain, brain 1	lINSGHSDAAT	2.6	A2	0.52	11	17	0.569	Cervical cancer
Q6PF15	KLHL35	Kelch-like protein 35	HTWIkVASLHk	2.8	A2	0.64	11	24	0	
P51665	PSMD7	26S proteasome non-ATPase regulatory subunit 7	RIGkVGNQk	3.3	A3	0.46	9	29	3	
Q14839	CHD4	Chromodomain-helicase-DNA-binding protein 4	sLYKEGHSk	3.9	A3	0.61	9	30	100	
P04844	RPN2	Dolichyl-diphosphooligosaccharide–protein glycosyltransferase subunit 2	rVTYPAKAk	3.9	A3	0.51	9	28	1.5	Cervical cancer
P05114	HMGN1	Non-histone chromosomal protein HMG-14	rLSAKPPAk	3.8	A3	0.62	9	29	20	
Q9NUT2	ABCB8	ATP-binding cassette sub-family B member 8, mitochondrial	lLGPmVLSk	2.4	A3	0.52	9	28	180	Breast and colorectal
Q8WVF1	OSCP1	Protein OSCP1	rLAHASImk	2.7	A3	0.67	9	26	40	Nasopharyngeal carcinoma
Q04864	REL	Proto-oncogene c-Rel	PVTVkMQLRRP	2.4	A3	0.65	11	17	0.08	

Small amino acid letters denote the site of modification by iTRAQ labeling reagent.

[a] This peptide was confirmed to have normal binding affinity to HLA-A2 molecule [38].

[b] This peptide could be originated from two different histone proteins.

Table 4 – Quantitative analysis of differentially presented MHC peptides. List of up-regulated and down-regulated MHC peptides in SKOV3-A2 and SKOV3-A2-CP cells compared to OVCAR3 cells, their sequences, motif's, protein names, ID's, gene ID's, Xcorr scores, number of amino acids (#AA) SYFPEITHI scores and Bimas.

Accession ID	Gene ID	Protein	Peptide sequence	XCorr	Motif	SKOV3-A2(114)/ OVCAR3 (115) ratio	SKOV3-A2-CP (116)/ OVCAR3 (115) ratio	#AA	SYFPEITHI score	Bimas score
Up-regulated										
P54315	PNLIPRP1	Pancreatic lipase-related protein 1	kVGATKITVQk	4.2	A2	43.51	60.07	11	17	0.00
P39019	RPS19	40S ribosomal protein S19	rIAGQVAAANkkH	5.1	A2	1.56	1.88	13	23	0.01
P62888	RPL30	60S ribosomal protein L30	iIRSMPEQTGEk	3.7	A2	3.26	3.59	12	16	0.001
P22307	SCP2	Non-specific lipid-transfer protein	rVFVVGVGmTk	5.3	A2	2.86	4.49	11	12	0.721
P58876	HIST1H2BD	Histone H2B type 1-D	AmGImNSFVNDIFER	3.2	A2			15	25	46.389
			gTkAVTkYTSSk	2.4	A2	2.32	3.01	12	10	0.001
O60814	HIST1H2BK	Histone H2B type 1-K	AmGImNSFVNDIFER	3.2	A2			15	25	46.389
			gTkAVTkYTSAk	2.3	A2	5.83	5.77	12	12	0.1
P08238	HSP90AB1	Heat shock protein HSP 90-beta	ILDKkVEkV	2.7	A2	3.18	2.99	9	29	53.302
P84098	RPL19	60S ribosomal protein L19	iLmEHIHkL	3.7	A2	7.93	12.31	9	32	1267.104
Q14697	GANAB	Neutral alpha-glucosidase AB	hLIHEVTkV	4.5	A2	3.70	6.60	9	28	5.439
Q8WZ42	TTN	Titin	SAKLKVEAVkIk	2.3	A2	7.19	8.22	12	22	0.054
P42766	RPL35	60S ribosomal protein L35	rVAkVTGGAASk	3.5	A2	3.93	6.53	12	13	0.057
Q9NU23	LYRM2	LYR motif-containing protein 2	rLPPATLTLk	3.4	A2	2.78	4.33	10	16	0.034
P63220	RPS21	40S ribosomal protein S21	nVAEVDkVTGR	3.3	A2	8.28	14.29	11	11	0.027
			sASNRIIGAk	2.5	A2	8.43	12.76	10	11	0
O14775	GNB5	Guanine nucleotide-binding protein subunit beta-5	iLFGHENRV	3.2	A2	100.00	85.00	9	26	437.482
Q02224	CENPE	Centromere-associated protein E	rVFHGNETTk	4.8	A2	96.00	100.00	10	7	0.005
P62829	RPL23	60S ribosomal protein L23	tVkkGKPELR	2.7	A2	7.44	6.03	10	3	0
P21333	FLNA	Filamin-A	vLFAGQHIAk	4.3	A2	44.40	41.80	10	13	0.094
O75381	PEX14	Peroxisomal membrane protein PEX14	rVRQSPLATR	3.8	A2	6.18	6.80	10	12	0
Q9HBR0	SLC38A10	Putative sodium-coupled neutral amino acid transporter 10	rLGEAEGLmkV	3.6	A2	2.15	2.73	11	23	0.114
			eVAATGTSILk	2.5	A2	7.78	9.23	11	21	0.057
Q86XT4	TRIM50	E3 ubiquitin-protein ligase TRIM50	rLGVIKGTASRk	3.2	A2	100.00	94.00	12	16	0.075
Q5VYK3	ECM29	Proteasome-associated protein ECM29 homolog	nLAEkPKTV	3.2	A2	10.08	8.29	9	26	285.163
P33316	DUT	Deoxyuridine 5′-triphosphate nucleotidohydrolase, mitochondrial	rVAPRSGLAAk	3.4	A2	3.58	4.49	11	12	0.4
Q99436	PSMB7	Proteasome subunit beta type-7	rVVTANRmLk	3.0	A2	2.85	5.45	10	4	0.0
Q9Y5W9	SNX11	Sorting nexin-11	hTNSkAFTAk	5.1	A2	18.69	33.41	10	None	
P83731	RPL24	60S ribosomal protein L24	rAITGASLAD	2.2	A2	4.70	5.50	10	8	0
P49841	GSK3B	Glycogen synthase kinase-3 beta	rLLEYTPTAR	4.5	A2	3.81	4.17	10	15	0.226
P0C7M2	HNRPA1L3	Putative heterogeneous nuclear ribonucleoprotein A1-like 3	amNARPHkV	2.8	A2	15.72	16.23	9	24	50.232
Q5T653	MRPL2	39S ribosomal protein L2, mitochondrial	rTkYTITPVk	3.9	A2	18.66	26.00	10	3	0
Q02543	RPL18A	60S ribosomal protein L18a	rIFAPNHVVAk	3.8	A2	6.36	9.89	11	21	1.036
Q06787	FMR1	Fragile × mental retardation 1 protein	sVNPNkPATk	3.1	A2	89.00	100.00	10	13	0.001
P11217	PYGM	Glycogen phosphorylase, muscle form	nLAENISRV	2.7	A2	14.91	23.73	9	28	655.875
O00299	CLIC1	Chloride intracellular channel protein 1	tIPEAFRGVHR	2.5	A2	3.46	5.24	11	21	0.009
P0C7U0	ELFN1	Extracellular leucine-rich repeat and fibronectin type-III domain-containing protein 1	tLLHAGGLARA	3.0	A2	3.64	3.92	11	22	19.425
Q96PK2	MACF1	Microtubule-actin cross-linking factor 1, isoform4	gLIDRQVTV	2.1	A2	1.62	2.19	9	28	285.163

Up-regulated										
Q5VSL9	FAM40A	Protein FAM40A	iVkAISAVLL	2.6	A2	2.28	3.01	10	17	0.111
Q9NUB1	ACSS1	Acetyl-coenzyme A synthetase 2-like, mitochondrial	tTCRLANTLk	2.7	A2	6.81	7.27	10	4	0
O95721	SNAP29	Synaptosomal-associated protein 29	dAYPkNPHLR	3.5	A2	5.03	5.33	10	7	0
Q5JTW2	CEP78	Centrosomal protein of 78 kDa	sVkEPSKTAk	3.5	A2	13.05	6.64	10	8	0
Q8WVZ7	RNF133	E3 ubiquitin-protein ligase RNF133	gVFGRSSTLk	2.4	A2	49.83	58.04	10	8	0.005
O15511	ARPC5	Actin-related protein 2/3 complex subunit 5	aLkNPPINTk	4.9	A2	100.00	101.39	10	18	0.001
Q9Y283	INVS	Inversin	aLSGHVSTVk	3.1	A2	12.50	12.52	10	14	0.006
P30622	CLIP1	CAP-Gly domain-containing linker protein 1	gLFAPVHkV	3.0	A2	2.43	2.76	9	30	591.888
P13639	EEF2	Elongation factor 2	tTFEHAHNmRV	4.5	A2	4.21	13.21	11	12	0.003
P53621	COPA	Coatomer subunit alpha	gLkNGVPAV	2.4	A2	4.24	5.48	9	28	5.599
P62269	RPS18	40S ribosomal protein S18	fAITAIkGVGR	2.7	A2	5.39	13.49	11	21	0.002
Q96QD9	FYTTD1	UAP56-interacting factor	rTAVPSFLTk	4.0	A2	1.72	3.33	10	9	0
Q5T160	RARS2	Probable arginyl-tRNA synthetase, mitochondrial	LTLSHLAAVAHk	2.5	A2	75.71	100.00	12	25	0.178
Q9Y4C2	FAM115A	Protein FAM115A	rIYLSkGPNVk	2.6	A2	4.46	4.67	11	20	30.603
Q14258	TRIM25	E3 ubiquitin/ISG15 ligase TRIM25	aVYQARPQLHk	4.0	A2	5.22	8.97	11	18	0.021
P07195	LDHB	L-lactate dehydrogenase B chain	rIHPVSTmVk	4.0	A2	5.20	6.96	10	10	0.001
Q92540	SMG7	Protein SMG7	CTLEKLQETGk	2.5	A2	9.15	10.11	11	19	0.008
Q13098	GPS1	COP9 signalosome complex subunit 1	yLAPHVRTL	3.6	A2	9.21	12.45	9	32	45.203
Q9NVQ4	FAIM	Fas apoptotic inhibitory molecule 1	aLSDGVHkI	3.2	A2	1.93	4.90	9	30	98.381
Q8N4Q1	CHCHD4	Mitochondrial intermembrane space import and assembly protein 40	eTAPIEATATk	3.3	A2	9.01	13.36	11	13	0.008
Q9Y5Y0	FLVCR1	Feline leukemia virus subgroup C receptor-related protein 1	aVAPGHPLAk	3.1	A2	33.45	54.95	10	12	0.001
Q9UJ78	ZMYM5	Zinc finger MYM-type protein 5	sIQPPSISAPAIA	3.0	A2	8.76	8.20	13	19	0.856
Q49MG5	MAP9	Microtubule-associated protein 9	iLISTSATASSk	3.0	A2	11.20	13.23	12	22	0.127
Q96DB5	FAM82B	Regulator of microtubule dynamics protein 1	eTYQVISQAAV	2.9	A2	6.82	7.17	11	15	0.017
O00192	ARVCF	Armadillo repeat protein deleted in velo-cardio-facial syndrome	lLDHPRAEV	2.8	A2	6.97	8.42	9	27	47.295
Q15154	PCM1	Pericentriolar material 1 protein	eVYDGPkNVR	2.8	A2	16.69	18.48	10	4	0.004
Q8NCM8	DYNC2H1	Cytoplasmic dynein 2 heavy chain 1	iTYESPPGLkk	3.6	A2	13.67	18.76	11	21	0.001
Q13547	HDAC1	Histone deacetylase 1	rmLPHAPGV	3.2	A2	3.04	4.57	9	24	185.858
P00403	MT-CO2	Cytochrome c oxidase subunit 2	eVNDPSLTIk	2.8	A2	100.00	147.17	10	7	0
P63218	GNG5	Guanine nucleotide-binding protein G(I)/G(S)/G(O) subunit gamma-5	rVkVSQAAADLk	2.9	A2	3.00	3.99	12	17	0.05
Q96HS1	PGAM5	Serine/threonine-protein phosphatase PGAM5, mitochondrial	aVAVGkPRAGGD	2.7	A2	2.95	3.91	12	15	0.002
P13693	TPT1	Translationally-controlled tumor protein	kLEEQRPERVk	2.8	A2	30.02	19.47	11	22	31.3
O95347	SMC2	Structural maintenance of chromosomes protein 2	dVFDPHGTLSGGAR	2.8	A2	10.97	10.92	14	18	0.007
P26639	TARS	Threonyl-tRNA synthetase, cytoplasmic	gLADNTVIAkV	2.8	A2	29.05	49.49	11	24	1.511
Q5TB30	DEPDC1A	DEP domain-containing protein 1A	lLQPHLERV	2.7	A2	2.20	2.40	9	28	133.255
Q96NU1	SAMD11	Sterile alpha motif domain-containing protein 11	gLRPAGDLLGk	2.6	A2	100.00	59.14	11	23	0.006
O15372	EIF3H	Eukaryotic translation initiation factor 3 subunit H	rLTPkLmEV	2.9	A2	1.73	3.83	9	28	159.97
Q96CS2	HAUS1	HAUS augmin-like complex subunit 1	rLkQQTIPLk	2.7	A2	7.40	9.01	10	14	0.001
Q9H7M9	C10orf54	Platelet receptor Gi24	LAASLGPVAAFk	2.6	A2	2.57	3.00	12	16	0.117
O95777	LSM8	U6 snRNA-associated Sm-like protein LSm8	iLDESHERV	2.5	A2	16.03	17.86	9	24	95.016
O95235	KIF20A	Kinesin-like protein KIF20A	eMkKLSLLNG	2.6	A2	42.14	48.99	10	9	0
Q9H920	RNF121	RING finger protein 121	lIYKISYATGIV	2.6	A2	34.22	34.12	12	20	0.084

(continued on next page)

Table 4 *(continued)*

Accession ID	Gene ID	Protein	Peptide sequence	XCorr	Motif	SKOV3-A2(114)/ OVCAR3 (115) ratio	SKOV3-A2-CP (116)/ OVCAR3 (115) ratio	#AA	SYFPEITHI score	Bimas score
P29353	SHC1	SHC-transforming protein 1	rVPPPPQSV	2.6	A2	3.59	5.11	9	19	6.086
P10809	HSPD1	60 kDa heat shock protein, mitochondrial	yAkDVkFGAD	2.5	A2	5.07	6.83	10	7	0
Q5JW98	FAM26D	Protein FAM26D	aAEQHSRLLm	2.7	A2	40.37	43.55	10	10	0.004
A8MUV8	ZNF727	Putative zinc finger protein 727	gLAIFKPDLI	2.4	A2	100.00	106.90	10	21	5.112
O43524	FOXO3	Forkhead box protein O3	rAAkkkAALQ	2.5	A2	1.58	2.06	10	8	0
Q8IZT6	ASPM	Abnormal spindle-like microcephaly-associated protein	ImKKAALLIQk	2.5	A2	4.61	5.17	11	18	0.001
P23246	SFPQ	Splicing factor, proline- and glutamine-rich	iVDDRGRSTGk	2.6	A2	20.83	18.92	11	13	0.018
P33991	MCM4	DNA replication licensing factor MCM4	rVNPRVSNVk	2.6	A2	4.82	4.59	10	8	0.001
Q01082	SPTBN1	Spectrin beta chain, brain 1	lINSGHSDAAT	2.6	A2	12.40	6.50	11	17	0.569
Q9BWE0	REPIN1	Replication initiator 1	aLEEAAAkALGP	2.5	A2	72.78	100.00			
Q63ZY3	KANK2	KN motif and ankyrin repeat domain-containing protein 2	eVADPTAHRR	2.3	A2	12.99	13.61	10	5	0
Q9BYV8	TSGA14	Centrosomal protein of 41 kDa	rLDTGNSmTk	2.5	A2	4.79	7.94	10	12	0.006
Q9UM00	TMCO1	Transmembrane and coiled-coil domain-containing protein 1	sIFDGRVVAk	2.4	A2	100.00	73.00	10	19	0.072
Q16512	PKN1	Serine/threonine-protein kinase N1	fLDNERHEV	2.4	A2	4.94	5.06	9	24	127.976
Q9Y6K5	OAS3	2′-5′-oligoadenylate synthetase 3	sLAEGLRTV	2.1	A2	1.74	1.68	9	34	131.175
O14980	XPO1	Exportin-1	vLIDYQRNV	2.1	A2	11.34	11.90	9	25	96.955
A6NMY6	ANXA2P2	Putative annexin A2-like protein	aLSGHLETV	2.2	A2	2.51	3.33	9	30	78.385
P56270	MAZ	Myc-associated zinc finger protein	hLNSHVRQV	3.9	A2	2.58	3.21	9	25	1.088
P34925	RYK	Tyrosine-protein kinase RYK	aLSRDLFPmD	2.3	A2	1.56	1.71	10	13	0.028
Q68D10	SPTY2D1	Protein SPT2 homolog	gLGPPGRSV	2.2	A2	3.09	3.23	9	26	13.91
Q9Y675	SNURF	SNRPN upstream reading frame protein	hVPEVEVQVkR	3.3	A2	2.71	3.83	11	18	0
Q09019	DMWD	*Dystrophia myotonica* WD repeat-containing protein	vLYPHPPLAR	3.2	A2	6.66	6.09	10	16	0.081
Q99715	COL12A1	Collagen alpha-1 (XII) chain	IkAADAKELk	3.2	A2	4.15	6.23	10	4	0
Q9BXR0	QTRT1	Queuine tRNA-ribosyltransferase	gLRPGPELIQk	3.1	A2	5.49	8.19	11	23	0
P46776	RPL27A	60S ribosomal protein L27a	kLPkQPVIVk	3.1	A2	2.88	3.03	10	15	0.049
Q9NV56	MRGBP	MRG-binding protein	dVFSSSGSLGk	3.0	A2	23.08	15.69	11	16	0.002
Q5T6V5	C9orf64	UPF0553 protein C9orf64	dVFIDSGGVRR	2.9	A2	5.11	7.03	11	15	0
O95573	ACSL3	Long-chain-fatty-acid--CoA ligase 3	hVSSkPSTmk	2.9	A2	100.00	87.00	10	4	0
P52948	NUP98	Nuclear pore complex protein Nup98–Nup96	rLkPTNPAAQk	2.9	A2	95.16	100.00	11	17	0.001
Q6PF15	KLHL35	Kelch-like protein 35	HTWIkVASLHk	2.8	A2	4.91	3.12	11	24	0

Q8TCP9	C7orf38	Uncharacterized protein C7orf38	FLVEkQSHLANIF	2.8	A2	50.63	49.61	13	24	93.696
O75747	PIK3C2G	Phosphatidylinositol-4-phosphate 3-kinase C2 domain-containing subunit gamma	LQGHVLMLIVKSk	2.8	A2	2.22	2.23	13	17	11.305
P01106	MYC	Myc proto-oncogene protein	sTRkDYPAAk	2.8	A2	8.82	30.58	10	9	0
Q15042	RAB3GAP1	Rab3 GTPase-activating protein catalytic subunit	sVSNmVHTAk	2.6	A2	37.34	25.88	10	7	0.001
Q9Y5V0	ZNF706	Zinc finger protein 706	rTQmPDPkTFk	2.6	A2	2.80	3.56	11	12	0.031
P11532	DMD	Dystrophin	RIKTGkASIPLk	2.6	A2	11.09	14.66	12	21	0.05
O60318	MCM3AP	80 kDa MCM3-associated protein	rILANWLKVK	2.5	A2	3.75	6.03	10	13	0.007
Q96RT8	TUBGCP5	Gamma-tubulin complex component 5	FVkEAImkVL	2.5	A2	6.24	6.67	10	15	1.164
Q15121	PEA15	Astrocytic phosphoprotein PEA-15	vVDYRTRVLk	2.4	A2	26.12	31.53	10	6	0.001
Q9P2G1	ANKIB1	Ankyrin repeat and IBR domain-containing protein 1	qIYENNPQLk	2.4	A2	22.02	31.21	10	11	0.027
O14787	TNPO2	Transportin-2	aLLGDLTkA	2.4	A2	7.50	12.96	9	26	42.278
P20132	SDS	L-serine dehydratase/L-threonine deaminase	qLGVPATIVVPSTTP	2.4	A2	4.52	4.92	15	21	28.516
O00244	ATOX1	Copper transport protein ATOX1	rVLNkLGGVk	2.4	A2	17.77	27.65	10	6	0
Q9Y4E8	USP15	Ubiquitin carboxyl-terminal hydrolase 15	gTWPRGPSTPk	2.3	A2	6.07	7.25	11	15	0.002
O43511	SLC26A4	Pendrin	tTALSRTAVQ	2.0	A2	4.75	6.70	10	8	0
P22090	RPS4Y1	40S ribosomal protein S4, Y isoform 1	hTNSkAFTAk	5.1	A2	18.69	33.41	10	6	0
P09237	MMP7	Matrilysin	lPGSLALPLPQ	2.9	B7	52.10	100.00	11	24	0.2
Q15785	TOMM34	Mitochondrial import receptor subunit TOM34	lPSENHkEm	2.3	B7	4.09	4.20	9	18	20
Down-regulated										
P05783	KRT18	Keratin, type I cytoskeletal 18	rLAADDFRV	3.8	A2	0.45	0.57	9	22	403.402
P62805	HIST1H4A	Histone H4	nIQGITkPAIRR	3.0	A2	0.60	0.39	12	15	1.435
Q04637	EIF4G1	Eukaryotic translation initiation factor 4 gamma 1	aARPATSTL	2.7	A2	0.17	0.18	9	22	0.023
P16403	HIST1H1C	Histone H1.2	aASkERSGVSL	2.5	A2	0.05	0.04	11	17	0.02
Q53H82	LACTB2	Beta-lactamase-like protein 2	rLSNRVVRV	2.5	A2	0.45	0.45	9	26	159.97
Q6P1A2	LPCAT3	Lysophospholipid acyltransferase 5	rLIQESPTL	2.4	A2	0.62	1.01	9	25	21.362
Q9UBU8	MORF4L1	Mortality factor 4-like protein 1	aPPEYHRkAV	2.8	B7	0.15	0.15	10	20	18
P22090	RPS4Y1	40S ribosomal protein S4, Y isoform 1	rPkEGTSTL	2.7	B7	0.50	0.53	9	22	80
P57086	SCAND1	SCAN domain-containing protein 1	gPREAFRQL	2.5	B7	0.40	0.37	9	23	800
P48444	ARCN1	Coatomer subunit delta	rPSGPSkAL	4.5	B7	0.30	0.33	9	29	120
P04818	TYMS	Thymidylate synthase	ePRPPHGEL	3.5	B7	0.37	0.42	9	27	1200
O94964	C20orf117	Uncharacterized protein C20orf117	aPHSRETEL	3.1	B7	0.33	0.27	9	23	240
Q9P2P1	NYNRIN	Protein NYNRIN	aPRQPPRHL	3.0	B7	0.46	0.55	9	27	3600

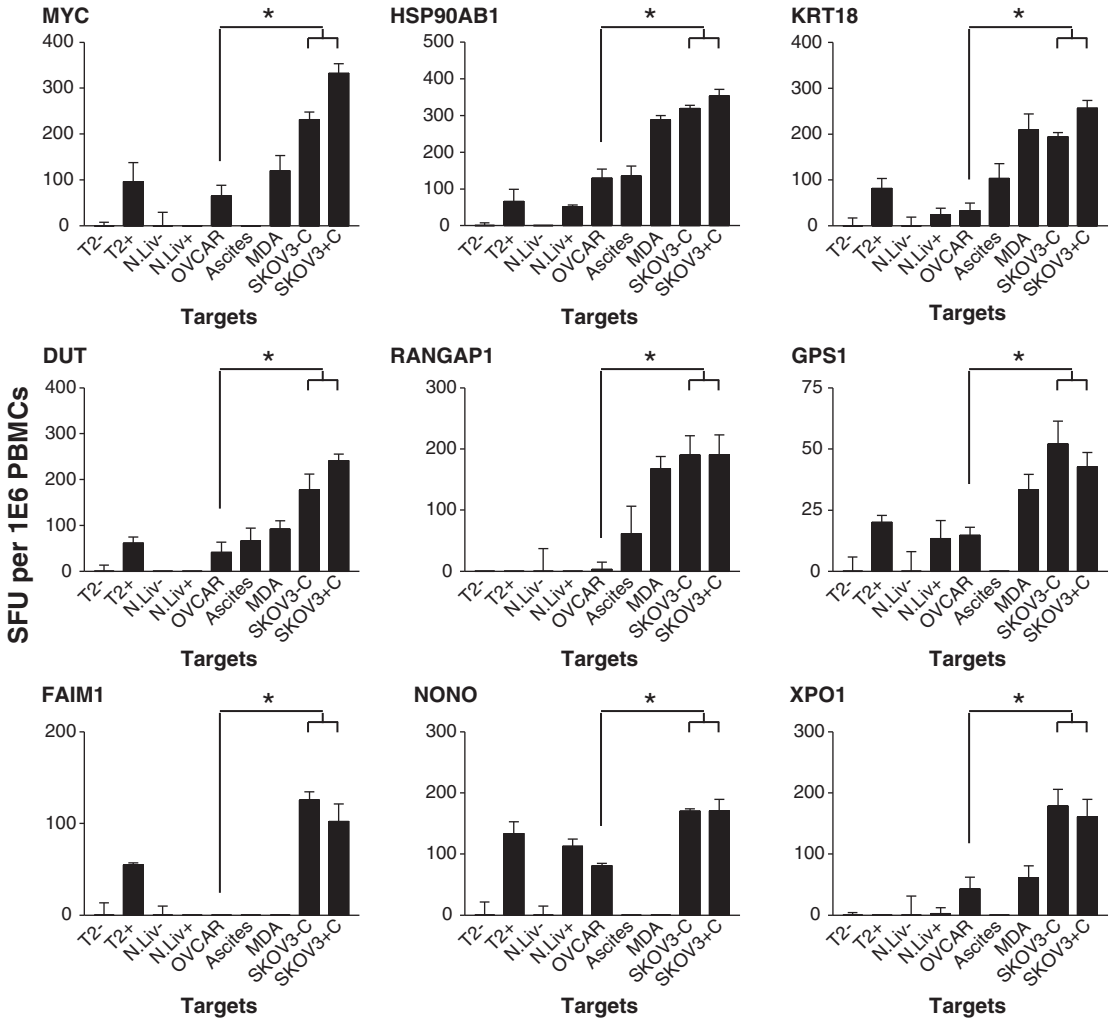

Fig. 4 – Cytotoxic T cells generated against differentially presented peptides recognize both cisplatin-resistant and sensitive ovarian cancer cells. PBMC from healthy HLA-A2+ donors were stimulated in vitro with synthetic peptides corresponding to each of the ovarian cancer epitopes. These cells were analyzed in an ELISpot assay using T2 cells loaded with the synthetic peptides, normal cells suspensions obtained from HLA-A2+ healthy liver tissues and HLA-A2+ ovarian and breast cancer cells. IFN-γ-producing cells were quantitated using an immunospot reader. Error bars represent SEM of experimental replicates normalized to negative controls. Asterisks denote p-values between OVCAR and SKOV3-A2+/– cisplatin treatment. All p-values are <.01.

to evaluate the therapeutic value of vaccination with these peptides, our results strongly support the concept that high-throughput analysis of the MHC peptide repertoire is a promising discovery platform for the identification of tumor associated antigens for cancer therapeutics and diagnostics [50].

5. Conclusions

In this study, we demonstrated that many novel MHCI peptides are processed and presented on ovarian cancer cells and cisplatin treatment of resistant ovarian cancer cells further enhanced the presentation of numerous MHCI peptides of various HLA types using the immunoproteomics approach. Furthermore, we demonstrated CTLs specific for the selected differentially presented peptides recognize the intrinsically-resistant ovarian cancer cells significantly higher than the sensitive cells. The MHCI peptidome, including the differentially presented MHCI peptides identified in our study, will contribute valuable information to the understanding of the cisplatin effect on ovarian cancer and potentially form the basis for the development of an immunotherapeutic strategy for the treatment of cisplatin-resistant ovarian cancer.

Supplementary data to this article can be found online at doi:10.1016/j.jprot.2012.03.044.

Acknowledgments

This work was supported by DOD grant #W81XWH-08-1-0224 and by the Immunotope corporate funding source.

REFERENCES

[1] Jemal A, Siegel R, Xu J, Ward E. Cancer statistics, 2010. CA Cancer J Clin 2010;60:277–300.

[2] Zhang Z, Bast Jr RC, Yu Y, Li J, Sokoll LJ, Rai AJ, et al. Three biomarkers identified from serum proteomic analysis for the detection of early stage ovarian cancer. Cancer Res 2004;64: 5882–90.

[3] Ozols RF. Systemic therapy for ovarian cancer: current status and new treatments. Semin Oncol 2006;33:S3–S11.

[4] Henkels KM, Turchi JJ. Induction of apoptosis in cisplatin-sensitive and -resistant human ovarian cancer cell lines. Cancer Res 1997;57:4488–92.

[5] Zhang L, Conejo-Garcia JR, Katsaros D, Gimotty PA, Massobrio M, Regnani G, et al. Intratumoral T cells, recurrence, and survival in epithelial ovarian cancer. N Engl J Med 2003;348:203–13.

[6] Babcock B, Anderson BW, Papayannopoulos I, Castilleja A, Murray JL, Stifani S, et al. Ovarian and breast cytotoxic T lymphocytes can recognize peptides from the amino enhancer of split protein of the Notch complex. Mol Immunol 1998;35:1121–33.

[7] Yoshino I, Peoples GE, Goedegebuure PS, Maziarz R, Eberlein TJ. Association of HER2/neu expression with sensitivity to tumor-specific CTL in human ovarian cancer. J Immunol 1994;152:2393–400.

[8] Ramakrishna V, Ross MM, Petersson M, Gatlin CC, Lyons CE, Miller CL, et al. Naturally occurring peptides associated with HLA-A2 in ovarian cancer cell lines identified by mass spectrometry are targets of HLA-A2-restricted cytotoxic T cells. Int Immunol 2003;15:751–63.

[9] Fisk B, Blevins TL, Wharton JT, Ioannides CG. Identification of an immunodominant peptide of HER-2/neu protooncogene recognized by ovarian tumor-specific cytotoxic T lymphocyte lines. J Exp Med 1995;181:2109–17.

[10] Ioannides CG, Fisk B, Pollack MS, Frazier ML, Taylor Wharton J, Freedman RS. Cytotoxic T-cell clones isolated from ovarian tumour infiltrating lymphocytes recognize common determinants on non-ovarian tumour clones. Scand J Immunol 1993;37:413–24.

[11] Brossart P, Wirths S, Stuhler G, Reichardt VL, Kanz L, Brugger W. Induction of cytotoxic T-lymphocyte responses in vivo after vaccinations with peptide-pulsed dendritic cells. Blood 2000;96:3102–8.

[12] Hwu P, Freedman RS. The immunotherapy of patients with ovarian cancer. J Immunother 2002;25:189–201.

[13] Morse MA, Nair SK, Mosca PJ, Hobeika AC, Clay TM, Deng Y, et al. Immunotherapy with autologous, human dendritic cells transfected with carcinoembryonic antigen mRNA. Cancer Invest 2003;21:341–9.

[14] Wagner U, Schlebusch H, Kohler S, Schmolling J, Grunn U, Krebs D. Immunological responses to the tumor-associated antigen CA125 in patients with advanced ovarian cancer induced by the murine monoclonal anti-idiotype vaccine ACA125. Hybridoma 1997;16:33–40.

[15] Admon A, Barnea E, Ziv T. Tumor antigens and proteomics from the point of view of the major histocompatibility complex peptides. Mol Cell Proteomics 2003;2:388–98.

[16] Fortier MH, Caron E, Hardy MP, Voisin G, Lemieux S, Perreault C, et al. The MHC class I peptide repertoire is molded by the transcriptome. J Exp Med 2008;205:595–610.

[17] Shetty V, Sinnathamby G, Nickens Z, Shah P, Hafner J, Mariello L, et al. MHC class I-presented lung cancer-associated tumor antigens identified by immunoproteomics analysis are targets for cancer-specific T cell response. J Proteomics 2011;74:728–43.

[18] Hunt DF, Henderson RA, Shabanowitz J, Sakaguchi K, Michel H, Sevilir N, et al. Characterization of peptides bound to the class I MHC molecule HLA-A2.1 by mass spectrometry. Science 1992;255:1261–3.

[19] Bonner PL, Lill JR, Hill S, Creaser CS, Rees RC. Electrospray mass spectrometry for the identification of MHC class I-associated peptides expressed on cancer cells. J Immunol Methods 2002;262:5–19.

[20] Engelhard VH, Brickner AG, Zarling AL. Insights into antigen processing gained by direct analysis of the naturally processed class I MHC associated peptide repertoire. Mol Immunol 2002;39:127–37.

[21] Ross PL, Huang YN, Marchese JN, Williamson B, Parker K, Hattan S, et al. Multiplexed protein quantitation in *Saccharomyces cerevisiae* using amine-reactive isobaric tagging reagents. Mol Cell Proteomics 2004;3:1154–69.

[22] Schmidt F, Hustoft HK, Strozynski M, Dimmler C, Rudel T, Thiede B. Quantitative proteome analysis of cisplatin-induced apoptotic Jurkat T cells by stable isotope labeling with amino acids in cell culture, SDS-PAGE, and LC-MALDI-TOF/TOF MS. Electrophoresis 2007;28:4359–68.

[23] Wang HX, Sun W, Li HL, Zhang WY. Quantitative differences in protein expression between cisplatin sensitive C0C1 ovarian carcinoma cells and cisplatin resistant C0C1/DDP cells. Chin Med J (Engl) 2009;122:865–9.

[24] Flick DA, Gifford GE. Comparison of in vitro cell cytotoxic assays for tumor necrosis factor. J Immunol Methods 1984;68:167–75.

[25] Rammensee H, Bachmann J, Emmerich NP, Bachor OA, Stevanovic S. SYFPEITHI: database for MHC ligands and peptide motifs. Immunogenetics 1999;50:213–9.

[26] Parker KC, Bednarek MA, Coligan JE. Scheme for ranking potential HLA-A2 binding peptides based on independent binding of individual peptide side-chains. J Immunol 1994;152:163–75.

[27] Pyndiah S, Tanida S, Ahmed KM, Cassimere EK, Choe C, Sakamuro D. c-MYC suppresses BIN1 to release poly (ADP-ribose) polymerase 1: a mechanism by which cancer cells acquire cisplatin resistance. Sci Signal 2011;4:ra19.

[28] Kim DY, Kim MJ, Kim HB, Lee JW, Bae JH, Kim DW, et al. Suppression of multidrug resistance by treatment with TRAIL in human ovarian and breast cancer cells with high level of c-Myc. Biochim Biophys Acta 2011;1812:796–805.

[29] Bertram J, Palfner K, Hiddemann W, Kneba M. Increase of P-glycoprotein-mediated drug resistance by hsp 90 beta. Anticancer Drugs 1996;7:838–45.

[30] Parekh HK, Simpkins H. The differential expression of cytokeratin 18 in cisplatin-sensitive and -resistant human ovarian adenocarcinoma cells and its association with drug sensitivity. Cancer Res 1995;55:5203–6.

[31] Urbani A, Poland J, Bernardini S, Bellincampi L, Biroccio A, Schnolzer M, et al. A proteomic investigation into etoposide chemo-resistance of neuroblastoma cell lines. Proteomics 2005;5:796–804.

[32] Gong F, Peng X, Zeng Z, Yu M, Zhao Y, Tong A. Proteomic analysis of cisplatin resistance in human ovarian cancer using 2-DE method. Mol Cell Biochem 2011;348:141–7.

[33] Li HX. Expression of COP9, JAK2, HSP and NADH in ovarian carcinoma tissues after taxol-chemotherapy and their significance. Zhonghua Fu Chan Ke Za Zhi 2008;43:528–32.

[34] Jenkins CC, Mata J, Crane RF, Thomas B, Akoulitchev A, Bahler J, et al. Activation of AP-1-dependent transcription by a truncated translation initiation factor. Eukaryot Cell 2005;4: 1840–50.

[35] Sengupta S, den Boon JA, Chen IH, Newton MA, Dahl DB, Chen M, et al. Genome-wide expression profiling reveals EBV-associated inhibition of MHC class I expression in nasopharyngeal carcinoma. Cancer Res 2006;66:7999–8006.

[36] Brieger A, Adam R, Passmann S, Plotz G, Zeuzem S, Trojan J. A CRM1-dependent nuclear export pathway is involved in the regulation of MutLalpha subcellular localization. Genes Chromosomes Cancer 2011;50:59–70.

[37] Sumi K, Tago K, Kasahara T, Funakoshi-Tago M. Aurora kinase A critically contributes to the resistance to anti-cancer drug cisplatin in JAK2 V617F mutant-induced transformed cells. FEBS Lett 2011;585:1884–90.
[38] Barnea E, Beer I, Patoka R, Ziv T, Kessler O, Tzehoval E, et al. Analysis of endogenous peptides bound by soluble MHC class I molecules: a novel approach for identifying tumor-specific antigens. Eur J Immunol 2002;32:213–22.
[39] Boon T, Coulie PG, Van den Eynde B. Tumor antigens recognized by T cells. Immunol Today 1997;18:267–8.
[40] Morse MA, Secord AA, Blackwell K, Hobeika AC, Sinnathamby G, Osada T, et al. MHC class I-presented tumor antigens identified in ovarian cancer by immunoproteomic analysis are targets for T-cell responses against breast and ovarian cancer. Clin Cancer Res 2011;17:3408–19.
[41] Weinschenk T, Gouttefangeas C, Schirle M, Obermayr F, Walter S, Schoor O, et al. Integrated functional genomics approach for the design of patient-individual antitumor vaccines. Cancer Res 2002;62:5818–27.
[42] Moore DH, Fowler Jr WC, Olafsson K. Class I histocompatibility antigen expression: a prognostic factor for aneuploid ovarian cancers. Gynecol Oncol 1990;38:458–61.
[43] Ohtsukasa S, Okabe S, Yamashita H, Iwai T, Sugihara K. Increased expression of CEA and MHC class I in colorectal cancer cell lines exposed to chemotherapy drugs. J Cancer Res Clin Oncol 2003;129:719–26.
[44] Nicosia SV, Bai W, Cheng JQ, Coppola D, Kruk PA. Oncogenic pathways implicated in ovarian epithelial cancer. Hematol Oncol Clin North Am 2003;17:927–43.
[45] Counter CM, Hirte HW, Bacchetti S, Harley CB. Telomerase activity in human ovarian carcinoma. Proc Natl Acad Sci U S A 1994;91:2900–4.
[46] Murakami J, Nagai N, Ohama K. Telomerase activity in body cavity fluid and peritoneal washings in uterine and ovarian cancer. J Int Med Res 1998;26:129–39.
[47] Brun JL, Cortez A, Commo F, Uzan S, Rouzier R, Darai E. Serous and mucinous ovarian tumors express different profiles of MMP-2, -7, -9, MT1-MMP, and TIMP-1 and -2. Int J Oncol 2008;33:1239–46.
[48] Hanahan D, Weinberg RA. The hallmarks of cancer. Cell 2000;100:57–70.
[49] Weinzierl AO, Lemmel C, Schoor O, Muller M, Kruger T, Wernet D, et al. Distorted relation between mRNA copy number and corresponding major histocompatibility complex ligand density on the cell surface. Mol Cell Proteomics 2007;6:102–13.
[50] Bassani-Sternberg M, Barnea E, Beer I, Avivi I, Katz T, Admon A. Soluble plasma HLA peptidome as a potential source for cancer biomarkers. Proc Natl Acad Sci U S A 2010;107:18769–76.
[51] Kawahara A, Akagi Y, Hattori S, Mizobe T, Shirouzu K, Ono M, et al. Higher expression of deoxyuridine triphosphatase (dUTPase) may predict the metastasis potential of colorectal cancer. J Clin Pathol 2009;62:364–9.
[52] Takatori H, Yamashita T, Honda M, Nishino R, Arai K, Takamura H, et al. dUTP pyrophosphatase expression correlates with a poor prognosis in hepatocellular carcinoma. Liver Int 2010;30:438–46.
[53] Wilson PM, Fazzone W, LaBonte MJ, Lenz HJ, Ladner RD. Regulation of human dUTPase gene expression and p53-mediated transcriptional repression in response to oxaliplatin-induced DNA damage. Nucleic Acids Res 2009;37:78–95.
[54] Noske A, Weichert W, Niesporek S, Roske A, Buckendahl AC, Koch I, et al. Expression of the nuclear export protein chromosomal region maintenance/exportin 1/Xpo1 is a prognostic factor in human ovarian cancer. Cancer 2008;112:1733–43.